AD_____

Award Number: W81XWH-05-1-0572

TITLE: Hypoxia and Prx1 in Malignant Progression of Prostate Cancer

PRINCIPAL INVESTIGATOR: Dr. Young-Mee Park

CONTRACTING ORGANIZATION: Roswell Park Cancer Institute
Buffalo, NY 14263-0001

REPORT DATE: September 2007

TYPE OF REPORT: Annual

PREPARED FOR: U.S. Army Medical Research and Materiel Command
Fort Detrick, Maryland 21702-5012

REPORT DOCUMENTATION PAGE

Form Approved
OMB No. 0704-0188

1. REPORT DATE *(DD-MM-YYYY)*	**2. REPORT TYPE**	**3. DATES COVERED** *(From - To)*
30-SEP-2007	Annual	1 SEP 2006 - 31 AUG 2007

4. TITLE AND SUBTITLE

Hypoxia and Prx1 in Malignant Progression of Prostate Cancer

5a. CONTRACT NUMBER

5b. GRANT NUMBER
W81XWH-05-1-0572

5c. PROGRAM ELEMENT NUMBER

6. AUTHOR(S)

Dr. Young-Mee Park

E-Mail: young-mee.park@roswellpark.org

5d. PROJECT NUMBER

5e. TASK NUMBER

5f. WORK UNIT NUMBER

7. PERFORMING ORGANIZATION NAME(S) AND ADDRESS(ES)

Roswell Park Cancer Institute
Buffalo, NY 14263-0001

8. PERFORMING ORGANIZATION REPORT NUMBER

9. SPONSORING / MONITORING AGENCY NAME(S) AND ADDRESS(ES)
U.S. Army Medical Research and Materiel Command
Fort Detrick, Maryland 21702-5012

10. SPONSOR/MONITOR'S ACRONYM(S)

11. SPONSOR/MONITOR'S REPORT NUMBER(S)

12. DISTRIBUTION / AVAILABILITY STATEMENT
Approved for Public Release; Distribution Unlimited

13. SUPPLEMENTARY NOTES

14. ABSTRACT Hypoxia has been proposed to function as a microenvironmental pressure to select for a subset of cancer cells with an increased ability to survive and proliferate. The activation of Nrf2 and the up-regulation of prx1 expression by changes of oxygenation are likely to contribute to the malignant progression of cancer and to modify the treatment response of cancer cells. The information provided in the current study suggests that the Nrf2-Prx1 axis may serve as a fruitful target for cancer prognosis and therapy. Identifying the key regulatory components and understanding the molecular basis of prx1 gene regulation by Nrf2 are critical to the development of intervention strategies. Future research will be aimed at finding out whether Nrf2-Prx1 activation can be suppressed by genetic and/or pharmacological approaches, and whether suppressing the Nrf2-Prx1 axis will inhibit the malignant progression or reverse treatment resistance in pre-clinical models. We provide the first evidence that suggests hypoxia increases AR function in human prostate cancer cells, and Prx1 enhances the hypoxia-mediated AR activation. Delineating the molecular mechanisms by which hypoxia affects AR function will provide insight into the treatment resistance and malignant progression of prostate cancer cells. Novel therapeutic approaches should be developed to prevent hypoxia and/or its consequences to enhance the efficacy of androgen deprivation therapy, a treatment that has not been Improved significantly since its introduction over 50 years ago

15. SUBJECT TERMS
Prx1, Hypoxic tumor microenvironment, Unstable oxygenation condition, Malignant progression

16. SECURITY CLASSIFICATION OF:			**17. LIMITATION OF ABSTRACT**	**18. NUMBER OF PAGES**	**19a. NAME OF RESPONSIBLE PERSON**
a. REPORT	**b. ABSTRACT**	**c. THIS PAGE**		51	USAMRMC
					19b. TELEPHONE NUMBER *(include area code)*

Standard Form 298 (Rev. 8-98)
Prescribed by ANSI Std. Z39.18

Table of Contents

Introduction

Last year, we reported the cloning and characterization of the promoter composition of human *prx1* gene and identified EpRE elements and Nrf2 as critical regulatory component of its up-regulation in prostate cancer cells. We also reported that androgen receptor (AR) is trans-activated by unstable oxygenation conditions. This year, we identified Kelch-like ECH-associated protein, Keap1, as one of the important mechanisms of *prx1* up-regulation by Nrf2 molecular mechanisms of Nrf2 activation. We were also able to demonstrate that AR activation is significantly increased by Prx1. We will continue to define the role of Prx1 in hypoxia-response of prostate cancer cells and the underlying regulatory mechanisms involved. This study will provide a sound scientific basis upon which the roles of Prx1 can be elucidated in prostate cancer, enabling the development of new therapeutic approaches to inhibit its malignant progression.

Body

Task 1. To establish the molecular basis for Prx1 regulation by hypoxia and its constitutive elevation in highly metastatic human prostate cancer cells (Months 1-36)

We hypothesized that the hypoxic and unstable oxygenation microenvironment of a tumor might be crucial for *prx1* up-regulation. We cloned the human *prx1* promoter and identified NF-E2-related factor 2 (Nrf2) as a key transcription factor. In our progress report of the last funding period, we showed that hypoxia/reoxygenation, an *in vitro* condition suited to mimic changes of oxygenation, increased Nrf2 nuclear localization and its binding to the electrophile responsive elements (EpRE) located at the proximal (EpRE1, -536 to -528) and distal (EpRE2, -1429 to -1421) regions of the *prx1* promoter. A significant reduction of both steady-state and hypoxia/reoxygenation-mediated *prx1* gene expression was demonstrated in Nrf2 knockout cells. Our research accomplishment for Task1 during the current period is described below.

Keap1 is reduced by hypoxia/reoxygenation

Keap1 (Kelch-like ECH-associated protein 1) is known to suppress the nuclear accumulation of Nrf2. Liberation of Nrf2 from Keap1 has been suggested to stabilize cytoplasmic Nrf2 and increase its nuclear translocation/trans-activation (1). Our results showed that hypoxia/reoxygenation significantly reduced Keap1 protein level in LNCaP cells (Figure 1A). A detailed time-course experiment revealed that the decrease of Keap1 occurred as early as 0.5 h of reoxygenation, which was accompanied by the simultaneous increase of Nrf2 accumulation in the nuclear fractions. Keap1 down-regulation under hypoxia/reoxygenation conditions is not

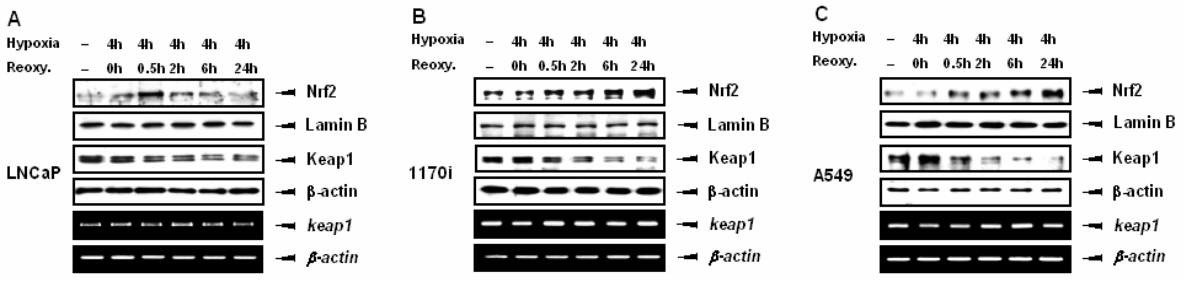

Figure 1. Reduction of Keap1 protein in response to hypoxia/reoxygenation. LNCap (panel A), 1170i (panel B), and A549 (panel C) cells were exposed to 4 h of hypoxia and reoxygenated for 0, 0.5, 2, 6 or 24 h. Nuclear and cytosolic protein extracts were prepared from each cell line and subjected to Western blot analysis with an anti-Nrf2 and an anti-Keap1 antibody, respectively. Lamin B is a loading control for nuclear fraction, and β-actin is a loading control for cytosolic fraction. Total RNA was isolated from and RT-PCR was performed using the primer pairs specific for the human *keap1* mRNA. *β-actin* gene was analyzed as a control.

unique to LNCaP cells. Similar results were obtained in the A549 and 1170i cells (Figure 1B and 1C). When A549 and 1170i cells were re-oxygenated for a longer period of time, *i.e.,* 6 h or 24 h, an additional increase of Nrf2 was noted. This is likely due to the *de novo* synthesis of Nrf2. Nrf2 itself was shown to contain an EpRE-like element in its promoter (2).

Reduced Keap1 protein, however, was not due to reduced mRNA. Comparable levels of *Keap1* mRNA were observed in control and hypoxic cells, suggesting an increased degradation of Keap1 during reoxygenation. Consistent with this interpretation, not only a constitutive elevation of Nrf2 protein (Figure 2A) but also an increased accumulation of *prx1* mRNA and protein (Figure 2B) was found in Keap1 -/- MEF cells.

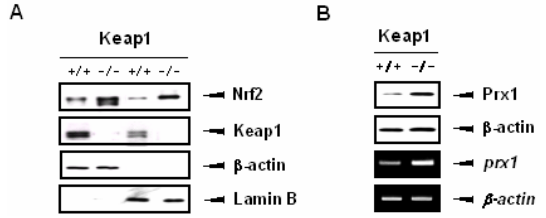

Figure 2. Effect of Keap1 knock-out on nuclear accumulation of Nrf2 and Prx1 expression. Panel A. Equal amounts of cytoplasmic and nuclear protein from Keap1+/+ and Keap1-/- MEF cells were subjected to Western blot analysis using an anti-Nrf2 or anti-Keap1 antibody. Western blots of β-actin and lamin B were carried out as the loading control for cytoplasmic and nuclear protein, respectively. Panel B. Total protein extract from Keap1+/+ or -/- cells was subjected to Western blot using an antibody specific to Prx1. β-actin was used as a loading control. Total RNA from Keap1+/+ or -/- cells were subjected to RT-PCR analysis using primer pairs specific to the mouse *prx1*. Mouse *β-actin* gene was analyzed as a control.

These results, together with those reported in the last funding period led to a publication in Cancer Research (3) (also see *Appendix 1*).

Plans

We plan to determine whether the increased Nrf2 binding to EpRE elements contributes to the increased Prx1 levels in highly metastatic human prostate cancer cells. We will compare Nrf2 binding activities in LNCaP *vs.* LN3 and PC3 *vs.* PC3M cells using EMSA and supershift assays. To cross-validate the EMSA/supershift assays, we will compare *prx1* promoter activities in LNCaP *vs.* LN3 and PC3 *vs.* PC3M cells. Various promoter reporter constructs we have generated will be used to this end. Since Nrf2 activity is primarily determined by the accumulation of stabilized Nrf2 in the nucleus, we also plan will to investigate the subcellular distribution and nuclear accumulation of Nrf2 in LNCaP *vs.* LN3 and PC3 *vs.* PC3M cells by Western blot analysis using cytosolic and nuclear fractions of the cells. These experiments will provide insight into the role of prx1-EpREs and Nrf2 in constitutive elevation of Prx1 in highly metastatic prostate cancer cells. A direct comparison of two isogenic pairs of prostate cancer cell lines will also provide a clue as to whether there exist shared mechanisms in different subsets of prostate cancer cells. Selenium has previously been shown to down-regulate AR in prostate cancer cells (4, 5). A recent collaborative study with Drs. Ip and Rustum at our Institute suggest a possibility that the anticancer action of selenium may also in part be mediated by suppressing the Nrf2-Prx1 pathway (also see *Appendix 2*). We plan to seek additional funding to pursue this intriguing possibility.

Task 2. To investigate the molecular mechanisms by which Prx1 regulates hypoxia-mediated PSA expression and AR activation in prostate cancer cells (Months 1-36)

Although hypoxia is accepted as an important microenvironmental factor influencing tumor progression and treatment response, it is regarded usually as a static global phenomenon. Consequently, less attention is given to the impact of dynamic changes in tumor oxygenation in regulating the behavior of cancer cells. AR signaling plays a critical role in prostate cancer. We reported previously that hypoxia/reoxygenation, an *in vitro* condition used to mimic an unstable

oxygenation climate in a tumor, stimulates AR activation (6). Results obtained from our study during the current funding period, we demonstrated that Prx1 acts as a key mediator in this process. Our results also show that Prx1 is capable of sensitizing a ligand-stimulated AR. Our research accomplishment for Task2 during the current period is described below.

Expression of Prx1 is elevated in the LNCaP derivatives, LN3, C4-2, and C4-2B cell lines

The LNCaP-lineage progression cell models, LN3, C4-2, and C4-2B, are less sensitive to androgen, and display an increased metastatic potential compared to the parental cells. Unlike LNCaP, all three are able to grow in a castrated host. Since Prx1 has been suggested to confer an aggressive survival phenotype, we postulated that Prx1 might influence AR activity and promote the malignant progression of prostate cancer. As a first step to test this hypothesis, we examined Prx1 expression in LN3, C4-2, and C4-2B cells. Our results revealed that Prx1 expression was increased in all three progeny cell lines compared to the parental LNCaP cells. The elevated expression of Prx1 appears to be controlled at the level of message abundance. We next examined whether elevated levels of Prx1 might influence AR activation by hypoxia/reoxygenation. LNCaP and LN3 cells were exposed to 4 h of hypoxia, and the androgen responsive element (ARE)-binding activities of AR were examined at 0, 0.5, 2 or 6 h during reoxygenation. As shown in Figure 3A, although the AR stimulatory effect of hypoxia/reoxygenation was observed in both LNCaP and LN3 cells, the degree of AR stimulation by hypoxia/reoxygenation was greater in LN3 than in LNCaP cells. The ARE-binding activity of AR reached a maximum at 2 h during reoxygenation for both cell lines. Since *PSA* is one of the best-characterized AR target genes, *PSA* mRNA accumulation was compared

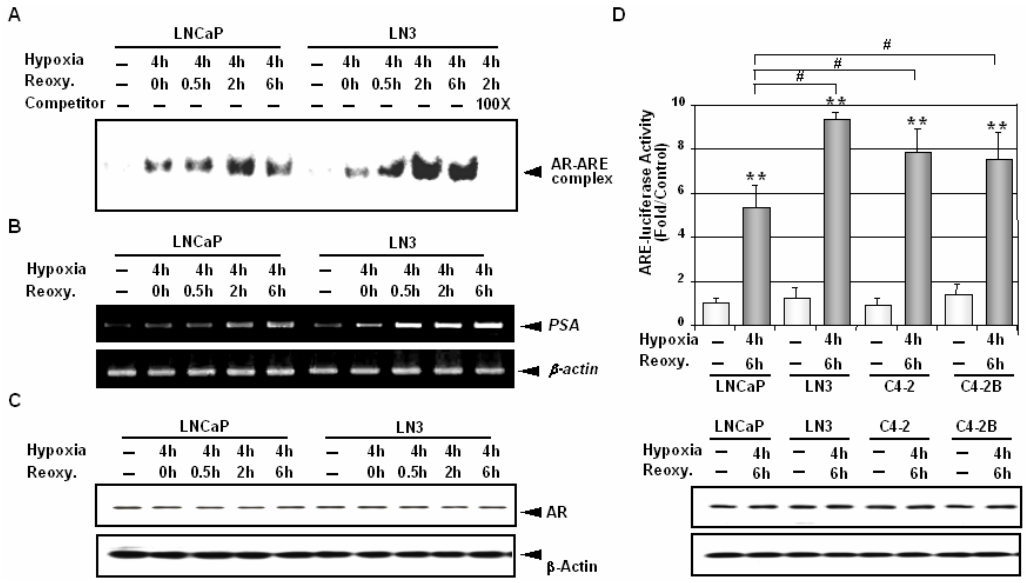

Figure 3. Effect of hypoxia/reoxygenation on AR-ARE binding activity and AR trans-activation. *A*, LNCaP or LN3 cells were exposed to 4 h of hypoxia, and EMSA was performed at the indicated times during reoxygenation. The ARE-containing oligonucleotides (Santa Cruz Biotechnology) radiolabeled with γ-^{32}P ATP (MP Biomedicals, Irvine, CA) were used as a probe. The location of AR-ARE complexes is indicated by an arrow. To confirm the specificity of the AR-ARE binding, molar excess of the unlabeled ARE was used as a competitor. *B*, LNCaP or LN3 were exposed to 4 h of hypoxia, and RT-PCR analysis was carried out using a PCR primer pair specific for the human *PSA* gene. *β-actin* gene was amplified as a control. *C*, LNCaP or LN3 were exposed to 4 h of hypoxia, and Western blot analysis was carried out using an anti-AR antibody (Santa Cruz Biotechnology) as a probe. β-Actin antibody was used as a loading control. *D*, Upper panel: LNCaP, LN3, C4-2 or C4-2B cells were transfected with an ARE-luciferase construct. The pRL-TK vector containing the *Renilla* luciferase gene was co-transfected to normalize the transfection efficiency. At 24 h after transfection, cells were treated with 4 h hypoxia/6 h reoxygenation, and luciferase activity was determined. Normalized mean luciferase activity obtained from cells transfected with ARE-luciferase without hypoxia exposure was set at 1.0. The data is presented as the ratio of the normalized luciferase activities. $^{**}P < 0.01$, compared with the respective non-hypoxia treated control. $^{\#}P < 0.05$, compared with hypoxia treated LNCaP. Lower panel: Western blot analysis was performed using an anti-AR antibody as a probe. β-Actin antibody was used as a loading control.

between LNCaP and LN3 cell lines using semi-quantitative RT-PCR. Consistent with the greater ARE-binding activity, the accumulation of *PSA* mRNA by hypoxia/reoxygenation was more pronounced in LN3 than in LNCaP cells (Figure 3B). Increased *PSA* mRNA accumulation was not due to increased AR protein level. No appreciable change in AR protein level was observed by hypoxia/reoxygenation (Figure 3C). Activated AR trans-activates its target genes by binding to the ARE-containing promoter region. LNCaP, LN3, C4-2, and C4-2B cells were transfected with an ARE-luciferase construct, and luciferase reporter activities were determined as a measure of AR trans-activation by hypoxia/reoxygenation. Our results demonstrated that increases of luciferase activity by hypoxia/reoxygenation were significantly higher in LN3, C4-2 and C4-2B when compared to that seen in LNCaP cells (Figure 3D), although the increases of luciferase activities were observed in all cell lines. The level of AR expression appeared to be comparable among the four cell lines; hypoxia/reoxygenation did not change the AR protein level.

Prx1 increases AR trans-activation by hypoxia/reoxygenation

To test the role of Prx1 directly, Prx1 was introduced exogenously into LNCaP cells using an adenoviral vector carrying the Prx1 gene (Ad.Prx1). As shown in Figure 4A, the ARE binding activity of AR was increased in cells transfected with Prx1 compared to that in the Ad.Con-infected control. Consistent with the enhanced ARE-binding activity, increased accumulation of *PSA* mRNA was observed in LNCaP cells infected with Ad.Prx1. The effect of Prx1 on AR trans-activation was also examined by transfecting an ARE-luciferase construct. As shown in Figure 4B, a significant increase of the reporter activity was observed in the Prx1 over-expressing cells, thus confirming that the enhanced AR activity by Prx1 is not limited to the *PSA* gene. We next examined the effect of reducing endogenous Prx1 expression on AR activity. To do this, LN3 cells were infected with a retroviral vector containing scramble-shRNA (scramble) or Prx1-shRNA (shPrx1). As shown in Figure 4C, the level of Prx1 was markedly reduced in shPrx1-infected cells, but not in scramble shRNA-infected cells. The Prx1 expression level of mock-infected LN3 cells is shown for comparison. When scramble- or shPrx1-infected cells were exposed to hypoxia/reoxygenation, the accumulation of *PSA* mRNA was significantly reduced in shPrx1-infected cells. This result is consistent with the findings from Prx1 over-expressing cells.

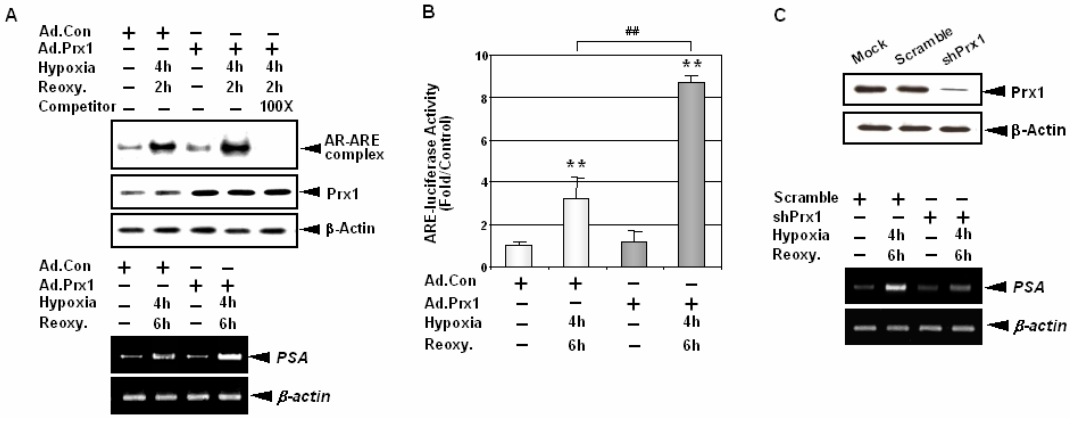

Figure 4. Prx1 increases the AR stimulatory effect of hypoxia/reoxygenation. *A*, LNCaP or LN3 cells were exposed to 4 h of hypoxia, and EMSA was performed at the indicated times during reoxygenation. The ARE-containing oligonucleotides (Santa Cruz Biotechnology) radiolabeled with γ-^{32}P ATP (MP Biomedicals, Irvine, CA) were used as a probe. The location of AR-ARE complexes is indicated by an arrow. To confirm the specificity of the AR-ARE binding, molar excess of the unlabeled ARE was used as a competitor. *B*, LNCaP or LN3 were exposed to 4 h of hypoxia, and RT-PCR analysis was carried out using a PCR primer pair specific for the human *PSA* gene. *β-actin* gene was amplified as a control. *C*, LNCaP or LN3 were exposed to 4 h of hypoxia, and Western blot analysis was carried out using an anti-AR antibody (Santa Cruz Biotechnology) as a probe. β-Actin antibody was used as a loading control.

Prx1 increases ligand-stimulated AR trans-activation

To examine whether Prx1 regulates ligand-stimulated AR activity independent of hypoxia/reoxygenation, LNCaP cells were switched to a charcoal-stripped FBS (CS-FBS) medium to deplete residual androgens present in the regular FBS medium. Cells were exposed to a CS-FBS medium supplemented with 10 nM of a synthetic androgen, R1881. It was shown that prostate tissue contains approximately 10 nM of dihydrotestosterone (7). A dominant tissue androgen in the prostate tissue is dihydrotestosterone. Our results show that Prx1 increased the ARE-binding activity of a ligand-stimulated AR (Figure 5A). To test whether Prx1 sensitizes AR to low levels of androgen, we exposed the cells to a lower concentration of R1881. We chose to use 2 nM R1881 since prostate cancer tissues that recurred during androgen deprivation therapy have been shown to contain approximately this level of dihydrotestosterone. Our results revealed that Prx1 over-expression significantly increased the ARE reporter activity at a sub-physiological level of R1881 (Figure 5B). The activity of the ARE-luciferase reporter at 10 nM R1881 is shown for comparison. To evaluate the effect of endogenous Prx1 knock-down on ligand-stimulated AR activity, scramble- or shPrx1-infected LN3 cells were exposed to 10 nM R1881. Our results clearly demonstrated that the accumulation of *PSA* mRNA was much lower in shPrx1-infected cells compared to scramble-shRNA infected cells (Figure 5C).

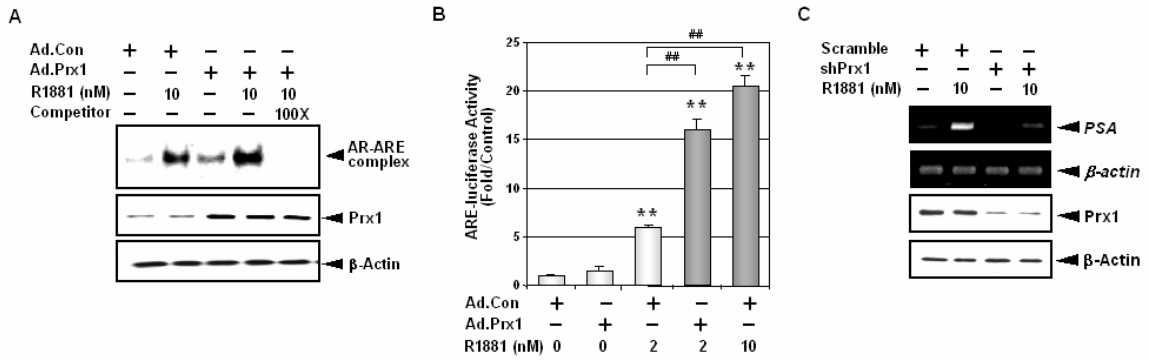

Figure 5. Prx1 enhances AR activation after exposure to synthetic androgen, R1881. *A,* Ad.Con- or Ad.Prx1-infected LNCaP cells grown in a CS-FBS containing medium were treated with 10 nM of R1881 for 6 h. Nuclear extract was obtained, and EMSA was performed using ARE-containing oligonucleotides as a probe. Western blot was carried out to monitor the expression levels of Prx1 at the time of experiment. β-Actin was used as a loading control. *B,* Ad.Con- or Ad.Prx1-infected cells grown in a CS-FBS containing medium were transfected with the ARE-luciferase construct. Cells were treated with 2 nM or 10 nM of R1881 for 6 h, and luciferase activities were determined. Normalized mean luciferase activity obtained from Ad.Con-infected cells without R1881 stimulation was set at 1.0. Data is presented as the ratio of the normalized luciferase activities. $^{**}P < 0.01$, compared with un-stimulated Ad.Con sample. $^{\#\#}P < 0.01$, compared with 2 nM R1881 stimulated Ad.Con sample. *C,* Scramble- or shPrx1-infected LN3 cells grown in a CS-FBS medium were treated with 10 nM of R1881 for 6 h. Total RNA was isolated and RT-PCR analysis was performed to analyze the levels of *PSA* mRNA accumulation. Western blot analysis was carried out to monitor the expression levels of Prx1 in scramble- or shPrx1-infected cells at the time of experiment.

The AR stimulatory function of Prx1 is independent of its antioxidant activity

The ability of Prx1 to sensitize a ligand-stimulated AR indicated that the antioxidant activity of Prx1 may not be necessary for its AR stimulatory function in response to hypoxia/reoxygenation. When we examined the oxidation status of Prx1 in LNCaP and LN3 cells, we found that the active site Cys^{52} residue in Prx1 was oxidized and inactivated by hypoxia/reoxygenation. Figure 6A shows the 2D Western blots of LN3 cells analyzed after 2 h of reoxygenation when the ARE-binding activity of AR was maximal based on EMSA results. Oxidation of Prx1 resulted in an acidic shift of the 2D Western blot when probed with a Prx1 antibody (upper panel). Oxidation of the active site Cys^{52}-SH to Cys^{52}-$SO_{2/3}H$ was further confirmed by using a Prx $SO_{2/3}H$ antibody which specifically recognizes the oxidized Cys^{52} (lower panel). The oxidation status of Prx1 was maintained at least after 6 h to 8 h during reoxygenation (data not shown). To test the effectiveness of an antioxidant activity-null Prx1 in modifying AR function, LNCaP cells were transfected with a plasmid containing a mutant Prx1 generated by replacing the catalytic site

Cys[52] with Ser[52] (pCR C52S). As shown in Figure 6B, regardless of whether the wild type Prx1 (pCR Prx1WT) or the mutant Prx1 was over-expressed, the ARE-luciferase activity was consistently increased. The effect of hypoxia/reoxygenation on AR activity in mock-transfected cells with an empty plasmid (pCR3.1) is shown for comparison. The enhancement of AR activity in mutant Prx1 over-expressing cells was comparable to that seen in wild type Prx1 over-expressing cells. This result clearly demonstrated that the antioxidant activity of Prx1 is not essential for the AR stimulatory function of Prx1.

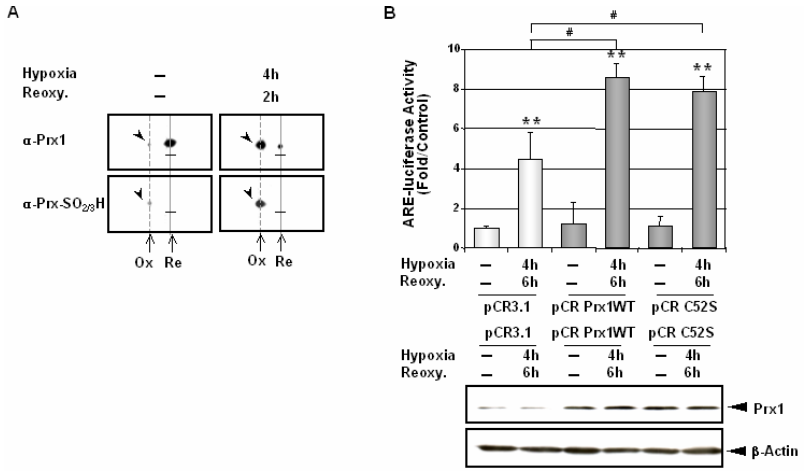

Figure 6. The antioxidant activity of Prx1 is not essential for AR trans-activation by hypoxia/reoxygenation. *A*, LN3 cells were treated with 4 h hypoxia/2 h rexoxygenation. The oxidation status of Prx1 was analyzed by 2-dimensional gel electrophoresis followed by Western blot using a Prx1 antibody (upper panel). The Prx1 antibody recognizes both oxidized (Ox) and reduced (Re) forms of Prx1. Note the acidic shift of oxidized Prx1 after hypoxia/reoxygenation. Oxidation status of the active site Cys[52] was evaluated using Prx-$SO_{2/3}$H antibody (lower panel). *B*, Upper panel: LNCaP cells were transfected with pCR vectors containing wild type Prx1 (pCR Prx1WT) or mutant Prx1 lacking antioxidant activity (pCR C52S). Empty vector (pCR3.1) was transfected as a negative control. At 24 h after transfection, cells were treated with 4 h hypoxia/6 h rexoxygenation. Normalized mean luciferase activity obtained from cells without hypoxia exposure was set at 1.0. The data is presented as the ratio of the normalized luciferase activities. $^{**}P < 0.01$ compared with the respective non-hypoxia treated control. $^{\#}P < 0.05$, compared with hypoxia treated pCR3.1 sample. Lower panel: Western blot analysis of Prx1 was carried out to monitor the levels of Prx1 expression after transfection. β-Actin was used as a loading control.

Prx1 interacts with AR, and is recruited to the PSA promoter

Since accumulating evidence suggests that Prx1 interacts with various proteins to modulate their activities (8-11), we tested whether Prx1 interacts with AR. Immunoprecipitation and reciprocal immuneoprecipitation experiments were carried out using a Prx1 antibody or an AR antibody in LN3 cells, these cells possess a relatively high level of endogenous Prx1. As shown in Figure 7A, AR was co-precipitated with Prx1 after hypoxia/regoxygenation when a Prx1 antibody was used for immunoprecipitation. Similarly, Prx1 was co-precipitated with AR after hypoxia/reoxygenation when an AR antibody was used for immunoprecipitation, indicating a possible interaction of Prx1 and AR after hypoxia/reoxygenation. In order to examine whether Prx1 is recruited to the androgen-responsive element (ARE) of the *PSA* promoter in the natural chromatin milieu, chromatin immunoprecipitaion (ChIP) assays were carried out using a Prx1 antibody. To control for possible nonspecific interactions and DNA contamination, samples precipitated with rabbit IgG were analyzed in parallel. As shown in Figure 7B, our results demonstrated a recruitment of Prx1 to the ARE region in response to hypoxia/reoxygenation. The results obtained from DNA that was PCR amplified from chromatin extracts before immunoprecipitation (input) are shown for comparison. The specific recruitment of AR to the same ARE region was also confirmed in cells treated with hypoxia/reoxygenation. Neither Prx1 nor AR was recruited to the non-specific region (intervening) that does not contain an ARE site. No signal was detected in DNA samples obtained from the corresponding IgG samples. These and related findings led to a publication on Cancer Research (7) (also see *Appendix 3*).

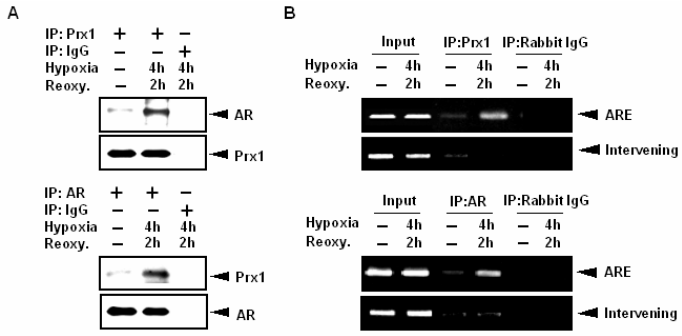

Figure 7. Prx1 interacts with AR, and is recruited to the *PSA* promoter with AR. *A*, Upper panel: LN3 cells were treated with 4 h hypoxia/2 h reoxygenation. Equal amounts of protein were used for immunoprecipitation (IP) with a Prx1 antibody. The immunoprecipitates were probed for the presence of AR by Western blot. Prx1 Western blot was performed as a loading control. Rabbit IgG immunoprecipiation was done as a negative control. Lower panel: Aliquots of protein were subjected to reciprocal immunoprecipitation using an AR or rabbit IgG antibody. The immunoprecipitates were probed for the presence of Prx1 by Western blot. AR Western blot was performed as a loading control. *B*, Upper panel: LN3 cells treated with 4 h hypoxia/2 h reoxygenation were processed for ChIP assays using an anti-Prx1 antibody. Primer pairs used to amplify the ARE containing region (ARE) and the non-ARE containing region (intervening) are described in the Materials and Method. The input lane shows results obtained from DNA that was PCR amplified from chromatin extracts before immunoprecipitation. The rabbit IgG lane shows PCR results obtained after immunoprecipitation with rabbit IgG. The gels shown are representative of three independent experiments. Lower panel: Aliquots of samples were processed for ChIP assays using an anti-AR antibody. The ARE region and intervening regions were amplified with the respective primer pairs.

We also crystallized the human Prx1 protein for the first time and revealed its three-dimensional structure (12) (also see *Appendix 4*). Based on the results from a combination of mutagenesis, biochemical, computer modeling, mass spectrometry, and x-ray crystallographic studies, we demonstrated that the Cys^{83} residue in Prx1 is critical for its structural and chaperone-like properties.

Plans

The N terminal to C terminal dimerization of the AR is suggested to play an important role in AR trans-activation. We plan to examine whether Prx1 levels affect the N-C interaction of the AR. A mammalian two-hybrid system will be employed. This system consists of the N-terminus of AR fused with VP16 (VP16-ARN) and the C-terminal hinge and ligand-binding domain of AR fused with the GAL4-DBD (GAL-ARHLBD), and a pG5-luciferase reporter. This experiment will provide information on the possible role for Prx1 on AR dimerization. Having uncovered the importance of Cys^{83} residue in molecular behaviors of Prx1, we plan to test whether or not a Cys^{83} to Ser^{83} mutant protein (C83S) can interact with AR. These experiments will provide vital biological and clinical information to unravel the functional significance of Prx1 in malignant progression of human prostate cancer.

Task 3. To test the prognostic value of Prx1 in disease relapse and progression (Months 12-36)

We have established a database for a total of 249 patients who underwent curative surgical resection. Study subjects were mostly white (232/249 = 93%) with median age at diagnosis 61 years (range 41-81). Diagnosis was between May 1987 and June 2002. Last follow-up date was Dec 2002 with median patient follow-up of 69 months (range 1-162).

Immunohistochemical analysis of Prx1 in these tissue specimens is expected to be completed within 2 months. In brief, tissue specimens were fixed in neutral buffered formalin (10% vol/vol formalin in water; pH, 7.4) and embedded in paraffin wax. Serial sections of 4-µm thickness

were cut and mounted on charged glass slides (Superfrost Plus; Fisher Scientific, Rochester, NY). IHC conditions for Prx1 were optimized and evaluated by two independent pathologists. Sections were microwaved twice for 10 minutes in citrate buffer (pH 6.0) for antigen retrieval. The sections were then treated with 3% hydrogen peroxide in methanol to quench the endogenous peroxidase activity followed by incubation with 1% BSA to block the non-specific binding. A rabbit polyclonal antibody against Prx1 (Lab Frontier, Korea) was used at dilutions of 1:2000. The avidin-biotin detection method was used on a Ventana Automated System (Ventana Medical Systems, AZ). An irrelevant rabbit antiserum served as a negative control. Prx1 immunoreactivity was observed in the cytosol and nucleus.

Plans

Research proposed is in good progress as originally planned. Each slide will be evaluated for Prx1 using a semi-quantitative scoring system for both the intensity of the stain and the percentage of positive malignant cells. The intensity of Prx1 will be coded as: 0, lower than the adjacent normal-appearing prostatic epithelium; 1, similar to the adjacent prostatic epithelium; 2, stronger than the adjacent prostatic epithelium. The percentage of cells displaying a stronger staining intensity than the adjacent prostatic epithelium was scored as 1 (0% to 24% tumor cells stained); 2 (25% to 49% tumor cells stained); 3 (50% to 74% tumor cells stained); 4 (75% to 100% tumor cells stained). Statistical analysis will be performed to evaluate the predictive value of Prx1 on patient survival and PSA recurrence, and its correlations with various parameters predictive of clinical outcomes. Having found the critical role of Nrf2 in Prx1 up-regulation, we also plan to analyze Nrf2 as well as Prx1.

Key Research Accomplishments

- Validated the functional significance of *prx1*-EpRE sites in *prx1* regulation
- Mutation analysis of *prx1*-EpRE sites and identified critical nucleotide sequences
- Confirmed *in vivo* Nrf2 occupancy to *prx1*-EpRE by chromatin immunoprecipitation
- Demonstrated the effect of Prx1 levels on *PSA* and AR-target gene expression
- Demonstrated the effect of Prx1 levels on ARE-binding activity of AR
- Purified human Prx1 and characterized its behavior at the molecular level
- Crystallized human Prx1 and resolved 3-D structure
- Demonstrated the effect of Prx1 levels on nuclear localization of AR
- Establishd a detailed database of patient cohorts by medical chart review
- Identified the human CaP tissue specimens that match with the database

Reportable Outcomes

The following four manuscripts resulted from this research.

Kim Y-J, Ahn J-Y, Liang P, Ip C, Zhang Y, and **Park Y-M.** Human *prx1* gene is a target of Nrf2 and is up-regulated by hypoxia/reoxygenation: implication to tumor biology. Cancer Res, 67:546-554, 2007

Kim Y-J, Baek S-H, Bogner PN, Ip C, Rustum YM, Fakih MG, Ramnath N, and **Park Y-M**. Targeting the Nrf2-Prx1 pathway with selenium to enhance the efficacy and selectivity of cancer therapy. J Cancer Mol, 3(2): 37-43, 2007

Park S-Y, Yu X, Ip C, Mohler JL, Bogner PN and **Park Y-M**. Prx1 interact with androgen receptor and enhances its trans-activation by hypoxia/reoxygenation. Cancer Res, *in press*, 2007

Lee WS, Choi K-S, Riddell J, Ip C, Ghosh D, Park J-H, and **Park Y-M**. Human Prx1 and Prx2 are not duplicate proteins: The unique presence of Cys83 in Prx1 underscores the structural and functional differences between Prx1 and Prx2. J of Biol Chem, 282(30): 22011-22022, 2007

Conclusions

Our research will provide vital new information in elucidating the molecular mechanisms by which Prx1 promotes the aggressive phenotype of the prostate cancer cells and its malignant progression. The information generated and the approaches we have taken in this study will serve as a fundamental basis upon which the role of Prx1 can be elucidated in prostate cancer and in other human malignancies, ultimately leading to the development of new prognostic/therapeutic approaches. Nearly 30% of men who undergo radical prostatectomy for localized prostate cancer have been reported to experience a biochemical recurrence. Improved prognostic methods to predict the likelihood of recurrence will help both clinicians and patients when making treatment decisions. Results obtained from Task 3 will provide information applicable to the clinic for the rational decision of therapeutic options. Task 3 will also cross validate the clinical relevance of the biological information to be obtained from Tasks 1 and 2.

References

1. Itoh K, Wakabayashi N, Katoh Y, et al. Keap1 represses nuclear activation of antioxidant responsive elements by Nrf2 through binding to the amino-terminal Neh2 domain. Genes Dev 1999;13:76-86.
2. Kwak MK, Itoh K, Yamamoto M, et al. Enhanced expression of the transcription factor Nrf2 by cancer chemopreventive agents: role of antioxidant response element-like sequences in the nrf2 promoter. Mol Cell Biol 2002;22:2883-92.
3. Kim YJ, Ahn JY, Liang P, et al. Human prx1 gene is a target of Nrf2 and is up-regulated by hypoxia/reoxygenation: implication to tumor biology. Cancer Res 2007;67:546-54.
4. Dong Y, Lee SO, Zhang H, et al. Prostate specific antigen expression is down-regulated by selenium through disruption of androgen receptor signaling. Cancer Res 2004;64:19-22.
5. Lee SO, Chun JY, Nadiminty N, et al. Monomethylated selenium inhibits growth of LNCaP human prostate cancer xenograft accompanied by a decrease in the expression of androgen receptor and prostate-specific antigen (PSA). Prostate 2006;66:1070-5.
6. Park SY, Kim YJ, Gao AC, et al. Hypoxia increases androgen receptor activity in prostate cancer cells. Cancer Res 2006;66:5121-9.
7. Park SY, Yu X, Ip C, et al. Prx1 interacts with androgen receptor and enhances its trans-activation by hypoxia/reoxygenation. Cancer Res 2007;*in press*.
8. Kim YJ, Lee WS, Ip C, et al. Prx1 suppresses radiation-induced c-Jun NH2-terminal kinase signaling in lung cancer cells through interaction with the glutathione S-transferase Pi/c-Jun NH2-terminal kinase complex. Cancer Res 2006;66:7136-42.
9. Wen ST, Van Etten RA. The PAG gene product, a stress-induced protein with antioxidant properties, is an Abl SH3-binding protein and a physiological inhibitor of c-Abl tyrosine kinase activity. Genes Dev 1997;11:2456-67.
10. Mu ZM, Yin XY, Prochownik EV. Pag, a putative tumor suppressor, interacts with the Myc Box II domain of c-Myc and selectively alters its biological function and target gene expression. J Biol Chem 2002;277:43175-84.
11. Jung H, Kim T, Chae HZ, et al. Regulation of macrophage migration inhibitory factor and thiol-specific antioxidant protein PAG by direct interaction. J Biol Chem 2001;276:15504-10.

12. Lee W, Choi KS, Riddell J, et al. Human peroxiredoxin 1 and 2 are not duplicate proteins: the unique presence of CYS83 in Prx1 underscores the structural and functional differences between Prx1 and Prx2. J Biol Chem 2007;282:22011-22.

Appendix

Appendix 1. Kim Y-J, Ahn J-Y, Liang P, Ip C, Zhang Y, and **Park Y-M,** Human *prx1* gene is a target of Nrf2 and is up-regulated by hypoxia/reoxygenation: Implication to tumor biology. Cancer Res, 67:546-554, 2007

Appendix 2. Kim Y-J, Baek S-H, Bogner PN, Ip C, Rustum YM, Fakih MG, Ramnath N, and **Park Y-M**. Targeting the Nrf2-Prx1 pathway with selenium to enhance the efficacy and selectivity of cancer therapy. J Cancer Mol, 3(2): 37-43, 2007

Appendix 3. Park S-Y, Yu X, Ip C, Mohler JL, Bogner PN and **Park Y-M**. Prx1 interact with androgen receptor and enhances its trans-activation. Cancer Res, *in press*, 2007

Appendix 4. Lee WS, Choi K-S, Riddell J, Ip C, Ghosh D, Park J-H, and **Park Y-M**. Human Prx1 and Prx2 are not duplicate proteins: The unique presence of Cys83 in Prx1 underscores the structural and functional differences between Prx1 and Prx2. J of Biol Chem, 282(30): 22011-22022, 2007

Human *prx1* Gene Is a Target of Nrf2 and Is Up-regulated by Hypoxia/Reoxygenation: Implication to Tumor Biology

Yun-Jeong Kim,[1] Ji-Yeon Ahn,[1] Ping Liang,[2] Clement Ip,[3] Yuesheng Zhang,[3] and Young-Mee Park[1]

Departments of [1]Cell Stress Biology, [2]Cancer Genetics, and [3]Cancer Chemoprevention, Roswell Park Cancer Institute, Buffalo, New York

Abstract

Peroxiredoxin 1 (Prx1) has been found to be elevated in several human cancers. The cell survival–enhancing function of Prx1 is traditionally attributed to its reactive oxygen species–removing capacity, although the growth-promoting role of Prx1 independent of this antioxidant activity is increasingly gaining attention. Although much progress has been made in understanding the behavior of Prx1, little information is available on the mechanism responsible for the abnormal elevation of Prx1 level in cancer. We hypothesized that the hypoxic and unstable oxygenation microenvironment of a tumor might be crucial for *prx1* up-regulation. In this study, we cloned the human *prx1* promoter and identified nuclear factor (erythroid-derived 2)–related factor 2 (Nrf2) as a key transcription factor. Hypoxia/reoxygenation, an *in vitro* condition suited to mimic changes of oxygenation, increased Nrf2 nuclear localization and its binding to the electrophile-responsive elements located at the proximal (−536 to −528) and distal (−1429 to −1421) regions of the *prx1* promoter. A significant reduction of both steady-state and hypoxia/reoxygenation–mediated *prx1* gene expression was shown in Nrf2 knock-out cells. Our results indicated that decreased Kelch-like ECH-associated protein, Keap1, might be an important mechanism for the increased nuclear translocation and activation of Nrf2 in response to hypoxia/reoxygenation. A constitutive elevation of *prx1* mRNA and protein was observed in Keap1 knock-out cells. The above information suggests that the Nrf2-Prx1 axis may be a fruitful target for intervention with respect to inhibiting the malignant progression and/or reducing the treatment resistance of cancer cells. [Cancer Res 2007;67(2):546–54]

Introduction

Peroxiredoxins (Prx) are thiol-specific antioxidant proteins. They are found in mammals, yeast, and bacteria and are classified largely on the basis of having either one (1-Cys) or two (2-Cys) conserved cysteine residues (1). Prx1 is a major 2-Cys Prx family member. It contains a cysteine at the catalytic site (Cys^{52}) and detoxifies peroxides at the expense of Cys^{52} oxidation through intermolecular disulfide formation with the other conserved Cys^{173} residue. The disulfide bond is reduced back to the active thiol form, Cys-SH, by various mechanisms (1, 2).

Despite the initial biochemical characterization of Prx1 as a peroxide-detoxifying enzyme, the physiologic significance of its peroxidase activity is unclear because Prx1 is highly susceptible to inactivation by oxidative stress. Overoxidation of the Cys-SH to Cys-sulfinic ($-SO_2H$) or Cys-sulfonic acid ($-SO_3H$) has been reported with various Prx family members during peroxide detoxification (3). When the catalytic Cys^{52}-SH of Prx1 is overoxidized, the peroxidase activity is lost. Recent studies have suggested that overoxidation of the active site Cys in itself may be physiologically significant because it allows a mechanism of structural and functional switching of the 2-Cys Prx from a peroxidase enzyme to a molecular chaperone under stress conditions (4, 5). The wide range of effects attributed to Prx1 (6–9) may in part be explained by the physical interaction of Prx1 with growth regulatory proteins to modulate their activities (10–12).

Elevated expression of Prx1 has been observed in several human cancers (13–15), including lung cancer (16–18). We recently reported that Prx1 suppresses radiation-induced c-*Jun*-NH_2-kinase (JNK) signaling and apoptosis in lung cancer cells (19). The peroxidase activity of Prx1, however, is not essential for inhibiting JNK activation. The latter effect is mediated through the association of Prx1 with the GSTpi-JNK complex, thereby preventing JNK release from the complex. The JNK inhibitory and antiapoptotic activities of Prx1 suggest that lung cancer with high Prx1 levels is likely to be resistant not only to radiation but also to multiple anticancer agents targeting JNK and the associated apoptotic pathways. Studies by Chen et al. (20) have recently shown the role of Prx1 in radioresistance using human lung cancer xenograft models. They observed a significant growth inhibition and radiosensitization, as well as reduced metastasis of lung cancer cells stably transfected with antisense Prx1. These studies suggest that Prx1, in addition to serving as a potential prognostic marker, may also serve as a therapeutic target and/or a target for inhibiting malignant tumor progression. Delineating the molecular basis of *prx1* gene regulation is expected to provide valuable clues for the development of new intervention strategies. Although much effort has been devoted to the investigation of the various functions of Prx1, virtually nothing is known about the molecular basis of abnormal *prx1* gene regulation in cancer cells.

Hypoxia is one of the key factors influencing tumor growth and progression (21, 22). Generally speaking, hypoxia is considered a global phenomenon and is defined as an overall reduction in oxygen availability or partial pressure below critical levels (23). Tissue oxygenation within a tumor, however, is highly unstable and heterogeneous as a consequence of the architectural and functional abnormalities of the vascular network (24). Blood flow fluctuations in the tumor microvasculature can lead to perfusion-limited hypoxia in the tumor parenchyma (25, 26). In terms of the ultrastructure, tumor vasculature has numerous “holes” or “openings”, widened interendothelial junctions, and a discontinuous or absent basement membrane (27, 28). Aberrant blood vessels can be shut down locally at any time; the same defects can cause a reversal of blood flow. In addition to the reopening of the temporarily closed or blocked vessels, dynamic changes of hypoxia/reoxygenation may also occur as a result of regional angiogenesis.

Requests for reprints: Young-Mee Park, Department of Cell Stress Biology, Roswell Park Cancer Institute, Buffalo, NY 14263. Phone: 716-845-3190; Fax: 716-845-8899; E-mail: young-mee.park@roswellpark.org.

doi:10.1158/0008-5472.CAN-06-2401

We hypothesized that the hypoxic and unstable oxygenation milieu of a tumor may trigger the transactivation of the *prx1* gene via redox-sensitive transcription factors and signaling molecules. In this study, we cloned the human *prx1* upstream region and identified the critical regulatory component of *prx1* gene expression. To mimic the dynamic changes of oxygenation, we treated A549 lung cancer cells to transient hypoxia followed by reoxygenation. We showed that *prx1* is a target gene of nuclear factor (erythroid-derived 2) (NF-E2)–related factor 2 (Nrf2) and is up-regulated by hypoxia/reoxygenation. We showed a specific binding of Nrf2 to the electrophile-responsive element (EpRE) or antioxidant-responsive element located at the proximal (−536 to −528) and distal (−1429 to −1421) regions of the *prx1* promoter. We found that both steady-state *prx1* and hypoxia/reoxygenation–induced *prx1* expression are severely compromised in mouse embryonic fibroblast (MEF) cells lacking Nrf2. Lastly, our results suggest that decreased Kelch-like ECH-associated protein (Keap1) might be an important mechanism for the increased nuclear translocation and activation of Nrf2 in response to hypoxia/reoxygenation.

Materials and Methods

Cell culture. Human lung cancer A549 [American Type Culture Collection (ATCC), Manassas, VA] and 1170i (29) cells were maintained in RPMI 1640 supplemented with 10% (v/v) bovine calf serum, 100 units/mL penicillin, and 100 μg/mL streptomycin. Human prostate cancer LNCaP (ATCC) cells were grown in RPMI 1640 supplemented with 10% (v/v) fetal bovine serum containing 2 mmol/L glutamine, 100 units/mL penicillin, and 100 μg/mL streptomycin. Wi-26 (ATCC) human embryonic epithelial cells, wild-type and Nrf2 knock-out MEF (30), and Keap1 knock-out MEF (30) cells were maintained in DMEM with 10% (v/v) fetal bovine serum, 100 units/mL penicillin, and 100 μg/mL streptomycin. All cells were grown at 37°C in an atmosphere of 5% CO_2 and 95% air.

Hypoxia treatment. Hypoxia treatment was done as reported previously (31). Briefly, the culture medium was replaced with deoxygenated RPMI 1640 before hypoxia treatment at 37°C in a hypoxic chamber (Forma Scientific, Marietta, OH). Deoxygenated medium was prepared before each experiment by equilibrating the medium with a hypoxic gas mixture containing 5% CO_2, 85% N_2, and 10% H_2 at 37°C. The oxygen concentration in the hypoxic chamber and the exposure medium was maintained at <0.05% and monitored by using an oxygen indicator (Forma Scientific). All experiments were done at 70–80% confluency, and the medium pH was maintained between 7.2 and 7.4 for the duration of hypoxia exposure.

Plasmid construction. A 2,100-bp fragment of the human *prx1* promoter was isolated via PCR using the 5′-atatgctagcCAGCCTCCCAAAGTGCTGGG-3′ and 5′-atatctcgagCGGAACGGACGGGGGTGCCG-3′ primer pairs and high-fidelity platinum Taq DNA polymerase with proofreading capability (Invitrogen, Carlsbad, CA). A *Xho*I site was added to the 3′-primer, and a *Nhe*I site was added to the 5′-*prx1* primer. The PCR product was digested with *Nhe*I/*Xho*I, gel-isolated, and subcloned into the pGL3-Basic (Promega, Madison, WI) upstream of the luciferase reporter, and the construct was designated as pGL3-p2100 (−2,100/+1; +1 meaning the transcription initiation site). A series of deletion constructs were generated using pGL3-p2100 as a template. The information from various promoter analysis programs, including TransFac,[4] was taken into consideration when generating the deletion constructs. The sequences of the PCR primers were p1500 forward, 5′-atatgctagcGTTGCCAGGCTGGAGTGCAG-3′; p1000 forward, 5′-atatgctagcCCTCGTCTCTACTAAAAATA-3′; p700 forward, 5′-atatgctagcGCAAATAATTAATTATGATT-3′; p500 forward, 5′-atatgctagcTAAGTTTAGGAGTCCTGATA-3′; p300 forward, 5′-atatgctagcGCAGCTAAGACGCTTACTCC-3′; and p100 forward, 5′-atatgctagcACGAGGGAAAGCGCCGAGTC-3′. The same reverse primer, 5′-atatctcgagCGGAACGGACGGGGGTGCCG-3′, was used to generate the deletion constructs. The sequence accuracy of all constructs was confirmed by using an ABI 3700 capillary sequencer (Applied Biosystems, Foster City, CA).

Site-directed mutagenesis. Site-directed mutagenesis was done by using the GeneTailor Site-Directed Mutagenesis kit (Invitrogen). To generate mtEpRE1 (TGAATCAGC → GTAATCATA) and mtEpRE2 (TGCCTCAGC → GTCCTCATA), mtEpRE1, mt1F 5′-GGAGAGGATGGTCGTGTAACGTAATCATACTCCCAAGAT-3′ and mt1R 5′-GTTACACGACCATCCTCTCCCCGGATGAAT-3′, mtEpRE2, mt2F 5′-CCGGGTTCAAGCGATTCCCCGTCCTCATACTCCCAAGTA-3′, and mt2R 5′-GGGGAATCGCTTGAACCCGGAGGCAGAGGT-3′ were used, respectively. For the construction of the double mutant, mt1mt2, mtEpRE1 was used as a template, and site-directed mutagenesis was done using the mtEpRE2 primer pairs. The constructs were verified by DNA sequencing in both directions.

RNA isolation and reverse transcription-PCR analysis. Total cellular RNA was extracted with TRIzol Reagent (Invitrogen) according to the manufacturer's instructions. RNA concentration was determined by measuring UV absorption, and samples with comparable A_{260}/A_{280} ratios were used for reverse transcription-PCR analysis. The sequences of the PCR primer pairs used for the amplification of human *prx1, keap1*, and *β-actin* were forward 5′-ATGTCTTCAGGAAATGCTAAAAT-3′ and reverse 5′-TCACTTCTGCTTGGAGAAATATTC-3′; forward 5′-CCTGTCCCACTGCCAACTGGTGAC-3′ and reverse 5′-CCTTGCAGCGGGAGTCGGACTGCA-3′; and forward 5′-CAAGAGATGGCCACGGCTGCT-3′ and reverse 5′-TCCTTCTGCATCCTGTCGGCA-3′, respectively. The sequences of the PCR primer pairs used for the amplification of mouse *prx1* and *β-actin* were forward 5′-GTCCCACGGAGATCATTGCTTTC-3′ and reverse 5′-CCCCTGAAAGAGATACCTTCATC-3′; and forward 5′-ACTTGCGCTCAGGAGGAGCAATG-3′ and reverse 5′-GAGATGGCCACTGCCGCATCCTCTT-3′, respectively. PCR was carried out with a thermal cycler (Perkin-Elmer 9600, Boston, MA). Amplification conditions were 25 cycles for *prx1* and *β-actin*, or 30 cycles for *keap1*, of 30 s at 94°C, 30 s at 55°C, and 40 s at 72°C. The amplified products were separated by electrophoresis on a 1.5% agarose gel, stained with ethidium bromide, and photographed under UV illumination.

Transfection and reporter gene assay. Transient reporter gene assays were done by standard transfection methods using 1.5×10^4 cells in 24-well plates. Plasmid constructs (0.2 μg of reporter gene plasmid and 0.02 μg of pRLTK normalizing vector) were transfected into cells by using Fugene 6 reagent (Roche, Branchburg, NJ) according to manufacturer's instruction. Twenty-four hours after transfection, cells were exposed to hypoxia or treated with 20 μmol/L *tert*-butylhydroquinone (tBHQ), and luciferase activities were measured by the luciferase assay system (Promega). Relative luciferase activities were calculated by normalizing the *Renilla* luciferase activity from the pRLTK plasmid. All transfection experiments were done in triplicate and repeated at least thrice.

Nuclear extracts and electrophoretic mobility shift assay. Nuclear lysates were prepared as described previously (31). Briefly, cells were harvested, washed thrice with PBS, resuspended in a hypotonic buffer [10 mmol/L HEPES-KOH (pH 7.9), 1.5 mmol/L $MgCl_2$, 10 mmol/L KCl, and 0.1% NP40], and incubated on ice for 10 min. Nuclei were precipitated with 12,000 × *g* centrifugation for 10 min at 4°C. After washing once with the hypotonic buffer, nuclei were lysed in a lysis buffer [50 mmol/L Tris-HCl (pH 8.0), 150 mmol/L NaCl, and 1% Triton X-100], incubated on ice for 30 min, and precleared with 20,000 × *g* centrifugation for 15 min at 4°C. For the electrophoretic mobility shift assay, 8 μg of nuclear protein extract was incubated in 20 μL of a solution with 10 mmol/L HEPES (pH 7.9), 80 mmol/L NaCl, 10% glycerol, 1 mmol/L dithiothreitol, 1 mmol/L EDTA, 100 μg/mL poly(deoxyinosinic-deoxycytidylic acid), and radiolabeled double-stranded oligonucleotide containing the EpRE elements present in the human *prx1* promoter. EpRE-binding complexes were resolved on native 4.5% polyacrylamide gels in 0.25× Tris-borate-EDTA at 140 V for 1 h. Competition experiments were done by adding 100-fold excess of unlabeled oligonucleotides or nonspecific heat shock element (HSE) containing oligonucleotides. For Nrf2 supershift experiments, nuclear protein extract was incubated with the Nrf2 antibody (Santa Cruz Biotechnology, Santa Cruz, CA). Rabbit immunoglobulin G (Santa Cruz Biotechnology) was used as the negative control.

[4] http://transfac.gbf.de/cgi-bin/matsearch.

Chromatin immunoprecipitation assay. Chromatin immunoprecipitation assays were carried out following the previously described procedure with minor modifications (31). Briefly, formaldehyde was added directly to cells before or after hypoxia/reoxygenation. The crosslinking process was limited to <30 min because longer incubation with formaldehyde caused cells to aggregate and prevented the efficient sonication of the chromatin. After crosslinking, cells were lysed in buffer containing protease inhibitors. Nuclei were isolated, and chromatin was sheared to an average length of 250 to 500 bp using sonication. The sheared chromatin was precleared with salmon sperm DNA/protein A-sepharose and precipitated with an antibody specific to Nrf2 (2 μg/mL; Santa Cruz Biotechnology). Rabbit immunoglobulin G was used as a control to monitor nonspecific interactions. Immune complexes were adsorbed onto salmon sperm DNA/protein A-sepharose beads. After an extensive wash to reduce background, Ab/Nrf2/DNA complexes were eluted. After precipitation, DNA was resuspended in water, and PCR was carried out to amplify the EpRE1- or EpRE2-containing regions in the *prx1* promoter gene. The following primer sequences were used to amplify the two EpRE regions: EpRE1, forward 5′-GAGAGGATGGTCGTGTAACTG-3′, reverse 5′-CAGGGTTGCTGCTTTCTGTTG-3′; and EpRE2, forward 5′-TTGAGACGGAGTCTTGCTCTG-3′, reverse 5′-GTAGTCCTAGCTACTTGGGAG-3′, respectively. The intervening region between the EpRE1 and EpRE2 regions of the human *prx1* promoter was amplified as a negative control by using a forward 5′-GGATCACCTGAGGTCAGGCGT-3′ and reverse 5′-CACGCACCACCACGCCCAGCT-3′ primer pair. Triplicate PCR reactions were conducted for each sample, and the experiments were repeated at least thrice.

Western blot analysis. Cells were rinsed thrice with ice-cold PBS and lysed in radioimmunoprecipitation assay buffer [50 mmol/L Tris-Cl (pH 7.4), 1% NP40, 150 mmol/L NaCl, 1 mmol/L EDTA, 1 mmol/L phenylmethylsulfonyl fluoride, 1 μg/mL each of aprotinin and leupeptin, and 1 mmol/L Na_3VO_4]. After centrifugation at 12,000 × *g* for 30 min, the supernatant was collected, and protein concentration was determined by the Lowry method (32). Equal amounts of protein were separated on 12% (for Prx1 and Keap1) or 7.5% (for Nrf2) SDS-PAGE gel and blotted onto nitrocellulose membranes. The blots were incubated with anti-Prx1 (Lab Frontier, Seoul, Korea), anti-Nrf2 (Santa Cruz Biotechnology) or anti-Keap1 (Santa Cruz Biotechnology) antibody. Antibody to β-actin (Sigma, St. Louis, MO) or Lamin B (Santa Cruz Biotechnology) was used as a loading control. Immunoreactive bands were detected with horseradish peroxidase-conjugated secondary antibodies and enhanced chemiluminescence reagents (Amersham Biosciences, Piscataway, NJ). The experiments were repeated at least thrice.

Immunocytochemistry. Cells seeded on coverslips in six-well plates were allowed to grow for 24 h. After exposure to hypoxia or treatment with 20 μmol/L tBHQ, the cells were washed with PBS, fixed in 4% paraformaldehyde for 30 min at room temperature, permeabilized with 1% Triron X-100 for 10 min, and blocked with 1% bovine serum albumin in PBS for 15 min. The cells were then incubated with anti-Nrf2 antibody (Santa Cruz Biotechnology) for 45 min, followed by incubation with FITC-conjugated antirabbit secondary antibody (Molecular Probes, Eugene, OR) for 45 min. For filamentous actin staining, cells were incubated with rhodamine-conjugated phalloidin (Molecular Probes) for 10 min. The coverslips were mounted on slides using Vectashield mounting medium containing 4′,6-diamidino-2-phenylindole (Vector Laboratories, Burlingame, CA). Fluorescence images were visualized with the Nikon Eclipse E600 inverted microscope.

Statistical analysis. Statistical significance was examined using Student's *t* tests. The two-sample *t* test was used for two-group comparisons. Values were reported as means ± SD. *P* values <0.05 were considered significant and indicated by asterisks in the figures.

Results

Up-regulation of *prx1* expression by hypoxia/reoxygenation and multiple sequence alignment analysis of the *prx1* upstream sequences. To test whether a hypoxic and unstable oxygenation condition activates *prx1* gene expression, human lung cancer A549 cells were exposed to 4 h of hypoxia, followed by reoxygenation in a CO_2 incubator. Reverse transcription-PCR analysis showed a significant up-regulation of *prx1* expression during reoxygenation (Fig. 1*A*). The accumulation of Prx1 protein closely correlated with the mRNA level (Fig. 1*B*). Hypoxia treatment alone, however, did not up-regulate *prx1* gene expression even when the cells were treated with longer periods of hypoxia (Fig. 1*C*). The effect of an unstable oxygenation condition on *prx1* up-regulation was not unique to A549 cells. Similar responses were observed in several other cancer cell models, including human lung cancer 1170i and prostate cancer LNCaP cells (data not shown). Increased *prx1* mRNA level was reproducibly observed in reoxygenated cells regardless of the prior duration of hypoxia. These results are consistent with the hypothesis that dynamic changes of oxygenation of a tumor trigger the transcriptional activation of *prx1* expression. The human *prx1* gene may not be a target of hypoxia-inducible factor-1α because hypoxia-inducible factor-1α binding to the hypoxia-responsive element is known to increase during continuous exposure to hypoxia and to decline immediately by oxygen replenishment (21).

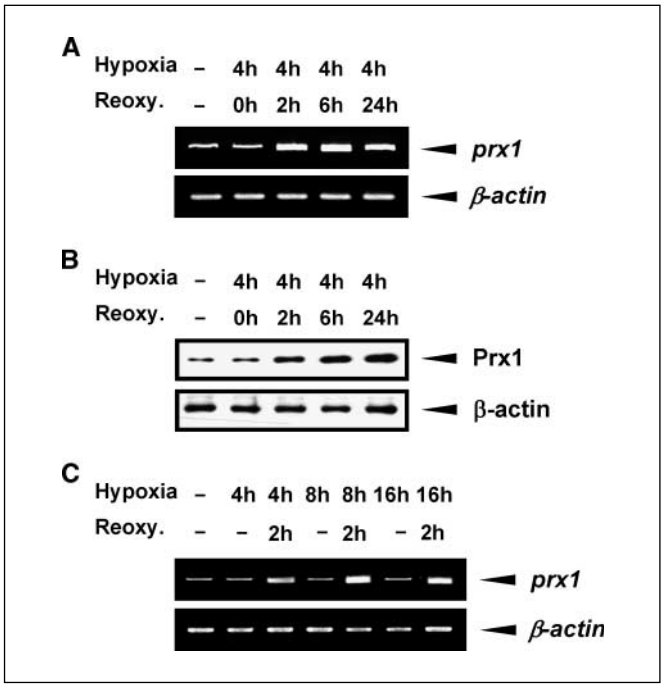

Figure 1. Up-regulation of *prx1* expression by hypoxia/reoxygenation. *A,* human lung cancer A549 cells were exposed to hypoxia for 4 h, followed by reoxygenation for 0, 2, 6, or 24 h. Total RNA was isolated, and reverse transcription-PCR analysis was carried out using primer pairs specific for human *prx1* gene. *β-actin* gene was used as a control. *B,* protein extracted from cells treated as above was subjected to Western blot analysis. Equal amounts of protein (10 μg) were separated by SDS-PAGE and probed with an antibody specific to Prx1. β-actin was used as a loading control. *C,* cells were exposed to 4, 8, or 16 h of hypoxia, followed by 2 h of reoxygenation. Total RNA was isolated, and reverse transcription-PCR was carried out using human *prx1* primer pairs. *β-actin* gene was used as a control.

Because no information is available on the transcriptional regulation of the human *prx1* gene, we carried out a computer-based sequence analysis of the mouse, rat, and human *prx1* upstream sequences. About 5 kb genomic sequences upstream of *prx1* were retrieved in Fasta format from the UCSC genome browser.[5] Multiple sequence alignment analysis was done with a

[5] http://genome.ucsc.edu.

locally installed Clustal X (33) program in combination with MEME (Multiple Em for Motif Elicitation; ref. 34), and CONREAL (CONserved Regulatory Elements anchored ALignment; ref. 35) programs. The computer-based sequence analysis revealed that the 5′ 2.1-kb segment upstream of the human *prx1* gene contains most of the sequence conservation across the three mammalian species (data not shown). No obvious hypoxia-inducible factor-1α–responsive element was found in these *prx1* upstream regions.

Cloning of the human *prx1* promoter and identification of two EpRE sites as critical cis-elements for *prx1* up-regulation in response to hypoxia. The 5′ 2.1-kb region upstream of the human *prx1* gene was PCR cloned, and the luciferase reporter vector, pGL3-2100, was generated. Genomic DNA from the Wi-26 human embryonic epithelial cells was used to avoid possible mutations of the promoter region in cancer cells. A series of deletion vectors were constructed as described in Materials and Methods for the purpose of examining the transcriptional activation of *prx1*. The pGL3-2100 reporter vector was transfected into A549 cells, and the luciferase activities were analyzed at 0, 0.5, 2, 6, or 24 h during reoxygenation after 4 h of hypoxia treatment. The luciferase activity was highest at 6 h of reoxygenation (data not shown). This time point was chosen to study the promoter activities of the deletion constructs. The importance of the 5′ −1,500 to −1,000 and −700 to −500 regions to hypoxia/reoxygenation–mediated *prx1* activation became evident from the analysis. As shown in Fig. 2*A*, a significant reduction of the promoter activity was observed in cells transfected with pGL3-1000 and pGL3-500 when compared with the pGL3-2100 transfected cells.

An examination of these two regions with the use of various promoter analysis programs, including TransFac, indicated that both regions contain potential EpRE, also known as antioxidant-responsive element. The consensus sequence of EpRE, 5′-TGAC*NNN*GC-3′, is a DNA-binding element of the transcription factor, NF-E2–related factor 2, or Nrf2 (36). The proximal EpRE site is at −536 to −528 (EpRE1), and the distal site is at −1,429 to −1,421 (EpRE2; Fig. 2*B*). The conventional EpRE displays sequence similarity to the activator protein 1 response element (5′-TGAC/GTCA-3′). One of the critical features of EpRE is the "GC" at the 3′ end of the EpRE core; this feature is met by *prx1*-EpRE1 and *prx1*-EpRE2. Suffice it to note that EpRE1 and EpRE2 possess one sequence mismatch in the fourth and third nucleotide, respectively. Previous studies have also reported a correlation between *prx1* mRNA accumulation and activation of Nrf2 (37).

To verify the significance of EpRE1 and EpRE2, EpRE1 mutant (pGL3-mtEpRE1), EpRE2 mutant (pGL3-mtEpRE2), and the double mutant (pGL3-mt1mt2) reporter vectors were constructed from pGL3-p2100 (Fig. 2*C*). The mutations were designed to disrupt the Nrf2 recognition sequences of EpRE1 and EpRE2. When pGL3-mtEpRE1 was transfected, both steady-state and hypoxia/reoxygenation–responsive reporter activities were completely lost. When pGL3-mtEpRE2 was transfected, hypoxia/reoxygenation–responsive promoter activity was significantly reduced, although EpRE1 was intact, indicating that both EpRE1 and EpRE2 are required for hypoxia/reoxygenation–mediated activation of *prx1*. The fact that the steady-state promoter activity of pGL3-mtEpRE2 was comparable to that of pGL3-2100 suggests that EpRE1, but not EpRE2, may be critical for baseline *prx1* expression.

EpRE-binding activity of Nrf2 is increased by hypoxia/reoxygenation. The EpRE-binding activities were examined during reoxygenation after 4 h of hypoxia treatment in A549 cells. As shown in Fig. 3*A*, increases of EpRE1- and EpRE2-binding activities were observed as early as 0.5 h during reoxygenation upon withdrawal from hypoxia. The EpRE-binding activities were specific because the DNA-binding complexes became undetectable when molar excess of the unlabeled competitor of the EpRE1- or EpRE2-containing probe was added. The addition of HSE, a classic stress-response element, did not inhibit EpRE-binding activities. The binding activity of EpRE1 declined with time, in contrast to the sustained activity of EpRE2. The reason for this difference is unclear, although a possible role of the adjacent sequences of the EpRE1- and EpRE2-containing probes and the profile of Nrf2 interaction with other nuclear factors may be responsible. When nuclear extracts of A549 cells were incubated with the Nrf2 antibody, the disappearance of the EpRE-binding complexes was clearly evident (Fig. 3*B*). To investigate the recruitment of Nrf2 to the EpRE sites of the human *prx1* promoter in the natural chromatin milieu, we did chromatin immunoprecipitation assays on EpRE1 and EpRE2 with the Nrf2-specific antibody. To control for possible nonspecific interactions and DNA contaminations, samples precipitated with rabbit immunoglobulin G were included. As shown in Fig. 3*C*, our results validated an increased occupancy of Nrf2 in the EpRE1 and EpRE2 regions of the *prx1* promoter in response to hypoxia/reoxygenation. The recruitment of Nrf2 to these EpRE sites was specific because no signal was detected in the immunoglobulin G control samples. We did not find an increase of Nrf2 recruitment to the nonspecific intervening region located between EpRE1 and EpRE2. The results obtained from DNA that was PCR amplified from chromatin extracts before immunoprecipitation (input) are shown for comparison.

Increased nuclear localization and transactivation of Nrf2 by hypoxia/reoxygenation. To test whether the *prx1* promoter is functional with other Nrf2 inducers, pGL3-2100 promoter activities were examined in A549 cells treated with tBHQ. The latter is one of the classic activators of Nrf2. As shown in Fig. 4*A*, treatment with 20 μmol/L tBHQ also increased the *prx1* promoter activity. Immunofluorescence studies confirmed the increased nuclear localization of Nrf2 in cells subjected to hypoxia/reoxygenation or treated with tBHQ (Fig. 4*B*). Nrf2 localization was examined by incubation with an anti-Nrf2 antibody; the location and integrity of the nucleus was probed by 4′,6-diamidino-2-phenylindole staining of the same cells. Overlaying the Nrf2 and 4′,6-diamidino-2-phenylindole images (cyan color) confirms the nuclear localization of Nrf2. In control cells, low levels of Nrf2 expression were observed in the cytoplasm and the nucleus. The Nrf2/filamentous actin overlay (orange color) images display the cytoplasmic localization of Nrf2. Nuclear fractions were then prepared, and as shown in Fig. 4*C*, there was significantly increased Nrf2 accumulation in the nucleus as shown by Western blot analysis. It should be noted that the Nrf2 band seemed at ~100 kDa, although the expected MW is at 68 kDa. The occurrence of the higher molecular mass of Nrf2 in Western blot analysis has been described by others and is suggested to represent a Nrf2-actin complex (38).

An important role of Nrf2 in *prx1* transactivation was also shown in Nrf2 knock-out cells. The accumulation of *prx1* mRNA was significantly diminished in Nrf2 −/− cells when compared with Nrf2 +/+ MEF cells (Fig. 4*D*). However, neither baseline nor hypoxia/reoxygenation–responsive expression of *prx1* mRNA was completely abolished in cells lacking Nrf2. It is conceivable that in addition to Nrf2, various regulatory factors might be involved in coordinating and relaying different cellular signals to the transcriptional machinery of the *prx1* gene, as is true for other genes involved in cell growth and survival regulation.

Keap1, an Nrf2 suppressor, is reduced by hypoxia/reoxygenation. Keap1 is known to suppress the nuclear accumulation of Nrf2. Liberation of Nrf2 from Keap1 has been suggested to stabilize cytoplasmic Nrf2 and increase its nuclear translocation and transactivation (39). Our results showed that hypoxia/reoxygenation significantly reduced Keap1 protein level in A549 cells (Fig. 5*A*). A detailed time course experiment revealed that the decrease of Keap1 occurred as early as 0.5 h of reoxygenation, which was accompanied by the simultaneous increase of Nrf2 accumulation in the nuclear fractions. Keap1 down-regulation under hypoxia/reoxygenation conditions is not unique to A549 cells. Similar results were obtained in the 1170i and LNCaP cells. When A549 and 1170i cells were reoxygenated for a longer period of time, i.e., 6 or 24 h, an additional increase of Nrf2 was noted. This is likely due to the *de novo* synthesis of Nrf2. Nrf2 itself was shown to contain an EpRE-like element in its promoter (40). Reduced Keap1 protein, however, was not due to reduced mRNA. Comparable levels of *keap1* mRNA were observed in control and hypoxic cells, suggesting an increased degradation of Keap1 during reoxygenation. Consistent with this interpretation, not only a constitutive elevation of Nrf2 protein (Fig. 5*B*) but also an increased accumulation of *prx1* mRNA and protein (Fig. 5*C*) was found in Keap1 −/− MEF cells.

Discussion

Although hypoxia is generally accepted as an important microenvironmental factor in influencing tumor progression and treatment response, it is usually regarded as a static global phenomenon. Consequently, much less attention is given to the

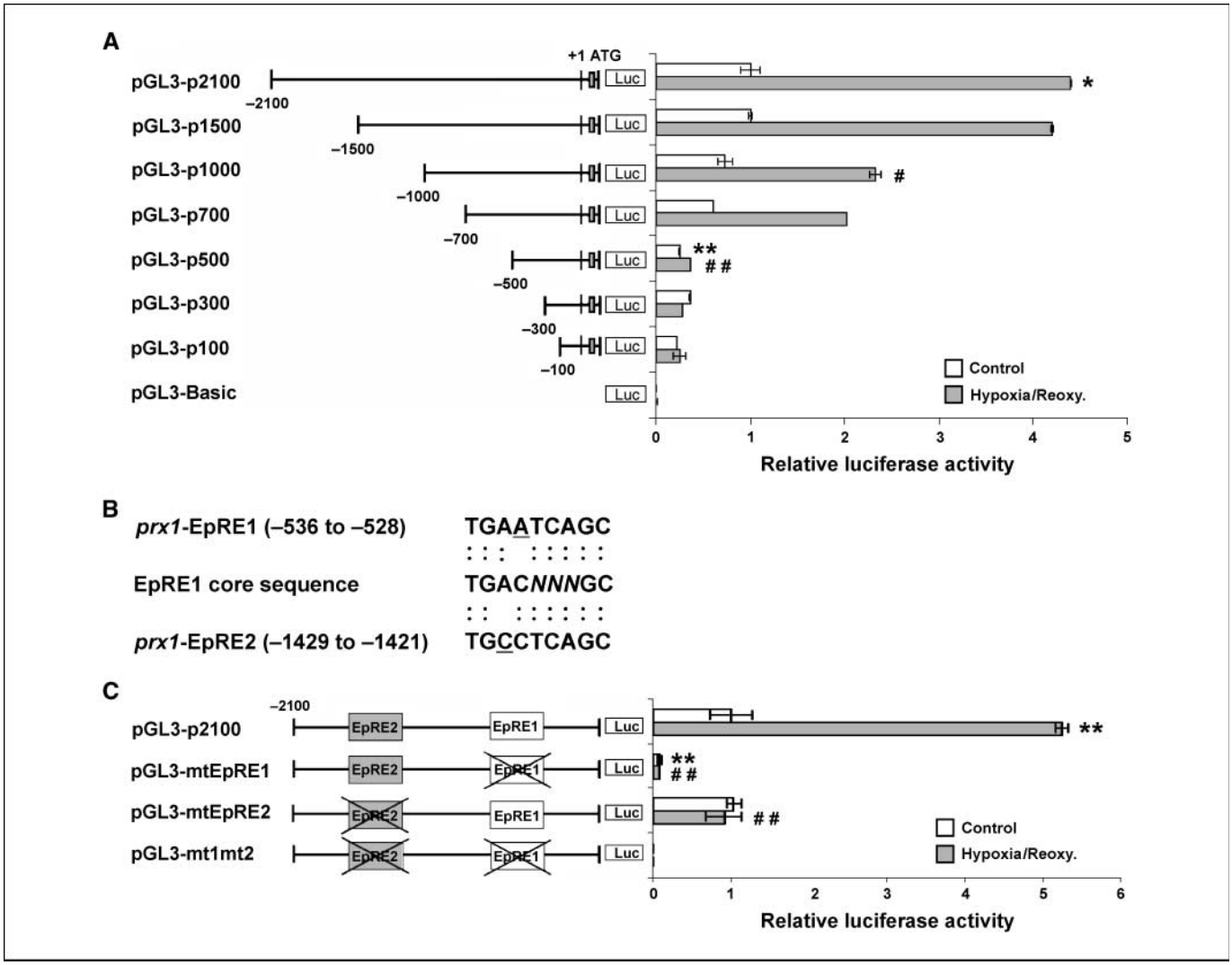

Figure 2. Analysis of hypoxia/reoxygenation–responsive *prx1* promoter activities. *A,* A549 cells were transfected with a series of *prx1* promoter reporter vectors. The pRLTK vector containing the *Renilla* luciferase gene was cotransfected to normalize the transfection efficiency. Twenty-four hours after transfection, cells were exposed to hypoxia for 4 h, followed by reoxygenation for 6 h. The data are presented as the ratio of the normalized luciferase activities. The numbers on the promoter vectors represent the positions starting from the transcription initiation site of the human *prx1* gene (+1). *, $P < 0.05$; **, $P < 0.01$, compared with control pGL3-2100 value. #, $P < 0.05$; ##, $P < 0.01$, compared with pGL3-2100 reporter activity after hypoxia/reoxygenation. *B,* EpRE1 and EpRE2 sequences present in the human *prx1* promoter were compared with the conventional EpRE core sequences. The nucleotide sequence of EpRE1 or EpRE2 that differs from the core sequence is underlined. *C,* the pGL3-mtEpRE1, pGL3-mtEpRE2, and the double mutant, pGL3-mt1mt2, were transfected into A549 cells together with the pRLTK normalizing vector. Relative luciferase activities were analyzed as described in *A*. **, $P < 0.01$, compared with control pGL3-2100 value. ##, $P < 0.01$, compared with pGL3-2100 reporter activity after hypoxia/reoxygenation.

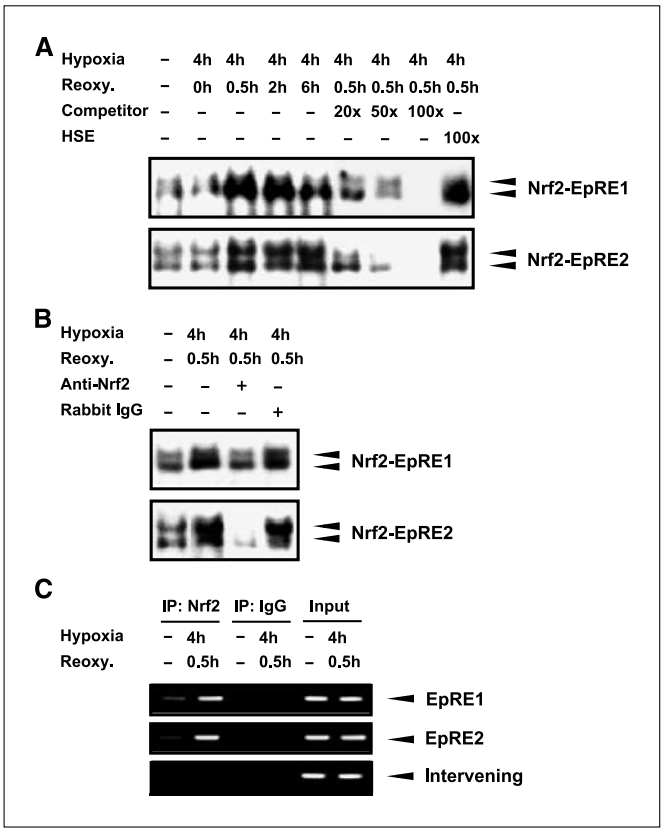

Figure 3. Binding of Nrf2 to EpRE1 and EpRE2 in response to hypoxia/reoxygenation. *A,* nuclear extracts were prepared from A549 cells immediately after 4 h of hypoxia (0 h) or 0.5, 2, or 6 h during reoxygenation. The electrophoretic mobility shift assay was done using radiolabeled EpRE1- or EpRE2-containing oligonucleotides. Unlabeled EpRE1 or EpRE2 was used as a specific competitor. Unlabeled heat shock responsive element (HSE) was used as a nonspecific competitor. Representative results from three independent experiments. *B,* nuclear extracts from cells treated with 4 h hypoxia/0.5 h reoxygenation were incubated with an anti-Nrf2 antibody. The specificity of Nrf2 binding to EpRE1 or EpRE2 was confirmed by using an antirabbit immunoglobulin G as a negative control. Representative results from three independent experiments. *C,* A549 cells treated with 4 h hypoxia/0.5 h reoxygenation were processed for ChIP assays using the primer pairs described in Materials and Methods. Input shows results obtained from DNA that was PCR amplified from chromatin extracts before immunoprecipitation. Rabbit immunoglobulin G lanes show PCR results obtained after immunoprecipitation with rabbit immunoglobulin G. Gels are representative of three independent experiments.

impact of the dynamic changes of tumor oxygenation in regulating the behavior of cancer cells. Our results showed that human *prx1* is up-regulated by hypoxia/reoxygenation, an *in vitro* condition that is suited to mimic the hypoxic and unstable oxygenation milieu of a tumor. We concluded that Nrf2 is one of the key transcription factors for *prx1* gene expression. Increased nuclear localization and transactivation of Nrf2 by hypoxia/reoxygenation was accompanied by a reduced level of Keap1 protein. Promoter cloning and characterization revealed two EpRE sites located at −536 to −528 (EpRE1) and −1,429 to −1,421 (EpRE2) as the Nrf2-binding sites responsible for both steady-state and hypoxia/reoxygenation–responsive regulation of *prx1* expression.

Based on the above information, we propose that the elevated expression of Prx1 observed in various cancers (13–18) may be explained in part by the activation of Nrf2 in response to the hypoxic and unstable oxygenation microenvironment of a tumor. The subpopulation of cells with elevated Prx1 may thus acquire an aggressive survival advantage that contributes to the malignant progression of cancer. Considering that Nrf2 is a major transcription factor responsible for the activation of EpRE-mediated drug–metabolizing/detoxifying genes (41), the impact of Nrf2 stimulation may also extend to the emergence of treatment-resistant cancers. Studies have suggested that the association of Nrf2 with Keap1 in response to electrophiles promotes Nrf2 degradation and prevents it from translocating to the nucleus (42, 43). However, a number of EpRE-dependent genes, including *prx1*, are constitutively expressed by Nrf2. This implies the existence of activated Nrf2 in the nucleus; the assumption is consistent with our immunocytochemistry results showing the nuclear expression of Nrf2 in control cells. How nuclear Nrf2 escapes Keap1 repression and activates the steady-state expression of its target genes is still an unresolved question. The precise mechanism by which Keap1 sequesters Nrf2 in the cytoplasm without causing its degradation is another question that begs for an answer. Given the short half-life of Nrf2, the purpose of its sequestration is also puzzling. An alternative role of Keap1 might be as a negative feedback regulator in returning Nrf2, and thereby the expression of Nrf2 target genes, to steady-state level after its activation (44). Such an event would have entailed the repression of Nrf2 by Keap1 only after Nrf2 exerts its transcriptional activity in the nucleus.

Phosphorylation of Nrf2 by various kinases has been implicated in its stabilization and nuclear localization and transactivation (38, 45–47). For example, phosphorylation at Ser^{40} by PKC (46) may disrupt Nrf2-Keap1 interaction and Nrf2 degradation in response to hypoxia/reoxygenation. The phosphoinositide-3-kinase pathway has also been proposed to regulate Nrf2 through actin rearrangement in response to oxidative stress (38). Various mitogen-activated protein kinases may regulate Nrf2 either positively or negatively depending on the signaling context of a particular EpRE-containing gene (45). It seems that Nrf2 transactivation is dependent on a number of regulatory mechanisms acting in concert to increase or decrease the Nrf2 protein level and to promote or suppress its stabilization and accumulation in the nucleus. However, the exact target sites of phosphorylation and the underlying mechanisms regulating Nrf2 stability and function have yet to be delineated. Additionally, the interaction of Nrf2 with other nuclear factors or components of the general transcriptional machinery may also influence Nrf2 activity (48). These may explain the variable levels of Prx1 expression observed in cancer cells and tissues.

Keap1 binds to the Neh2 domain of Nrf2 through the double glycine repeat and the COOH-terminal region to assert its repressive activity on Nrf2 (39, 49). Recent studies suggest a possible role of genetic abnormalities in Keap1 in eliminating or reducing its association with Nrf2 as a way of increasing Nrf2 activity in lung cancer cells (49, 50). Padmanabhan et al. (49) found the occurrence of glycine to cysteine mutations in the double glycine repeat domain of Keap1 in one lung cancer tissue (G430C, G/G to T/G) and in two lung cancer cell lines (G364C, G/G to TT). These mutations were found to alter the local conformation of Keap1 in the DC domain (double glycine repeat and COOH-terminal region) and to result in a reduced affinity of Keap1 to Nrf2. Because the mutations in Keap1 lead to a reduction, but not a complete abolishment, of its interaction with Nrf2, it is possible that the structural defects of Keap1 may augment the functionality of Nrf2 and give rise to a higher expression of *prx1* in response to an unstable oxygenation condition. Singh et al. (50) did a systematic analysis of the Keap1 genomic locus and sequencing of

Keap1 gene in 12 lung cancer cell lines and 54 tumor tissues. They showed that a mutation or an inactivation of Keap1 is a frequent event in lung cancer. Various mutations in Keap1 gene were found in 6 cell lines and 10 tumor tissues. Loss of heterozygosity was detected in the genomic locus of Keap1 (19q13.2) in 61% of the cell lines and 41% of the tumor samples that were examined. These findings led to a suggestion that the loss of function in Keap1 leads to a constitutive activation of Nrf2 in lung cancer.

These recent findings are consistent with our results in Keap1 −/− MEF cells in which we found not only an elevation of Nrf2 activity, but also an increased accumulation of *prx1* mRNA and protein. It is noteworthy, however, that not all cancer cell lines or tissues exhibit the genetic abnormalities in Keap1. Singh et al. (50) indeed noted an elevated Nrf2 activity in a number of tumor samples that contain a wild-type Keap1 gene, clearly suggesting that there are other mechanisms operating in these tissues. Our results offer a possible explanation that the decrease of Keap1 in an unstable oxygenation milieu of a tumor could serve as an important mechanism for the increased activation of Nrf2 in cells that contain a wild-type or a mutated but functional Keap1. The A549 cell line was found to possess a G-T transversion in the fourth exon of Keap1. This particular mutation, however, does not seem to affect the function of Keap1 in suppressing Nrf2 activation. Our results show that Keap1 suppresses an activation of Nrf2 in A549 cells as effectively as in other cell lines that were examined. Decrease of Keap1 by hypoxia/reoxygenation consistently released Nrf2 from Keap1 and enhanced a nuclear localization and activation of Nrf2 in several cell models including A549 (Figs. 4 and 5). The functional significance of various Keap1 mutations found in lung cancer cell lines and tissues warrants future investigation.

Hypoxia has been proposed to function as a microenvironmental pressure to select for a subset of cancer cells with an increased ability to survive and proliferate. The activation of Nrf2 and the up-regulation of *prx1* expression by changes of oxygenation are likely to contribute to the malignant progression of cancer and to modify the efficacy of chemo- and radiotherapies. The information provided in the current study suggests that the Nrf2-Prx1 axis may serve as a fruitful target for cancer prognosis and therapy. Identifying the key regulatory components and understanding the molecular basis of *prx1* gene regulation by Nrf2 are critical to the

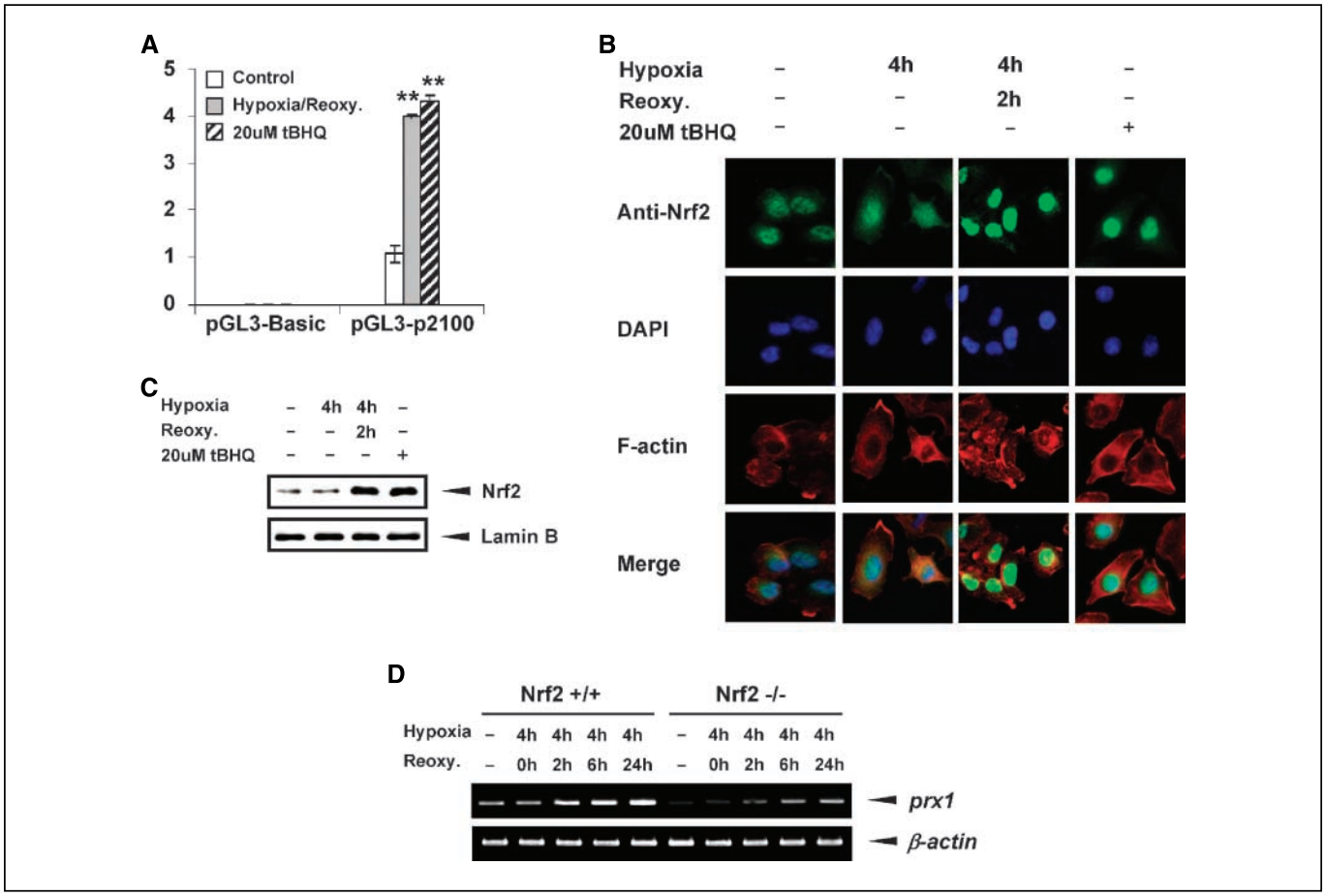

Figure 4. Stabilization of Nrf2 in the nucleus by hypoxia/reoxygenation. *A,* pGL3-p2100 was transfected into A549 cells together with pRLTK. Twenty-four hours after transfection, cells were treated with 4 h hypoxia/6 h reoxygenation or 20 μM tBHQ for 3 h. Luciferase activities were analyzed in cell extracts. **, $P < 0.01$, compared with control pGL3-2100 value. *B,* A549 cells were treated with 4 h hypoxia/2 h reoxygenation or 20 μM tBHQ for 3 h. Immunocytochemistry was done using an anti-Nrf2 antibody and FITC-conjugated secondary antibody. The location of the nuclei was visualized using 4′,6-diamidino-2-phenylindole (blue) counterstaining. Filamentous actin was stained with rhodamine-conjugated phalloidin for cytoplasmic counterstaining. The 4′,6-diamidino-2-phenylindole and filamentous actin images of the same field are shown separately or merged with the Nrf2 immunofluorescence images. *C,* equal amounts of nuclear protein (10 μg) from cells treated as described in *B* were subjected to Western blot analysis using an anti-Nrf2 antibody. Analysis of lamin B expression was done as a loading control for nuclear fraction. Representative results from three independent experiments are shown. *D,* Nrf2 +/+ and Nrf2 −/− MEF cells were exposed to 4 h of hypoxia, followed by 0, 2, 6, or 24 h of reoxygenation. Total RNA was isolated, and reverse transcription-PCR analysis was done by using primer pairs specific for the mouse *prx1* gene. *β-actin* gene was analyzed as a control. Representative results from three independent experiments are shown.

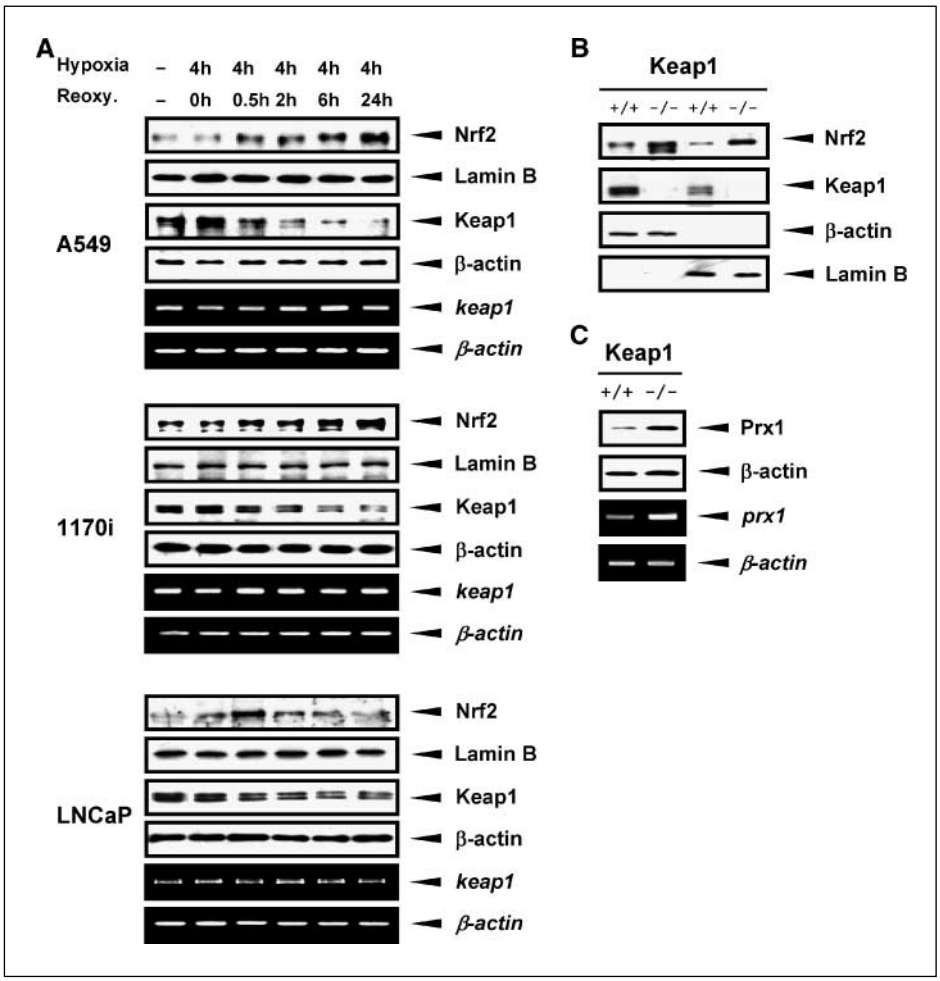

Figure 5. Reduction of Keap1 protein in response to hypoxia/reoxygenation. *A,* A549, 1170i, and LNCaP cells were exposed to 4 h of hypoxia and reoxygenated for 0, 0.5, 2, 6, or 24 h. Nuclear and cytosolic protein extracts were prepared from each cell line and subjected to Western blot analysis with an anti-Nrf2 and an anti-Keap1 antibody, respectively. Lamin B is a loading control for nuclear fraction, and β-actin is a loading control for cytosolic fraction. Total RNA was isolated from and reverse transcription-PCR was done using the primer pairs specific for the human *keap1* mRNA. *β-actin* gene was analyzed as a control. *B,* equal amounts of cytoplasmic and nuclear protein from Keap1 +/+ and Keap1 −/− MEF cells were subjected to Western blot analysis using an anti-Nrf2 or anti-Keap1 antibody. Western blots of β-actin and lamin B were carried out as the loading control for cytoplasmic and nuclear protein, respectively. *C,* total protein extract from Keap1 +/+ or −/− cells was subjected to Western blot using an antibody specific to Prx1. β-actin was used as a loading control. Total RNA from Keap1 +/+ or −/− cells were subjected to reverse transcription-PCR analysis using primer pairs specific to the mouse *prx1*. Mouse *β-actin* gene was analyzed as a control.

development of intervention strategies. Future research will be aimed at finding out whether Nrf2-Prx1 activation can be suppressed by genetic and/or pharmacologic approaches, and whether suppressing the Nrf2-Prx1 axis will inhibit the malignant progression or reverse treatment resistance in preclinical models. It would be important to investigate whether the Nrf2-Prx1 axis is dysregulated in lung cancer and other malignancies, and whether it correlates with a poor clinical outcome.

Acknowledgments

Received 6/30/2006; revised 10/31/2006; accepted 11/14/2006.

Grant support: NIH grants CA109480, CA111846, Department of Defense grant PC050127, and Cancer Center Support grant CA16056.

The costs of publication of this article were defrayed in part by the payment of page charges. This article must therefore be hereby marked *advertisement* in accordance with 18 U.S.C. Section 1734 solely to indicate this fact.

We are grateful to Dr. Masayuki Yamamoto (Center for Tsukuba Advanced Research Alliance, University of Tsukuba, Japan) for kindly providing the wild-type and knock-out Nrf2 and Keap1 MEF cells.

References

1. Rhee SG, Kang SW, Chang TS, Jeong W, Kim K. Peroxiredoxin, a novel family of peroxidases. IUBMB Life 2001;52:35–41.
2. Wood ZA, Schroder E, Robin Harris J, Poole LB. Structure, mechanism and regulation of peroxiredoxins. Trends Biochem Sci 2003;28:32–40.
3. Rabilloud T, Heller M, Gasnier F, et al. Proteomics analysis of cellular response to oxidative stress. Evidence for *in vivo* overoxidation of peroxiredoxins at their active site. J Biol Chem 2002;277:19396–401.
4. Jang HH, Lee KO, Chi YH, et al. Two enzymes in one; two yeast peroxiredoxins display oxidative stress-dependent switching from a peroxidase to a molecular chaperone function. Cell 2004;117:625–35.
5. Moon JC, Hah YS, Kim WY, et al. Oxidative stress-dependent structural and functional switching of a human 2-Cys peroxiredoxin isotype II that enhances HeLa cell resistance to H_2O_2-induced cell death. J Biol Chem 2005;280:28775–84.
6. Ishii T, Yamada M, Sato H, et al. Cloning and characterization of a 23-kDa stress-induced mouse peritoneal macrophage protein. J Biol Chem 1993;268:18633–6.
7. Kawai S, Takeshita S, Okazaki M, Kikuno R, Kudo A, Amann E. Cloning and characterization of OSF-3, a new member of the MER5 family, expressed in mouse osteoblastic cells. J Biochem (Tokyo) 1994;115:641–3.
8. Shau H, Kim A. Identification of natural killer enhancing factor as a major antioxidant in human red blood cells. Biochem Biophys Res Commun 1994;199:83–8.
9. Neumann CA, Krause DS, Carman CV, et al. Essential role for the peroxiredoxin Prdx1 in erythrocyte antioxidant defence and tumour suppression. Nature 2003;424:561–5.
10. Wen ST, Van Etten RA. The PAG gene product, a stress-induced protein with antioxidant properties, is an Abl SH3-binding protein and a physiological inhibitor of c-Abl tyrosine kinase activity. Genes Dev 1997;11:2456–67.
11. Mu ZM, Yin XY, Prochownik EV. Pag, a putative tumor suppressor, interacts with the Myc Box II domain of c-Myc and selectively alters its biological function and target gene expression. J Biol Chem 2002;277:43175–84.
12. Jung H, Kim T, Chae HZ, Kim KT, Ha H. Regulation of macrophage migration inhibitory factor and thiol-specific antioxidant protein PAG by direct interaction. J Biol Chem 2001;276:15504–10.
13. Yanagawa T, Ishikawa T, Ishii T, et al. Peroxiredoxin I expression in human thyroid tumors. Cancer Lett 1999;145:127–32.
14. Yanagawa T, Iwasa S, Ishii T, et al. Peroxiredoxin I expression in oral cancer: a potential new tumor marker. Cancer Lett 2000;156:27–35.
15. Noh DY, Ahn SJ, Lee RA, Kim SW, Park IA, Chae HZ.

Overexpression of peroxiredoxin in human breast cancer. Anticancer Res 2001;21:2085–90.
16. Chang JW, Jeon HB, Lee JH, et al. Augmented expression of peroxiredoxin I in lung cancer. Biochem Biophys Res Commun 2001;289:507–12.
17. Lehtonen ST, Svensk AM, Soini Y, et al. Peroxiredoxins, a novel protein family in lung cancer. Int J Cancer 2004;111:514–21.
18. Chang JW, Lee SH, Jeong JY, et al. Peroxiredoxin-I is an autoimmunogenic tumor antigen in non-small cell lung cancer. FEBS Lett 2005;579:2873–7.
19. Kim YJ, Lee WS, Ip C, Chae HZ, Park EM, Park YM. Prx1 suppresses radiation-induced c-*Jun* NH_2-terminal kinase signaling in lung cancer cells through interaction with the glutathione *S*-transferase Pi/c-*Jun* NH_2-terminal kinase complex. Cancer Res 2006;66:7136–42.
20. Chen MF, Keng PC, Shau H, et al. Inhibition of lung tumor growth and augmentation of radiosensitivity by decreasing peroxiredoxin I expression. Int J Radiat Oncol Biol Phys 2006;64:581–91.
21. Harris AL. Hypoxia—a key regulatory factor in tumour growth. Nat Rev Cancer 2002;2:38–47.
22. Greco O, Marples B, Joiner MC, Scott SD. How to overcome (and exploit) tumor hypoxia for targeted gene therapy. J Cell Physiol 2003;197:312–25.
23. Zander R, Vaupel P. Proposal for using a standardized terminology on oxygen transport to tissue. Adv Exp Med Biol 1985;191:965–70.
24. Vaupel P, Kallinowski F, Okunieff P. Blood flow, oxygen and nutrient supply, and metabolic microenvironment of human tumors: a review. Cancer Res 1989; 49:6449–65.
25. Brown JM. Evidence for acutely hypoxic cells in mouse tumours, and a possible mechanism of reoxygenation. Br J Radiol 1979;52:650–6.
26. Kimura H, Braun RD, Ong ET, et al. Fluctuations in red cell flux in tumor microvessels can lead to transient hypoxia and reoxygenation in tumor parenchyma. Cancer Res 1996;56:5522–8.
27. Brown JM, Giaccia AJ. The unique physiology of solid tumors: opportunities (and problems) for cancer therapy. Cancer Res 1998;58:1408–16.
28. Dewhirst MW. Concepts of oxygen transport at the microcirculatory level. Semin Radiat Oncol 1998;8:143–50.
29. Klein-Szanto AJ, Iizasa T, Momiki S, et al. A tobacco-specific *N*-nitrosamine or cigarette smoke condensate causes neoplastic transformation of xenotransplanted human bronchial epithelial cells. Proc Natl Acad Sci U S A 1992;89:6693–7.
30. Wakabayashi N, Dinkova-Kostova AT, Holtzclaw WD, et al. Protection against electrophile and oxidant stress by induction of the phase 2 response: fate of cysteines of the Keap1 sensor modified by inducers. Proc Natl Acad Sci U S A 2004;101:2040–5.
31. Park SY, Kim YJ, Gao AC, et al. Hypoxia increases androgen receptor activity in prostate cancer cells. Cancer Res 2006;66:5121–9.
32. Lowry OH, Rosebrough NJ, Farr AL, Randall RJ. Protein measurement with the Folin phenol reagent. J Biol Chem 1951;193:265–75.
33. Jeanmougin F, Thompson JD, Gouy M, Higgins DG, Gibson TJ. Multiple sequence alignment with Clustal X. Trends Biochem Sci 1998;23:403–5.
34. Bailey TL, Elkan C. Fitting a mixture model by expectation maximization to discover motifs in biopolymers. Proc Int Conf Intell Syst Mol Biol 1994;2:28–36.
35. Berezikov E, Guryev V, Plasterk RH, Cuppen E. CONREAL: conserved regulatory elements anchored alignment algorithm for identification of transcription factor binding sites by phylogenetic footprinting. Genome Res 2004;14:170–8.
36. Nguyen T, Sherratt PJ, Pickett CB. Regulatory mechanisms controlling gene expression mediated by the antioxidant response element. Annu Rev Pharmacol Toxicol 2003;43:233–60.
37. Ishii T, Itoh K, Takahashi S, et al. Transcription factor Nrf2 coordinately regulates a group of oxidative stress-inducible genes in macrophages. J Biol Chem 2000;275: 16023–9.
38. Kang KW, Lee SJ, Park JW, Kim SG. Phosphatidylinositol 3-kinase regulates nuclear translocation of NF-E2-related factor 2 through actin rearrangement in response to oxidative stress. Mol Pharmacol 2002;62: 1001–10.
39. Itoh K, Wakabayashi N, Katoh Y, et al. Keap1 represses nuclear activation of antioxidant responsive elements by Nrf2 through binding to the amino-terminal Neh2 domain. Genes Dev 1999;13:76–86.
40. Kwak MK, Itoh K, Yamamoto M, Kensler TW. Enhanced expression of the transcription factor Nrf2 by cancer chemopreventive agents: role of antioxidant response element-like sequences in the nrf2 promoter. Mol Cell Biol 2002;22:2883–92.
41. Rushmore TH, Kong AN. Pharmacogenomics, regulation and signaling pathways of phase I and II drug metabolizing enzymes. Curr Drug Metab 2002;3:481–90.
42. Velichkova M, Hasson T. Keap1 regulates the oxidation-sensitive shuttling of Nrf2 into and out of the nucleus via a Crm1-dependent nuclear export mechanism. Mol Cell Biol 2005;25:4501–13.
43. Zhang DD, Hannink M. Distinct cysteine residues in Keap1 are required for Keap1-dependent ubiquitination of Nrf2 and for stabilization of Nrf2 by chemopreventive agents and oxidative stress. Mol Cell Biol 2003; 23:8137–51.
44. Nguyen T, Sherratt PJ, Nioi P, Yang CS, Pickett CB. Nrf2 controls constitutive and inducible expression of ARE-driven genes through a dynamic pathway involving nucleocytoplasmic shuttling by Keap1. J Biol Chem 2005; 280:32485–92.
45. Kong AN, Owuor E, Yu R, et al. Induction of xenobiotic enzymes by the MAP kinase pathway and the antioxidant or electrophile response element (ARE/EpRE). Drug Metab Rev 2001;33:255–71.
46. Huang HC, Nguyen T, Pickett CB. Phosphorylation of Nrf2 at Ser-40 by protein kinase C regulates antioxidant response element-mediated transcription. J Biol Chem 2002;277:42769–74.
47. Numazawa S, Ishikawa M, Yoshida A, Tanaka S, Yoshida T. Atypical protein kinase C mediates activation of NF-E2–related factor 2 in response to oxidative stress. Am J Physiol Cell Physiol 2003;285:C334–42.
48. Nguyen T, Yang CS, Pickett CB. The pathways and molecular mechanisms regulating Nrf2 activation in response to chemical stress. Free Radic Biol Med 2004; 37:433–41.
49. Padmanabhan B, Tong KI, Ohta T, et al. Structural basis for defects of Keap1 activity provoked by its point mutations in lung cancer. Mol Cell 2006;21:689–700.
50. Singh A, Misra V, Thimmulappa RK, et al. Dysfunctional Keap1–2 interaction in non-small-cell lung cancer. PLoS Med 2006;3:1–12.

Review Article

Targeting the Nrf2-Prx1 Pathway with Selenium to Enhance the Efficacy and Selectivity of Cancer Therapy

Yun-Jeong Kim, Sun-Hee Baek, Paul N. Bogner, Clement Ip, Youcef M. Rustum, Marwan G. Fakih, Nithya Ramnath, and Young-Mee Park[1]

Departments of Cell Stress Biology [Y.-J. Kim, S.-H. Baek, Y.-M. Park], Pathology [P. N. Bogner], Cancer Chemoprevention [C. Ip], Pharmacology [Y. M. Rustum], and Medicine [M. G. Fakih, N. Ramnath], Roswell Park Cancer Institute, Buffalo, NY, USA

Peroxiredoxin 1 (Prx1) is frequently elevated in human cancer. Although the cell survival enhancing function of Prx1 has traditionally been attributed to its antioxidant activity, the growth promoting role of Prx1 independent of its antioxidant activity is increasingly gaining attention. Prx1 interacts with and modulates the activities of growth regulatory proteins in a fashion favoring cell survival. The human *prx1* promoter was recently cloned and characterized. It was found that hypoxia/reoxygenation, an *in vitro* condition mimicking unstable oxygenation of a tumor, up-regulates *prx1* through the activation of NF-E2-related factor 2, also known as Nrf2. Studies have shown that a Nrf2 suppressor Keap1 is often mutated in cancer cells resulting in a constitutive activation of Nrf2. These findings suggest that both genetic and microenvironmental abnormalities can contribute to the aberrant elevation of *prx1* in a subset of cancer cells, conferring on them an aggressive survival phenotype. Consistent with this hypothesis, elevated expression of Prx1 has been shown to predict disease recurrence and poor clinical outcome, indicating that the Nrf2-Prx1 pathway may prove to be a fruitful new target to inhibit malignant progression and/or reduce treatment resistance. Recent studies suggest that selenium is a highly effective modulator of various therapeutic agents, and that the anti-cancer activity of selenium may in part be mediated by suppressing the Nrf2-Prx1 pathway of a tumor. Our current research focus aims at investigating how selenium modulation of the Nrf2-Prx1 pathway may enhance the efficacy and selectivity of cancer therapy in both preclinical and clinical settings.

Journal of Cancer Molecules 3(2): 37-43, 2007.

Keywords:

Nrf2

Prx1

selenium

hypoxia

tumor microenvironment

Background

Peroxiredoxin 1 in cancer

Peroxiredoxins (Prx[2]) are thiol-specific antioxidant proteins. They are found in mammals, yeast and bacteria, and are classified largely on the basis of having either one (1-Cys) or two (2-Cys) conserved cysteine residues [1]. Prx1, a major 2-Cys Prx family member, has been found to be elevated in various human cancers [2-7]. Prx1 contains a cysteine at the catalytic site (Cys-52), and detoxifies peroxides at the expense of Cys-52 oxidation through inter-molecular disulfide formation with the other conserved Cys-173 residue. The disulfide bond is reduced back to the active thiol form, Cys-SH, by the action of the thioredoxin system. Despite the initial biochemical characterization of Prx1 as a peroxide-detoxifying enzyme, the physiological significance of its peroxidase activity is unclear, since Prx1 is highly susceptible to inactivation by reactive oxygen species (Figure 1). Over-oxidation of the Cys-SH moiety to Cys-sulfinic ($-SO_2H$) or -sulfonic acid ($-SO_3H$) has been reported with Prx family members during peroxide detoxification [8,9]. When the catalytic Cys-52-SH of Prx1 is over-oxidized, the peroxidase activity is lost. Recent studies have suggested that over-oxidation of the active site Cys in itself may be physiologically significant, because it allows for a mechanism of structural and functional switching of the 2-Cys Prx from a peroxidase enzyme to a molecular chaperone under stress conditions [10,11]. The wide range of effects attributed to Prx1 [12-19] may in part be explained by the physical interaction of Prx1 with growth and survival regulatory proteins to modulate their activities. Kim *et al.* recently reported that Prx1 suppresses radiation-induced JNK signaling and apoptosis [20]. The peroxidase activity of Prx1, however, is not essential for inhibiting JNK activation. This effect is in part mediated through the association of Prx1 with the GSTpi-JNK complex, thereby preventing JNK release from the complex. The JNK inhibitory and anti-apoptotic activities of Prx1 suggest that cancer cells with high Prx1 levels are likely to be resistant not only to radiation, but also to anti-

Received 3/12/07; Revised 3/29/07; Accepted 3/30/07.

[1]**Correspondence:** Dr. Young-Mee Park, Department of Cell Stress Biology, Roswell Park Cancer Institute, Elm and Carlton Streets, Buffalo, NY 14263, USA. Phone: 1-716-8453190. Fax: 1-716-8458899. E-mail: young-mee.park@roswellpark.org

[2]**Abbreviations:** Prx, peroxiredoxin(s); Nrf2, NF-E2-related factor 2; EpRE/ARE, electrophile or antioxidant responsive element; tBHQ, *tert*-butylhydroquinone; Keap1, Kelch-like ECH-associated protein 1; Se-Met, seleno-L-methionine; MSC, 5-methylselenocysteine.

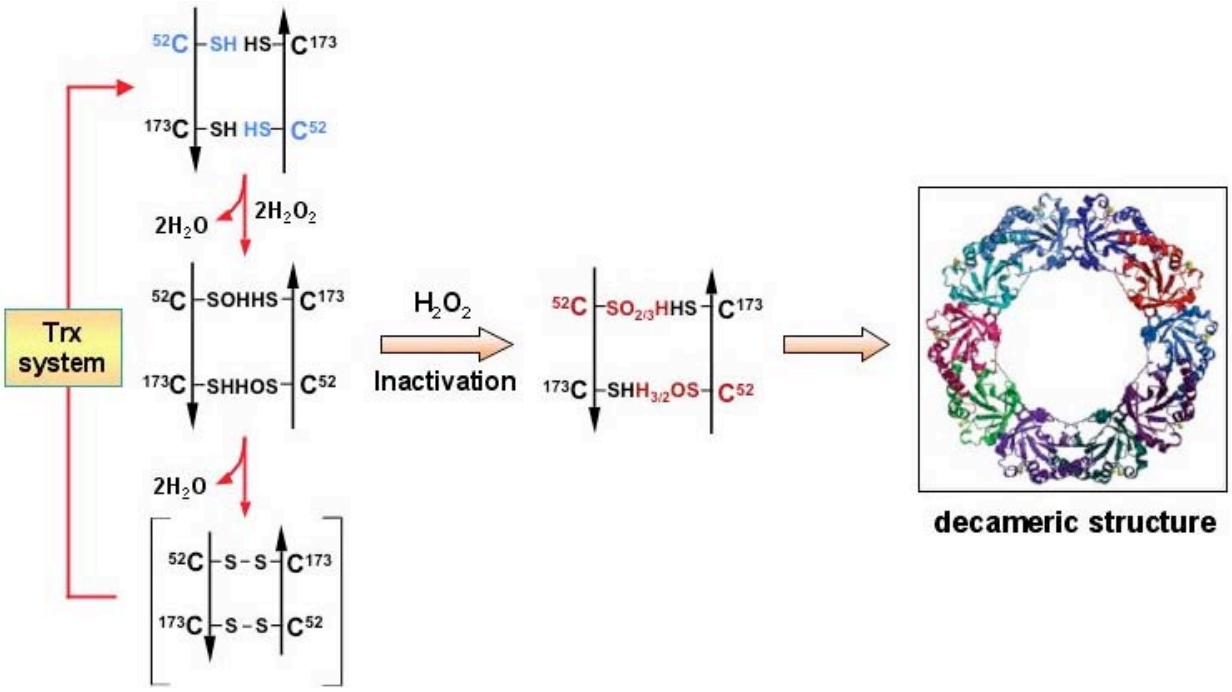

Figure 1: Structure and function of Prx1. The active site Cys-52 becomes oxidized to a sulfenic acid (-SOH) during the peroxide catalysis cycle. The Cys-52-SOH forms a transient inter-molecular disulfide bond with the Cys-173 of another Prx1 molecule and is reduced to Cys-52-SH by the thioredoxin system. Alternatively, the Cys-52-SOH may undergo over-oxidation to Cys-52-$SO_{2/3}$H under stress conditions. While the over-oxidation results in a loss of antioxidant activity, it may allow a mechanism for structural and functional switching of Prx1 from an antioxidant enzyme to a molecular chaperone which assumes a decameric structure (adapted from Parsonage *et al.* [71]).

cancer agents targeting JNK and related apoptotic pathways. Studies by Chen *et al.* [21] have demonstrated the role of Prx1 in radio-resistance using human cancer xenograft models. They observed significant growth inhibition, radio-sensitization, as well as reduced metastasis in lung cancer cells stably transfected with antisense Prx1. These studies suggest that Prx1, in addition to its usefulness as a potential diagnostic and/or prognostic marker, may also serve as a therapeutic target.

Nrf2 up-regulates human prx1 gene expression in hypoxic and unstable oxygenation conditions

Delineation of the molecular basis of *prx1* gene regulation is expected to provide valuable clues for the development of new intervention strategies. Hypoxia is one of the critical factors known to influence tumor progression and treatment response [22-24]. It has been hypothesized that a hypoxic tumor microenvironment may trigger trans-activation of the *prx1* gene *via* redox-sensitive transcription factors and signaling molecules [25]. Generally speaking, hypoxia is regarded as a static global phenomenon and is defined as an overall reduction in oxygen availability or partial pressure below critical levels [26]. Tissue oxygenation within a tumor, however, is highly unstable and heterogeneous as a consequence of architectural and functional abnormalities in the vascular network [27]. In ultra structural terms, tumor vasculature has numerous "holes" or "openings", widened inter-endothelial junctions, and a discontinuous or absent basement membrane [22,28]. Aberrant blood vessels can be shut down locally at any time; the same defects can cause a reversal of blood flow. In addition to re-opening of temporarily closed/blocked vessels, dynamic changes in hypoxia/reoxygenation may also occur as a result of regional angiogenesis. The resulting blood flow fluctuations in the tumor microvasculature can lead to perfusion-limited hypoxia in tumor parenchyma [29-32].

A recent study showed that a hypoxic and unstable oxygenation climate might be crucial for the abnormal elevation of Prx1 [25]. The *in vitro* condition of hypoxia/reoxygenation was used to mimic dynamic oxygenation changes present in the tumor microenvironment. This study demonstrated that unstable oxygenation conditions lead to increased trans-activation of NF-E2-related factor 2, also known as Nrf2, which in turn up-regulates *prx1* expression. The human *prx1* promoter was cloned and characterized to identify the enhancer elements critical to mediate this response. The *prx1* promoter was found to contain two specific binding sites for Nrf2; the electrophile or antioxidant responsive elements (EpRE/ARE) were located at the proximal (-536 to -528) and distal (-1429 to -1421) regions of the *prx1* promoter [25]. To test whether the *prx1* promoter is functional with other Nrf2 inducers, the activity of pGL3-2100 luciferase reporter plasmid containing the two EpRE regions of the *prx1* gene was examined in cells treated with *tert*-butylhydroquinone (tBHQ), one of the classical activators of Nrf2. It was shown that both unstable oxygenation conditions and tBHQ were capable of inducing nuclear translocalization of Nrf2, and thus the activation of the *prx1* promoter (Figure 2). The effect of unstable oxygenation conditions on *prx1* up-regulation appears to be relevant in several cancer cell models, including human lung cancer (A549 and 1170i), prostate cancer (LNCaP, PC3, and DU145), colon cancer (HCT116, HCT-8, and HT-29), and breast cancer (MCF7) cell lines (data not shown).

The potential significance of the Nrf2-Prx1 pathway to cancer progression and therapy

The information outlined above indicates that elevated expression of Prx1 in human cancer may in part be mediated by the activation of Nrf2 underlined by unstable oxygenation conditions. A sub-population of cells with elevated Prx1 may then acquire an aggressive survival advantage *via* vari-

Print ISSN 1816-0735; Online ISSN 1817-4256

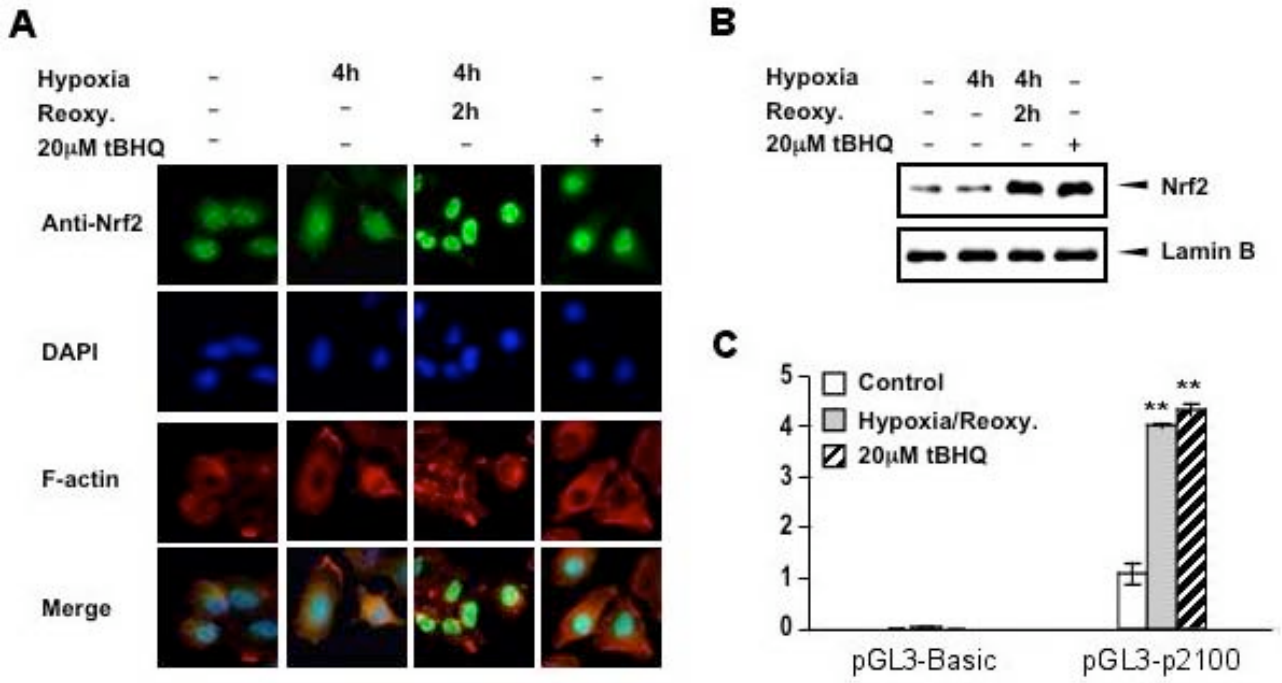

Figure 2: Activation of the human *prx1* promoter by Nrf2 in response to hypoxia/reoxygenation. (A) A549 cells were exposed to hypoxia or treated with 20 μM tBHQ. Nrf2 localization was examined by incubation with an anti-Nrf2 antibody; the location and integrity of the nucleus was probed by DAPI staining of the same cells. Overlaying the Nrf2 and DAPI images (cyan color) confirms the nuclear localization of Nrf2. F-actin was stained with rhodamine-conjugated phalloidin for cytoplasmic counter-staining. The DAPI and F-actin images of the same field are shown separately or merged with the Nrf2 fluorescence images. (B) Samples of nuclear protein were subjected to Western blot analysis using an anti-Nrf2 antibody. Lamin B was probed as a loading control for nuclear fraction. Representative results from three independent experiments are shown. (C) The 2.1-Kb human *prx1* promoter, pGL3-p2100, was transfected into A549 cells. Twenty-four hours after transfection, cells were exposed to hypoxia or 20 μM tBHQ, and luciferase activities were determined. $^{**}P < 0.01$, compared to the untreated pGL3-2100 value.

ous mechanisms influenced by Prx1. Nrf2 belongs to the "Cap'n'Collar" family of basic region-leucine zipper (bZip) transcription factors. The central role of Nrf2 in regulating EpRE-mediated expression of antioxidant proteins and drug metabolizing/detoxifying enzymes has been well documented [33-37]. The antioxidant proteins protect tissues from chemical and physical oxidative damage, while the detoxifying enzymes function to convert reactive electrophiles and xenobiotics to less toxic and more readily excretable products. Nrf2-null mice, for example, exhibit severe impairment in the basal expression or induction of several drug-metabolizing enzymes [38]. Accordingly, tissues of Nrf2-null mice are more susceptible to insult from xenobiotics [39-42]. The inducibility of Nrf2-mediated antioxidant gene expression is lost in Nrf2-deficient macrophages [43]. These studies suggest that Nrf2 is involved in the molecular mechanisms of cellular protection against oxidative stress and xenobiotic insult.

How is Nrf2 activation regulated? Previous work has suggested that in an un-stimulated condition, the association of Nrf2 with Kelch-like ECH-associated protein 1 (Keap1) promotes Nrf2 degradation and prevents it from translocating into the nucleus [44,45]. Many Nrf2 activators are capable of modifying the thiol (-SH) of cysteine, thus leading to the idea that the reactive Cys residues in Keap1 may function as a redox sensor [46]. As illustrated in Figure 3, the oxidation/modification of these reactive Cys residues in response to electrophile or oxidative stress may allow Nrf2 to dissociate from Keap1 [45-47]. A recent study by Eggler *et al.* [48], however, disagreed with this direct disruption model. Based on results from a combination of chemical, mass spectrometry, and isothermal titration calorimetry approaches, they suggested that the modification of Keap1 Cys residues was insufficient to disturb the interaction of Nrf2 and Keap1, and proposed that other mechanisms might be necessary to reduce the affinity of Keap1 for Nrf2. Phosphorylation of Nrf2 by various kinases has also been implicated in its liberation from Keap1, with subsequent nuclear localization and trans-activation function [49-52]. It appears that the regulation of EpRE-mediated Nrf2 trans-activation is subordinate to a number of control mechanisms acting in concert to increase Nrf2 protein level and promote its accumulation in the nucleus. Akt/protein kinase B (PKB) and MAPKs (mitogen-activated protein kinases) have been shown to regulate Nrf2 either positively or negatively depending on the specific signaling context of a given EpRE containing gene [49,50,53]. The molecular mechanisms regulating the Nrf2-Prx1 axis are not clearly defined at the present time.

Keap1, an Nrf2 suppressor, is frequently mutated in some cancer cells and tissues

Studies suggest that genetic abnormalities in Keap1 may be involved in eliminating or reducing its association with Nrf2, thus leading to constitutive activation of Nrf2 [54,55]. Glycine to cysteine mutations in the Nrf2-interacting domain of Keap1 have been observed in lung cancer tissues (G430C, G/G to T/G) and cell lines (G364C, G/G to T/T)[54]. These mutations were found to alter the local conformation of Keap1 and reduce the affinity of Keap1 for Nrf2. These findings may not be exclusive with those of Kim *et al.* [25] showing a down-regulation of Keap1 by hypoxia/reoxygenation. Considering that the mutations in Keap1 lead to a reduction, but not a complete abolishment, of its affinity for Nrf2, it is possible that the structural defects of Keap1 together with the decrease of Keap1 level may further facilitate the nuclear translocation of Nrf2 and give rise to higher expression of *prx1* in response to unstable oxygen-

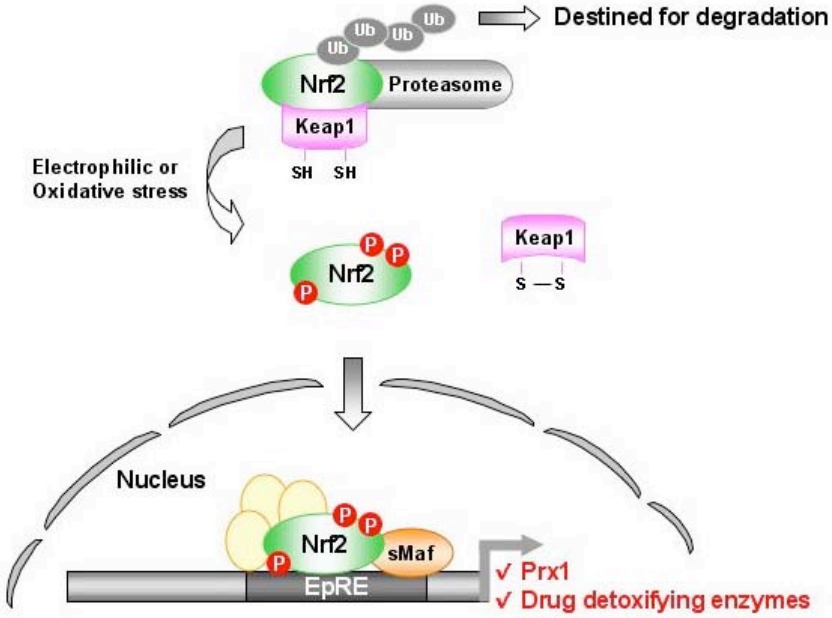

Figure 3: Proposed scheme of the signaling pathway for Nrf2 activation. Nrf2 sequestered by Keap1 is subject to ubiquitin-mediated degradation. Oxidative stress and electrophiles modify the cysteine residues of Keap1, resulting in the release of Nrf2. Nrf2 binds to EpRE and forms a transcription complex with small Maf and other nuclear factors to induce the expression of a group of EpRE-containing genes [72,73]. Phosphorylation of Nrf2 by various kinases has also been implicated in the liberation, stability, and trans-activation of Nrf2, although exact target sites and how phosphorylation regulates Nrf2 stability and activation are not fully understood.

ation conditions. Recently, Singh *et al.* [55] performed a systematic analysis of the Keap1 genomic locus with sequencing of the Keap1 gene in several lung cancer cell lines and 54 lung tumor tissues. They demonstrated that mutation or inactivation of Keap1 was a frequent event in lung cancer. Various mutations in the Keap1 gene were observed in several lung cancer cell lines and tumor tissues. Loss of heterozygosity was detected at the genomic locus of Keap1 (19q13.2) in 61% of the cell lines and 41% of the tumor samples that were examined. These observations led to the suggestion that loss of Keap function led to constitutive activation of Nrf2 in lung cancer. It is noteworthy, however, that not all cancer cell lines or tissues exhibit genetic abnormalities of Keap1. Elevated Nrf2 activity was found in a number of lung tumor samples that contained the wild type Keap1 gene [55], suggesting that there were other mechanisms for Nrf2 activation in these tissues. It is possible that the decrease of Keap1 in the unstable oxygenation milieu of a tumor could also serve to increase the activation of Nrf2 in cells that contain a wild type, or mutated but functional Keap1. This interpretation is consistent with recent findings showing that Keap1 decreases induced by hypoxia/reoxygenation consistently released Nrf2 from Keap1, and enhanced nuclear localization and activation of Nrf2 in several cell models [25]. Collectively, the above information points to both genetic and environmental factors as contributors to the aberrant elevation of Prx1 in cancer cells and tissues. Future investigation is warranted to evaluate the functional significance of various Keap1 mutations, and to examine whether genetic abnormalities of Keap1 exist in other human malignancies.

Clinical-translational advances

Prx1 is predictive of disease recurrence and poor clinical outcome

Park and co-workers investigated the significance of Prx1 and/or Nrf2 levels as prognostic factors in human cancer [56]. Lung cancer is the leading cause of cancer death, with the best chance of survival restricted to a subset of non-small cell lung cancer (NSCLC) patients able to undergo surgical resection. Unfortunately, however, the recurrence rate of NSCLC after surgery remains high even in early stage patients, with few useful prognostic indicators [57]. The majority of these relapses occur at distant sites away from the primary tumor. This is probably due to early and occult metastatic spread, undetected at the time of treatment and initial staging [57]. It is likely that within a tumor the ability of malignant cells to survive varies widely. Some of them may possess a more aggressive survival phenotype and progress to fatal disease, even when the disease is found at a clinically favorable stage. Immunohistochemical expression of Prx1 and Nrf2 was evaluated in paraffin embedded tissues from a total of 90 stage I lung cancer patients who underwent surgical resection. Elevations in both Prx1 and Nrf2 were detectable in nearly all cases, albeit at different levels. Univariate and multivariate analysis unequivocally demonstrated that a high level of Prx1 expression was significantly associated with disease recurrence and shorter overall survival. The study showed that the median recurrence-free survival (RFS) and overall survival (OS) for patients with a low level of Prx1 expression was significantly better than for those with a high level of Prx1. Recent therapeutic efforts in early stage lung cancer have focused on neoadjuvant and adjuvant chemotherapy to reduce the high rate of systemic recurrence. The findings in this study suggest that the Prx1 expression status may be of practical utility in selecting additional treatment options for early stage lung cancer patients receiving surgical treatment.

The Nrf2 expression status was not found to be predictive of clinical outcome in this series of patients. Although the likelihood of expressing a high level of Prx1 in tumors containing a high level of nuclear Nrf2 was 1.51 times greater than in tumors with a low level of nuclear Nrf2 in this study, the association between the expressions of Prx1 and Nrf2 did not reach statistical significance ($P > 0.05$)[56]. It is conceivable that in addition to Nrf2, other transcription factors may be involved in coordinating and relaying various cellular signals to turn on/off the transcriptional machinery of the *prx1* gene, as is true for other genes involved in cell growth and survival regulation. Although the Nrf2 expression status was not associated with RFS or OS in early stage lung cancer, a possible role for Nrf2 in advanced and inoperable NSCLC cannot be ruled out. One of the major factors contributing to the failure of chemotherapy is the development of drug resistance in cancer cells. Several studies have shown that the expression of genes involved in xenobiotic

Print ISSN 1816-0735; Online ISSN 1817-4256

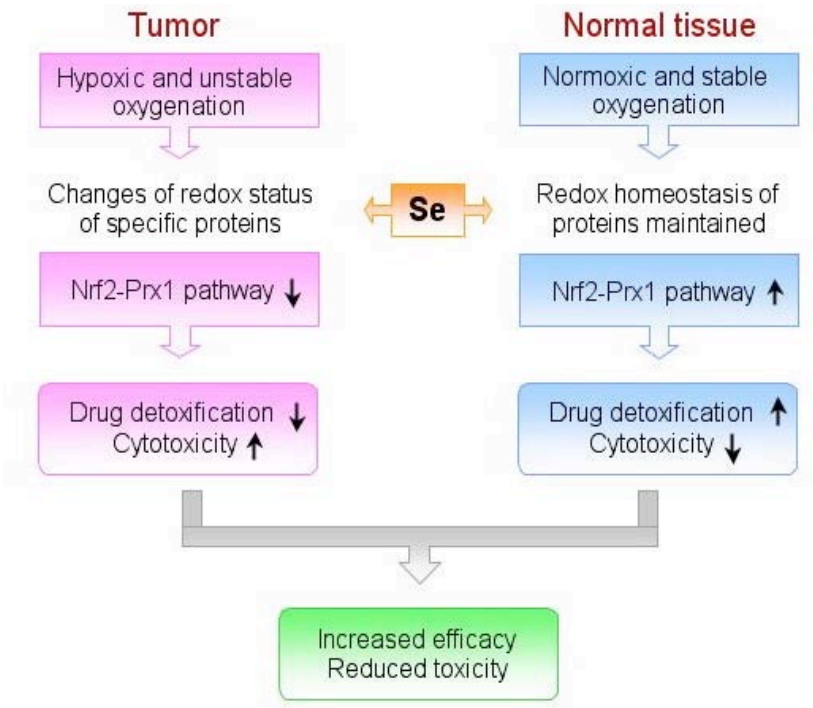

Figure 4: Effect of selenium on the Nrf2-Prx1 pathway in tumor *vs.* normal tissue. The hypoxic and unstable oxygenation milieu of a tumor makes redox-sensitive effector molecules of the Nrf2-Prx1 pathway vulnerable to modification by selenium, thus suppressing Nrf2 activation and Prx1 expression, and enhancing the therapeutic efficacy of anti-cancer agents. In contrast, the reactive Cys moieties of the redox-sensitive proteins are not susceptible to thiol modification by selenium in a normoxic condition. As a result, the Nrf2-Prx1 pathway may remain intact and protect normal tissues against treatment-related toxicity.

metabolism, oxidative stress defense, and drug efflux is increased in lung cancer [58-61]. Considering the role of Nrf2 in regulating a battery of genes that act to detoxify cancer drugs and/or attenuate drug-induced oxidative stress [33,34,37], it is possible that Nrf2 may play a role in increasing treatment resistance in advanced stage disease. Future investigation will be necessary to evaluate the potential of elevated Prx1 and/or Nrf2 levels in predicting response to chemo- and radio-therapy in advanced lung cancer and other malignancies.

Selective modulation of the therapeutic efficacy of anti-cancer agents by selenium

Selenium has been widely investigated as an anti-cancer agent, although most of the research was done under the setting of cancer prevention. Recent *in vivo* studies showed that selenium is a highly effective modulator of the therapeutic efficacy and selectivity of anti-cancer drugs [62]. The experimental design involved evaluating the cure rate of a number of human tumor xenografts in nude mice which were treated with selenium for 7 days before the first injection of irinotecan. The selenium compounds investigated in this study were seleno-L-methionine (Se-Met) and 5-methylselenocysteine (MSC). The concentration used for both selenium compounds was 200 μg/day. This dose of Se-Met or MSC was non-toxic and well-tolerated in mice. In mice given 200 μg of Se-Met or MSC daily for seven days, the steady-state plasma selenium concentration was > 10 μM. Irinotecan was given once a week for 4 weeks, and selenium treatment was continued during this 4-week period. Four different human tumor xenografts were examined: two head and neck squamous cell carcinomas (FaDu and A253) and two colon carcinomas (HCT-8 and HT-29). FaDu and HT-8 are sensitive to irinotecan, while A253 and HT-29 are resistant. Without the pre-treatment of selenium (either Se-Met or MSC), the cure rate was 30% and 20% for FaDu and HT-8 respectively, with the maximum tolerated dose (MTD) of irinotecan (100 mg/kg/week x 4). With selenium pre-treatment, complete cure rate (100%) was achieved for both xenografts. The same dose schedule of irinotecan was totally ineffective against A253 and HT-29. The administration of a high dose of irinotecan (300 mg/kg/week x 4) was required to reach 100% and 50% cure rate for A253 and HT-29 xenografts respectively, but only in the presence of selenium. The use of such a high dose of irinotecan was made possible due to the protection of normal tissues by selenium. Otherwise, this high dose of irinotecan alone would have caused 100% mortality. The selenium-mediated protection of the host against drug toxicity was also observed with 5-fluorouracil, oxaliplatin, cisplatin, paclitaxel and doxorubicin [63]. Thus the modulating effect of selenium appears not to be tumor specific or drug specific. That the maximal therapeutic gain is achieved when selenium is administered prior to drug treatment suggests the importance of selenium "pre-conditioning" in tumor sensitization and normal tissue protection.

Targeting the Nrf2-Prx1 pathway with selenium

These findings with selenium led us to investigate the effect of selenium treatment *per se* on the Nrf2-Prx1 pathway. Tumor-bearing mice were treated with selenium for 7 days as described previously [62]. The selenium compound used was Se-Met (200 μg/day) in view of the fact that this form of selenium was and is still being used in a number of human intervention trials. We found that selenium was capable of modulating Nrf2 activation differently in tumor *vs.* normal tissue in pre-clinical models. Our study showed that selenium suppressed Nrf2 activation and reduced the up-regulation of *prx1* in tumor tissues obtained from human lung cancer A549 and colon cancer HT-29 xenografts (unpublished). The effect of selenium on the Nrf2-Prx1 pathway appears to be quite significant in tumor tissue. Conversely, increased expression of Prx1 and several other Nrf2 target genes was observed in some normal tissues in the tumor-bearing mice. It warrants future investigation to test whether the effect observed is limited to a specific form of selenium compound.

How might selenium preferentially suppress the Nrf2-Prx1 pathway of a tumor? We proposed that the inherently hypoxic and unstable oxygenation milieu of a tumor might be one of the critical factors in this process. As proposed originally by Ip and coworkers, the metabolism of either

inorganic or organic selenium compounds to methylselenol (CH_3SeH) is an essential step for selenium to exert its anti-cancer effect [64-66]. In the whole animal (and in human), liver and kidney are the major organs for selenium metabolism. Methylselenolate is an avid protein redox modulator. At physiological pH, methylselenol is present as anionic methylselenolate (CH_3Se^-). Depending on the redox potential of the immediate microenvironment of individual proteins, methylselenolate appears to oxidize thiol groups to disulfides or reduce disulfides to thiol groups [67]. Previous studies describing the redox modification of protein kinase C and p53 by selenium and their resulting changes in activity are supportive of this concept [68-70]. Using a display thiol proteomics approach, it was demonstrated that monomethylated selenium causes global protein thiol/disulfide interchange which may lead to alterations of protein function [67]. It is tempting to speculate that selenium may suppress the Nrf2-Prx1 pathway directly by allowing the critical Cys residues of Keap1 to be protected from oxidation/modification in the unstable oxygenation climate of a tumor, thereby increasing the affinity of Keap1 for Nrf2 and promoting Nrf2 degradation (Figure 4). Selenium may also act indirectly by modifying the redox status of critical signaling molecules, and hence their activities, in favor of suppressing the Nrf2-Prx1 pathway. The reactive Cys moieties of these redox-sensitive signaling proteins may not be susceptible to modification by selenium under normoxic conditions. As a result, the Nrf2-Prx1 pathway may be activated and protect normal tissues against treatment-related toxicity in some normal tissues. Our *in vitro* and *in vivo* studies appear to support the notion that selenium suppresses the Nrf2-Prx1 axis effectively in tumor. Future research is focused on delineating/validating the molecular mechanisms of selenium action in modulating the Nrf2-Prx1 pathway in tumor *vs.* normal tissue, and developing ways to bring the new findings into clinical practice. At our institute, phase I and phase II clinical trials are underway to evaluate the potential of using selenium (Se-Met) in enhancing therapeutic efficacy and selectivity.

Acknowledgments

This work was supported by NIH grants CA109480, CA111846, DOD grant PC050127, and Cancer Center Support Grant CA16056.

References

1. Rhee SG, Kang SW, Chang TS, Jeong W, Kim K. Peroxiredoxin, a novel family of peroxidases. *IUBMB Life* 52: 35-41, 2001.
2. Yanagawa T, Ishikawa T, Ishii T, Tabuchi K, Iwasa S, Bannai S, Omura K, Suzuki H, Yoshida H. Peroxiredoxin I expression in human thyroid tumors. *Cancer Lett* 145: 127-132, 1999.
3. Yanagawa T, Iwasa S, Ishii T, Tabuchi K, Yusa H, Onizawa K, Omura K, Harada H, Suzuki H, Yoshida H. Peroxiredoxin I expression in oral cancer: a potential new tumor marker. *Cancer Lett* 156: 27-35, 2000.
4. Chang JW, Jeon HB, Lee JH, Yoo JS, Chun JS, Kim JH, Yoo YJ. Augmented expression of peroxiredoxin I in lung cancer. *Biochem Biophys Res Commun* 289: 507-512, 2001.
5. Noh DY, Ahn SJ, Lee RA, Kim SW, Park IA, Chae HZ. Overexpression of peroxiredoxin in human breast cancer. *Anticancer Res* 21: 2085-2090, 2001.
6. Lehtonen ST, Svensk AM, Soini Y, Paakko P, Hirvikoski P, Kang SW, Saily M, Kinnula VL. Peroxiredoxins, a novel protein family in lung cancer. *Int J Cancer* 111: 514-521, 2004.
7. Chang JW, Lee SH, Jeong JY, Chae HZ, Kim YC, Park ZY, Yoo YJ. Peroxiredoxin-I is an autoimmunogenic tumor antigen in non-small cell lung cancer. *FEBS Lett* 579: 2873-2877, 2005.
8. Rabilloud T, Heller M, Gasnier F, Luche S, Rey C, Aebersold R, Benahmed M, Louisot P, Lunardi J. Proteomics analysis of cellular response to oxidative stress. Evidence for in vivo overoxidation of peroxiredoxins at their active site. *J Biol Chem* 277: 19396-19401, 2002.
9. Yang KS, Kang SW, Woo HA, Hwang SC, Chae HZ, Kim K, Rhee SG. Inactivation of human peroxiredoxin I during catalysis as the result of the oxidation of the catalytic site cysteine to cysteine-sulfinic acid. *J Biol Chem* 277: 38029-38036, 2002.
10. Jang HH, Lee KO, Chi YH, Jung BG, Park SK, Park JH, Lee JR, Lee SS, Moon JC, Yun JW, Choi YO, Kim WY, Kang JS, Cheong GW, Yun DJ, Rhee SG, Cho MJ, Lee SY. Two enzymes in one; two yeast peroxiredoxins display oxidative stress-dependent switching from a peroxidase to a molecular chaperone function. *Cell* 117: 625-635, 2004.
11. Moon JC, Hah YS, Kim WY, Jung BG, Jang HH, Lee JR, Kim SY, Lee YM, Jeon MG, Kim CW, Cho MJ, Lee SY. Oxidative stress-dependent structural and functional switching of a human 2-Cys peroxiredoxin isotype II that enhances HeLa cell resistance to H_2O_2-induced cell death. *J Biol Chem* 280: 28775-28784, 2005.
12. Ishii T, Yamada M, Sato H, Matsue M, Taketani S, Nakayama K, Sugita Y, Bannai S. Cloning and characterization of a 23-kDa stress-induced mouse peritoneal macrophage protein. *J Biol Chem* 268: 18633-18636, 1993.
13. Prosperi MT, Ferbus D, Karczinski I, Goubin G. A human cDNA corresponding to a gene overexpressed during cell proliferation encodes a product sharing homology with amoebic and bacterial proteins. *J Biol Chem* 268: 11050-11056, 1993.
14. Kawai S, Takeshita S, Okazaki M, Kikuno R, Kudo A, Amann E. Cloning and characterization of OSF-3, a new member of the MER5 family, expressed in mouse osteoblastic cells. *J Biochem (Tokyo)* 115: 641-643, 1994.
15. Shau H, Kim A. Identification of natural killer enhancing factor as a major antioxidant in human red blood cells. *Biochem Biophys Res Commun* 199: 83-88, 1994.
16. Wen ST, Van Etten RA. The PAG gene product, a stress-induced protein with antioxidant properties, is an Abl SH3-binding protein and a physiological inhibitor of c-Abl tyrosine kinase activity. *Genes Dev* 11: 2456-2467, 1997.
17. Jung H, Kim T, Chae HZ, Kim KT, Ha H. Regulation of macrophage migration inhibitory factor and thiol-specific antioxidant protein PAG by direct interaction. *J Biol Chem* 276: 15504-15510, 2001.
18. Mu ZM, Yin XY, Prochownik EV. Pag, a putative tumor suppressor, interacts with the Myc Box II domain of c-Myc and selectively alters its biological function and target gene expression. *J Biol Chem* 277: 43175-43184, 2002.
19. Neumann CA, Krause DS, Carman CV, Das S, Dubey DP, Abraham JL, Bronson RT, Fujiwara Y, Orkin SH, Van Etten RA. Essential role for the peroxiredoxin Prdx1 in erythrocyte antioxidant defence and tumour suppression. *Nature* 424: 561-565, 2003.
20. Kim YJ, Lee WS, Ip C, Chae HZ, Park EM, Park YM. Prx1 Suppresses Radiation-Induced c-Jun NH2-Terminal Kinase Signaling in Lung Cancer Cells through Interaction with the Glutathione S-Transferase Pi/c-Jun NH2-Terminal Kinase Complex. *Cancer Res* 66: 7136-7142, 2006.
21. Chen MF, Keng PC, Shau H, Wu CT, Hu YC, Liao SK, Chen WC. Inhibition of lung tumor growth and augmentation of radiosensitivity by decreasing peroxiredoxin I expression. *Int J Radiat Oncol Biol Phys* 64: 581-591, 2006.
22. Brown JM, Giaccia AJ. The unique physiology of solid tumors: opportunities (and problems) for cancer therapy. *Cancer Res* 58: 1408-1416, 1998.
23. Harris AL. Hypoxia--a key regulatory factor in tumour growth. *Nat Rev Cancer* 2: 38-47, 2002.
24. Greco O, Marples B, Joiner MC, Scott SD. How to overcome (and exploit) tumor hypoxia for targeted gene therapy. *J Cell Physiol* 197: 312-325, 2003.
25. Kim YJ, Ahn JY, Liang P, Ip C, Zhang Y, Park YM. Human prx1 gene is a target of Nrf2 and is up-regulated by hypoxia/reoxygenation: implication to tumor biology. *Cancer Res* 67: 546-554, 2007.
26. Zander R, Vaupel P. Proposal for using a standardized terminology on oxygen transport to tissue. *Adv Exp Med Biol* 191: 965-970, 1985.
27. Vaupel P, Kallinowski F, Okunieff P. Blood flow, oxygen and nutrient supply, and metabolic microenvironment of human tumors: a review. *Cancer Res* 49: 6449-6465, 1989.
28. Jain RK. Molecular regulation of vessel maturation. *Nat Med* 9: 685-693, 2003.
29. Kallman RF. The phenomenon of reoxygenation and its implications for fractionated radiotherapy. *Radiology* 105: 135-142, 1972.
30. Brown JM. Evidence for acutely hypoxic cells in mouse tumours, and a possible mechanism of reoxygenation. *Br J Radiol* 52: 650-656, 1979.
31. Kimura H, Braun RD, Ong ET, Hsu R, Secomb TW, Papahadjopoulos D, Hong K, Dewhirst MW. Fluctuations in red cell flux in tumor microvessels can lead to transient hypoxia and reoxygenation in tumor parenchyma. *Cancer Res* 56: 5522-5528, 1996.

Print ISSN 1816-0735; Online ISSN 1817-4256

32. Dewhirst MW. Concepts of oxygen transport at the microcirculatory level. *Semin Radiat Oncol* 8: 143-150, 1998.
33. Itoh K, Chiba T, Takahashi S, Ishii T, Igarashi K, Katoh Y, Oyake T, Hayashi N, Satoh K, Hatayama I, Yamamoto M, Nabeshima Y. An Nrf2/small Maf heterodimer mediates the induction of phase II detoxifying enzyme genes through antioxidant response elements. *Biochem Biophys Res Commun* 236: 313-322, 1997.
34. Rushmore TH, Kong AN. Pharmacogenomics, regulation and signaling pathways of phase I and II drug metabolizing enzymes. *Curr Drug Metab* 3: 481-490, 2002.
35. Nguyen T, Sherratt PJ, Pickett CB. Regulatory mechanisms controlling gene expression mediated by the antioxidant response element. *Annu Rev Pharmacol Toxicol* 43: 233-260, 2003.
36. Jaiswal AK. Nrf2 signaling in coordinated activation of antioxidant gene expression. *Free Radic Biol Med* 36: 1199-1207, 2004.
37. Nguyen T, Yang CS, Pickett CB. The pathways and molecular mechanisms regulating Nrf2 activation in response to chemical stress. *Free Radic Biol Med* 37: 433-441, 2004.
38. Chanas SA, Jiang Q, McMahon M, McWalter GK, McLellan LI, Elcombe CR, Henderson CJ, Wolf CR, Moffat GJ, Itoh K, Yamamoto M, Hayes JD. Loss of the Nrf2 transcription factor causes a marked reduction in constitutive and inducible expression of the glutathione S-transferase Gsta1, Gsta2, Gstm1, Gstm2, Gstm3 and Gstm4 genes in the livers of male and female mice. *Biochem J* 365: 405-416, 2002.
39. Chan K, Han XD, Kan YW. An important function of Nrf2 in combating oxidative stress: detoxification of acetaminophen. *Proc Natl Acad Sci USA* 98: 4611-4616, 2001.
40. Enomoto A, Itoh K, Nagayoshi E, Haruta J, Kimura T, O'Connor T, Harada T, Yamamoto M. High sensitivity of Nrf2 knockout mice to acetaminophen hepatotoxicity associated with decreased expression of ARE-regulated drug metabolizing enzymes and antioxidant genes. *Toxicol Sci* 59: 169-177, 2001.
41. Cho HY, Jedlicka AE, Reddy SP, Kensler TW, Yamamoto M, Zhang LY, Kleeberger SR. Role of NRF2 in protection against hyperoxic lung injury in mice. *Am J Respir Cell Mol Biol* 26: 175-182, 2002.
42. Ramos-Gomez M, Kwak MK, Dolan PM, Itoh K, Yamamoto M, Talalay P, Kensler TW. Sensitivity to carcinogenesis is increased and chemoprotective efficacy of enzyme inducers is lost in nrf2 transcription factor-deficient mice. *Proc Natl Acad Sci USA* 98: 3410-3415, 2001.
43. Ishii T, Itoh K, Takahashi S, Sato H, Yanagawa T, Katoh Y, Bannai S, Yamamoto M. Transcription factor Nrf2 coordinately regulates a group of oxidative stress-inducible genes in macrophages. *J Biol Chem* 275: 16023-16029, 2000.
44. Velichkova M, Hasson T. Keap1 regulates the oxidation-sensitive shuttling of Nrf2 into and out of the nucleus via a Crm1-dependent nuclear export mechanism. *Mol Cell Biol* 25: 4501-4513, 2005.
45. Zhang DD, Hannink M. Distinct cysteine residues in Keap1 are required for Keap1-dependent ubiquitination of Nrf2 and for stabilization of Nrf2 by chemopreventive agents and oxidative stress. *Mol Cell Biol* 23: 8137-8151, 2003.
46. Dinkova-Kostova AT, Holtzclaw WD, Cole RN, Itoh K, Wakabayashi N, Katoh Y, Yamamoto M, Talalay P. Direct evidence that sulfhydryl groups of Keap1 are the sensors regulating induction of phase 2 enzymes that protect against carcinogens and oxidants. *Proc Natl Acad Sci USA* 99: 11908-11913, 2002.
47. Wakabayashi N, Dinkova-Kostova AT, Holtzclaw WD, Kang MI, Kobayashi A, Yamamoto M, Kensler TW, Talalay P. Protection against electrophile and oxidant stress by induction of the phase 2 response: fate of cysteines of the Keap1 sensor modified by inducers. *Proc Natl Acad Sci USA* 101: 2040-2045, 2004.
48. Eggler AL, Liu G, Pezzuto JM, van Breemen RB, Mesecar AD. Modifying specific cysteines of the electrophile-sensing human Keap1 protein is insufficient to disrupt binding to the Nrf2 domain Neh2. *Proc Natl Acad Sci USA* 102: 10070-10075, 2005.
49. Kang KW, Lee SJ, Park JW, Kim SG. Phosphatidylinositol 3-kinase regulates nuclear translocation of NF-E2-related factor 2 through actin rearrangement in response to oxidative stress. *Mol Pharmacol* 62: 1001-1010, 2002.
50. Kong AN, Owuor E, Yu R, Hebbar V, Chen C, Hu R, Mandlekar S. Induction of xenobiotic enzymes by the MAP kinase pathway and the antioxidant or electrophile response element (ARE/EpRE). *Drug Metab Rev* 33: 255-271, 2001.
51. Huang HC, Nguyen T, Pickett CB. Phosphorylation of Nrf2 at Ser-40 by protein kinase C regulates antioxidant response element-mediated transcription. *J Biol Chem* 277: 42769-42774, 2002.
52. Numazawa S, Ishikawa M, Yoshida A, Tanaka S, Yoshida T. Atypical protein kinase C mediates activation of NF-E2-related factor 2 in response to oxidative stress. *Am J Physiol Cell Physiol* 285: C334-342, 2003.
53. Salazar M, Rojo AI, Velasco D, de Sagarra RM, Cuadrado A. Glycogen synthase kinase-3beta inhibits the xenobiotic and antioxidant cell response by direct phosphorylation and nuclear exclusion of the transcription factor Nrf2. *J Biol Chem* 281: 14841-14851, 2006.
54. Padmanabhan B, Tong KI, Ohta T, Nakamura Y, Scharlock M, Ohtsuji M, Kang MI, Kobayashi A, Yokoyama S, Yamamoto M. Structural basis for defects of Keap1 activity provoked by its point mutations in lung cancer. *Mol Cell* 21: 689-700, 2006.
55. Singh A, Misra V, Thimmulappa RK, Lee H, Ames S, Hoque MO, Herman JG, Baylin SB, Sidransky D, Gabrielson E, Brock MV, Biswal S. Dysfunctional Keap1-Nrf2 interaction in non-small-cell lung cancer. *PLoS Med* 3: e420, 2006.
56. Kim JH, Bogner PN, Ramnath N, Park Y, Yu J, Park YM. Elevated expression of Prx1 and Nrf2 in stage I non-small cell lung cancer: Prx1, but not Nrf2, is an independent prognostic factor for disease recurrence and reduced survival after surgery. *Clin Cancer Res* 13: in press, 2007.
57. Mountain CF. Revisions in the International System for Staging Lung Cancer. *Chest* 111: 1710-1717, 1997.
58. Tew KD. Glutathione-associated enzymes in anticancer drug resistance. *Cancer Res* 54: 4313-4320, 1994.
59. Young LC, Campling BG, Cole SP, Deeley RG, Gerlach JH. Multidrug resistance proteins MRP3, MRP1, and MRP2 in lung cancer: correlation of protein levels with drug response and messenger RNA levels. *Clin Cancer Res* 7: 1798-1804, 2001.
60. Soini Y, Napankangas U, Jarvinen K, Kaarteenaho-Wiik R, Paakko P, Kinnula VL. Expression of gamma-glutamyl cysteine synthetase in non-small cell lung carcinoma. *Cancer* 92: 2911-2919, 2001.
61. Gottesman MM. Mechanisms of cancer drug resistance. *Annu Rev Med* 53: 615-627, 2002.
62. Cao S, Durrani FA, Rustum YM. Selective modulation of the therapeutic efficacy of anticancer drugs by selenium containing compounds against human tumor xenografts. *Clin Cancer Res* 10: 2561-2569, 2004.
63. Azrak RG, Cao S, Slocum HK, Toth K, Durrani FA, Yin MB, Pendyala L, Zhang W, McLeod HL, Rustum YM. Therapeutic synergy between irinotecan and 5-fluorouracil against human tumor xenografts. *Clin Cancer Res* 10: 1121-1129, 2004.
64. Ip C. Lessons from basic research in selenium and cancer prevention. *J Nutr* 128: 1845-1854, 1998.
65. Ip C, Ganther HE. Activity of methylated forms of selenium in cancer prevention. *Cancer Res* 50: 1206-1211, 1990.
66. Ip C, Hayes C, Budnick RM, Ganther HE. Chemical form of selenium, critical metabolites, and cancer prevention. *Cancer Res* 51: 595-600, 1991.
67. Park EM, Choi KS, Park SY, Kong ES, Zu K, Wu Y, Zhang H, Ip C, Park YM. A display thiol-proteomics approach to characterize global redox modification of proteins by selenium: Implication for the anticancer action of selenium. *Cancer Genomics Proteomics* 2: 25-36, 2005.
68. Gopalakrishna R, Gundimeda U, Chen ZH. Cancer-preventive selenocompounds induce a specific redox modification of cysteine-rich regions in Ca^{2+}-dependent isoenzymes of protein kinase C. *Arch Biochem Biophys* 348: 25-36, 1997.
69. Seo YR, Kelley MR, Smith ML. Selenomethionine regulation of p53 by a ref1-dependent redox mechanism. *Proc Natl Acad Sci USA* 99: 14548-14553, 2002.
70. Smith ML, Lancia JK, Mercer TI, Ip C. Selenium compounds regulate p53 by common and distinctive mechanisms. *Anticancer Res* 24: 1401-1408, 2004.
71. Parsonage D, Youngblood DS, Sarma GN, Wood ZA, Karplus PA, Poole LB. Analysis of the link between enzymatic activity and oligomeric state in AhpC, a bacterial peroxiredoxin. *Biochemistry* 44: 10583-10592, 2005.
72. Motohashi H, O'Connor T, Katsuoka F, Engel JD, Yamamoto M. Integration and diversity of the regulatory network composed of Maf and CNC families of transcription factors. *Gene* 294: 1-12, 2002.
73. Sun J, Brand M, Zenke Y, Tashiro S, Groudine M, Igarashi K. Heme regulates the dynamic exchange of Bach1 and NF-E2-related factors in the Maf transcription factor network. *Proc Natl Acad Sci USA* 101: 1461-1466, 2004.

Research Article

Peroxiredoxin 1 Interacts with Androgen Receptor and Enhances its Transactivation by Hypoxia/Reoxygenation

Soo-Yeon Park,[1] Xiaofei Yu,[1] Clement Ip,[2] James L. Mohler,[3] Paul N. Bogner,[4] and Young-Mee Park[1]

Departments of [1]Cell Stress Biology, [2]Cancer Chemoprevention, [3]Urologic Oncology, and [4]Pathology, Roswell Park Cancer Institute, Buffalo, New York

Abstract

Although hypoxia is accepted as an important microenvironmental factor influencing tumor progression and treatment response, it is usually regarded as a static global phenomenon. Consequently, less attention is given to the impact of dynamic changes in tumor oxygenation in regulating the behavior of cancer cells. Androgen receptor (AR) signaling plays a critical role in prostate cancer. We previously reported that hypoxia/reoxygenation, an *in vitro* condition used to mimic an unstable oxygenation climate in a tumor, stimulates AR activation. In the present study, we showed that peroxiredoxin 1 (Prx1), a member of the peroxiredoxin protein family, acts as a key mediator in this process. We found that the aggressive LN3, C4-2, and C4-2B prostate cancer cell lines derived from LNCaP possess constitutively elevated Prx1 compared with parental cells, and display greater AR activation in response to hypoxia/reoxygenation. Although the cell survival–enhancing property of Prx1 has traditionally been attributed to its antioxidant activity, the reactive oxygen species–scavenging activity of Prx1 was not essential for AR stimulation because Prx1 itself was oxidized and inactivated by hypoxia/reoxygenation. Increased AR transactivation was observed when wild-type Prx1 or mutant Prx1 (C52S) lacking antioxidant activity was introduced into LNCaP cells. Reciprocal immunoprecipitation, chromatin immunoprecipitation, and *in vitro* pull-down assays corroborated that Prx1 interacts with AR and enhances its transactivation. We also show that Prx1 is capable of sensitizing a ligand-stimulated AR. Based on the above information, we suggest that disrupting the interaction between Prx1 and AR may serve as a fruitful new target in the management of prostate cancer. [Cancer Res 2007;67(19):1–10]

Introduction

Microenvironmental hypoxia develops during tumor growth, and is known to influence cancer progression and treatment response. Previous studies have shown a strong correlation between tumoral pO_2 and tumor control and progression in patients with solid tumors, including prostate cancer (1–6). Hypoxia is usually considered a global phenomenon, defined as an overall reduced oxygen availability or partial pressure below critical levels (7). However, tumor vasculature is architecturally and functionally abnormal (8, 9); the vessels are chaotic, tortuous, and highly branched. Ultrastructurally, numerous "openings" (endothelial fenestrations, vesicles, and transcellular holes), widened interendothelial junctions, and discontinuous or absent basement membranes have been described. Aberrant blood vessels can be shut down or reopened temporarily at any time, and the same defects can cause reversal of blood flow. Consequently, local blood flow and oxygenation within a tumor are not homogeneous; these variables are changing dynamically (10, 11). Additionally, regional angiogenesis may also contribute to local oxygenation changes. Although hypoxia is generally accepted as an important microenvironmental factor influencing the survival and proliferation of cancer cells, little is known about the effect of dynamic oxygenation changes on the behavior of cancer cells.

Prostate cancer is the most common noncutaneous cancer and is the second leading cause of cancer death in men from the U.S. (12). Androgen signaling via the androgen receptor (AR) plays a critical role in the development, progression, and treatment response of prostate cancer (13, 14). The binding of androgen to AR causes a translocation of AR to the nucleus where AR activates the expression of a battery of androgen-responsive genes (15). Because prostate cancer arises in an androgen-stimulated environment, androgen-deprivation therapy (ADT) is used to treat advanced prostate cancer. Although initially effective in blocking tumor growth, ADT eventually fails and results in a high rate of relapse. Recurrent prostate cancer is commonly referred to as "androgen-independent." Despite this clinical androgen independence, recurrent tumors continue to express AR and AR-regulated genes. Immunohistochemical studies of both frozen and formalin-fixed, paraffin-embedded tissues have shown similar levels of AR expression in primary and recurrent cancer tissues (16–18). Androgens were shown to be present in recurrent tumors at levels that may be sufficient to activate AR (16). These findings suggest that the state of "androgen-independence" may be somewhat of a misnomer. Prostate cancer that recurs during ADT may continue to depend on AR activity for survival and growth.

Studies with castrated rat, transgenic mouse and xenograft models suggested that androgen deprivation itself generates a state of hypoxia in the prostate tissue (19–21). Androgen deprivation has been shown to cause endothelial cell death, degeneration of capillaries, and vasoconstriction in the prostate. These findings imply that an inherently hypoxic and unstable oxygenation climate of a tumor might be further disturbed by androgen deprivation. Recently, we investigated the effect of an unstable oxygenation milieu on AR activity (22). Hypoxia/reoxygenation, an *in vitro* condition used to mimic dynamic changes in tumor oxygenation, was found to increase AR binding to the androgen-responsive element (ARE), prostate-specific antigen (PSA) expression, and ARE reporter gene activity. AR activation by hypoxia/reoxygenation was also observed when AR was introduced exogenously into AR-null prostate cancer cells. These findings provide evidence that the AR-stimulatory effect of an unstable oxygenation climate is likely to contribute to resistance to ADT, and the emergence of recurrent prostate cancer.

Requests for reprints: Young-Mee Park, Department of Cell Stress Biology, Roswell Park Cancer Institute, Buffalo, NY 14263. Phone: 716-845-3190; Fax: 716-845-8899; E-mail: young-mee.park@roswellpark.org.

doi:10.1158/0008-5472.CAN-07-0651

Peroxiredoxin 1 (Prx1) is a member of the redox-regulating peroxiredoxin protein family. Prx1 has been shown to be elevated in several cancers, and its ability to enhance the survival and progression of cancer cells has been suggested (23–26). However, no information is available on the possible role of Prx1 in prostate cancer. Considering the effect of an unstable oxygenation condition on AR activity, and the redox changes that are likely to be exacerbated by ADT, we postulated that Prx1 might modify the activity of AR and influence the malignant progression of prostate cancer. Several lineage-related cell models have been developed in an attempt to delineate the molecular basis of prostate cancer progression. The LNCaP human prostate cancer cell line has been widely used because it is one of the limited androgen-sensitive cell lines. LNCaP cells possess a functional AR, and secrete PSA *in vitro* and *in vivo*. The C4-2 and C4-2B lines were established by Chung and coworkers (27, 28), and LN3 was established by Pettaway and coworkers (29) from LNCaP. The LN3 cell line was developed by repeated lymph node metastasis of LNCaP cells grown orthotopically in the prostate gland of athymic mice. The C4-2 and C4-2B cell lines were established by cocultivating LNCaP with stromal cells *in vivo* and *in vitro*. The LN3, C4-2, and C4-2B cells are able to grow in a castrated host, and display increased tumorigenic and metastatic potential compared with the parental LNCaP cells (27–31).

In the present study, we found that Prx1 is elevated constitutively in these aggressive LNCaP derivatives compared with the parental cells. We therefore investigated whether Prx1 plays a role in regulating AR activation by hypoxia/reoxygenation. We provided evidence that Prx1 directly interacts with AR and enhances its transactivation in response to hypoxia/reoxygenation. To the best of our knowledge, this is the first report showing the unique function and regulatory mechanism of Prx1 in prostate cancer.

Materials and Methods

Cell culture. LNCaP and DU145 cells were obtained from the American Type Culture Collection. C4-2 and C4-2B cells were provided by Dr. Leland Chung (Emory University). LN3 and PC3-AR (which stably overexpresses the full-length human AR) were provided by Dr. Curtis Pettaway (University of Texas M.D. Anderson Cancer Center) and Dr. Shuyuan Yeh (University of Rochester), respectively. All cells were cultured in RPMI 1640 supplemented with 10% fetal bovine serum (FBS), 2 mmol/L of glutamine, 100 units/mL of penicillin, and 100 μg/mL of streptomycin at 37°C in an atmosphere of 5% CO_2 and 95% air. In some experiments, cells were switched to a medium containing charcoal-stripped FBS (CS-FBS; Hyclone) at 24 h prior to the start of the experiment.

Hypoxia treatment. Culture medium was replaced with deoxygenated RPMI 1640 before hypoxia treatment as reported previously (22). In brief, deoxygenated medium was prepared prior to each experiment by equilibrating the medium with a hypoxic gas mixture containing 5% CO_2, 85% N_2, and 10% H_2 at 37°C. The oxygen concentration in the hypoxic chamber and the exposure medium was maintained at <0.05%. Oxygen concentration was monitored continuously using an oxygen indicator (Forma Scientific). All experiments were done at 70% to 80% confluency at a medium pH between 7.2 and 7.4.

Plasmid and adenoviral expression vectors. The pCR3.1 plasmids containing wild-type Prx1 or mutant Prx1 (pCR C52S) lacking antioxidant activity, and the construction of adenoviral vectors, Ad.Con, Ad.Prx1, and Ad.C52S, were described previously (32). The adenoviral vectors were used at a multiplicity of infection of 5.

Retroviral short hairpin RNA expression constructs and retroviral infection. For the expression of short hairpin RNA (shRNA) targeting Prx1, the pSilencer 5.1 system (Ambion) was used. Only one of the three target sequences tested effectively knocked-down Prx1 expression. Scrambled sequences were designed to generate a scramble shRNA construct. Both sequences were checked by searching the genome database (BLAST) to ensure that they shared no significant sequence homology with other human genes. The sequences of hairpin oligonucleotides targeting the human *Prx1* gene that we chose to use were: 5′-GATCCGTTCTCACTTCTGTCATCTATTCAAGAGATAGATGACAGAAGTGAGAATTTTTTGGAAA-3′ (top strand) and 5′-AGCTTTTCCAAAAAATTCTCACTTCTGTCATCTATCTCTTGAATAGATGACAGAAGTGAGAACG-3′ (bottom strand). The scrambled sequences used were: 5′-GATCCCGTTCTCCGAACGGTGCACGTTTCAAGAGAACGTGCACCGTTCGGAGAATTTTTTGGAAA-3′ (top strand) and 5′-AGCTTTTCCAAAAAATTCTCCGAACGGTGCACGTTCTCTTGAAACGTGCACCGTTCGGAGAACGG-3′ (bottom strand). Each pair of oligonucleotides was annealed, and cloned into the pSilencer vector. The sequence accuracy of the constructs was confirmed by using an ABI 3700 capillary sequencer (Applied Biosystems). Phoenix packaging cells were transfected with Prx1- or scramble-shRNA expression vector using LipofectAMINE 2000 reagents (Invitrogen). Culture supernatants were collected 48 h after transfection and filtered. LN3 cells were infected with the filtered Prx1- or scramble-shRNA viral preparations in the presence of 4 μg/mL of polybrene (Sigma). Fresh viral suspensions were added to the cells every 8 h during the subsequent 48 h. Infected cells were selected in a growth medium containing 2 μg/mL of puromycin for 10 days, and used for experiments.

Cell growth assays. Cells were seeded at 2×10^5 per well in six-well plates in the appropriate medium and allowed to grow for 24 h. Cells were washed with PBS and switched to a phenol-free medium containing 2% CS-FBS (Hyclone). Triplicate wells were counted on days 1, 2, 3, and 4 using a hemocytometer.

Western blot analysis. Equal amounts of protein were analyzed in duplicate by SDS-PAGE. Protein concentrations were measured by the method of Lowry et al. (33). The following monoclonal antibodies were used: anti-Prx1 (Lab Frontier), anti–Prx-$SO_{2/3}$H (Lab Frontier), anti-AR (Upstate), and anti–β-actin (Sigma). Immunoreactive proteins were detected with secondary antibody and visualized using an enhanced chemiluminescence detection system (Amersham Bioscience).

Determination of Prx1 oxidation status. Two-dimensional electrophoresis was carried out as described previously (32). Nonlinear gradient strips (3–10 pH; Amersham Biosciences) were used for isoelectric focusing. The immobilized pH gradient strips were then equilibrated in SDS buffer and placed on top of a 12% SDS-PAGE gel. After migration, the gels were transferred to nitrocellulose membrane and probed with anti-Prx1 (Lab Frontier) or anti–Prx-$SO_{2/3}$H (Lab Frontier) antibody to determine Prx1 oxidation status.

Transfection and luciferase assay. An aliquot of 3×10^5 cells was placed in a six-well plate and transfected with DNA using Fugene 6 reagent (Roche). The pSG5hAR expression vector was used to express AR (22). The ARE reporter plasmid containing three repeats of the ARE was used to assess the luciferase reporter as described previously (22). The total amount of plasmid DNA was normalized to 1 μg/well by the addition of empty plasmid. Luciferase activities were measured by using the Luciferase Assay System (Promega), and normalized by protein concentration and transfection efficiency. All transfection experiments were done in triplicate wells and experiments were repeated at least thrice.

Nuclear extract preparation and electromobility gel shift assay. Nuclear extract was prepared as described previously (22). Cells were harvested, washed twice with PBS, resuspended in a hypotonic buffer [10 mmol/L HEPES-KOH (pH 7.9), 1.5 mmol/L $MgCl_2$, 10 mmol/L KCl, and 0.1% NP40] and incubated on ice for 10 min. Nuclei were precipitated by $3,000 \times g$ centrifugation for 10 min at 4°C. After washing once with the hypotonic buffer, nuclei were lysed in a lysis buffer [50 mmol/L Tris-HCl (pH 8.0), 150 mmol/L NaCl, and 1% Triton X-100], incubated on ice for 30 min and precleared by $20,000 \times g$ centrifugation for 15 min at 4°C. For electromobility gel shift assays (EMSA), 10 μg of nuclear protein extract was incubated in 20 μL of a solution containing 10 mmol/L of HEPES (pH 7.9), 80 mmol/L of NaCl, 10% glycerol, 1 mmol/L of DTT, 1 mmol/L of EDTA, 100 μg/mL of poly(deoxyinosinic-deoxycytidylic acid), and radiolabeled double-stranded oligonucleotide containing the AR consensus binding motif 5′-CTAGAAGTCTGGTACAGGGTGTTCTTTTTGCA-3′ (Santa Cruz

Biotechnology). ARE-binding complexes were resolved on a 4.5% nondenaturing polyacrylamide gel containing 2.5% glycerol in 0.25× Tris-borate/EDTA at room temperature, and the gels were autoradiographed.

RNA isolation and reverse transcription-PCR analysis. Total RNA was isolated using TRIzol Reagent (Invitrogen), dissolved in DNase I buffer and incubated for 15 min with RNase-free DNase I (20 units/mL) in the presence of RNasin. RNA concentration was determined by UV absorption measurement and samples with comparable A_{260}/A_{280} ratios were used for reverse transcription-PCR (RT-PCR) analysis. The PCR primer pair sequences were: for PSA, forward 5′-GGCAGGTGCTTGTAGCCTTCTC-3′ and reverse 5′-CACCCGAGCAGGTGCTTTTGC-3′; for prx1, forward 5′-GTCCCACGGAGATCATTGCTTTC-3′ and reverse 5′-CCCCTGAAAGAGA-TACCTTCATC-3′; and for β-actin, forward 5′-GATCG TCTAGATTCCTATG-TGGGCGACGA-3′ and reverse 5′-GATCGGAATTCCAGCGAACCGCTC ATTG-3′. PCR was carried out by using a thermal cycler (Perkin-Elmer 9600). The amplified products were separated by electrophoresis on a 1.5% agarose gel, stained with ethidium bromide, and photographed under UV illumination.

Immunoprecipitation assay. Immunoprecipitation was carried out with 1 mg of cell lysate and 1 μg of anti-AR (Upstate) or anti-Prx1 (Lab Frontier) antibody overnight at 4°C. After the addition of 25 μL of Protein G-agarose (Santa Cruz Biotechnology), lysates were incubated for an additional 4 h. Rabbit IgG (Santa Cruz Biotechnology) or mouse IgG (Santa Cruz Biotechnology) was used as a negative control. The beads were washed thrice with the lysis buffer, separated by SDS-PAGE, and immunoblotted with AR or Prx1 antibody. The protein bands were detected using an enhanced chemiluminescence system (Amersham Biosciences).

Chromatin immunoprecipitation assay. Chromatin immunoprecipitation (ChIP) assays were carried out following a procedure described previously (22). After cross-linking with formaldehyde, cells were lysed in buffer containing protease inhibitors. Nuclei were isolated and chromatin was sheared to an average length of 250 to 500 bp using sonication. The sheared chromatin was precleared with salmon sperm DNA/protein A-Sepharose and precipitated with an antibody specific for AR (Upstate) or Prx1 (Lab Frontier). Rabbit IgG was used as a control to monitor nonspecific interactions. Immune complexes were adsorbed onto salmon sperm DNA/protein A-Sepharose beads. After an extensive wash to reduce background, Ab/AR/DNA or Ab/Prx1/DNA complexes were eluted. After precipitation, DNA was resuspended in water and PCR was carried out to amplify the proximal ARE-containing region of the PSA promoter using a forward 5′-TCTGCCTTTGTCCCCTAGAT-3′ and reverse 5′-AACCTT-CATTCCCCAGGACT-3′ primer pair. The intervening region of the *PSA* gene that does not contain ARE was amplified as a negative control using a forward 5′-CTGTGCTTGGAGTTTACCTGA-3′ and reverse 5′-GCA-GAGGTTGCAGTGAGCC-3′ primer pair. Triplicate PCR reactions were conducted for each sample and experiments were repeated at least thrice.

Prx1 and AR pull-down assay. Recombinant human Prx1 and Prx1C52S proteins were purified using sequential ion exchange chromatography and size exclusion chromatography, and oxidized Prx1 was generated *in vitro* as described previously (32). The pSG5hAR expression vector was used to translate AR *in vitro* with the TNT Quick coupled transcription/translation system (Promega). An *in vitro* pull-down assay was done as described previously with minor modifications (32). *In vitro*–translated [^{35}S]methionine-labeled AR and 0.5 μg each of purified wild-type Prx1, Prx1C52S, or oxidized Prx1 were incubated in 20 mmol/L of Tris-Cl (pH 7.4) at 4°C overnight. After 1 day, Prx1 pull-down assays were carried out. The pull-down proteins were separated by SDS-PAGE, and visualized by autoradiogram or Western blot.

Statistical analysis. Statistical significance was examined using Student's *t* tests. The two-sample *t* test was used for two-group comparisons. Values were reported as means ± SD. $P < 0.05$ was considered significant.

Results

Expression of Prx1 is elevated in the LNCaP derivatives, LN3, C4-2, and C4-2B cell lines. The LNCaP-lineage progression cell models, LN3, C4-2, and C4-2B, are less sensitive to androgen, and display an increased metastatic potential compared with the parental cells. Unlike LNCaP, all three are able to grow in a castrated host. Because Prx1 has been suggested to confer an aggressive survival phenotype, we postulated that Prx1 might influence AR activity and promote the malignant progression of prostate cancer. As a first step to test this hypothesis, we examined Prx1 expression in LN3, C4-2, and C4-2B cells. As shown in Fig. 1, F1 our results revealed that Prx1 expression was increased in all three progeny cell lines compared with the parental LNCaP cells. The elevated expression of Prx1 seems to be controlled at the level of message abundance.

AR stimulatory effect of hypoxia/reoxygenation is greater in LN3, C4-2, and C4-2B than in parental LNCaP cells. We next examined whether elevated levels of Prx1 might influence AR activation by hypoxia/reoxygenation. LNCaP and LN3 cells were exposed to 4 h of hypoxia, and the ARE-binding activities of AR were examined at 0, 0.5, 2, or 6 h during reoxygenation. As shown in Fig. 2*A*, although the AR stimulatory effect of hypoxia/reoxygena- F2 tion was observed in both LNCaP and LN3 cells, the degree of AR stimulation by hypoxia/reoxygenation was greater in LN3 than in LNCaP cells. The ARE-binding activity of AR reached a maximum at 2 h during reoxygenation for both cell lines. Because PSA is one of the best-characterized AR target genes, PSA mRNA accumulation was compared between LNCaP and LN3 cell lines using semiquantitative RT-PCR. Consistent with the greater ARE-binding activity, the accumulation of PSA mRNA by hypoxia/reoxygenation was more pronounced in LN3 than in LNCaP cells (Fig. 2*B*). Increased PSA mRNA accumulation was not due to increased AR protein level. No appreciable change in AR protein level was observed by hypoxia/reoxygenation (Fig. 2*C*). Activated AR transactivates its target genes by binding to the ARE-containing

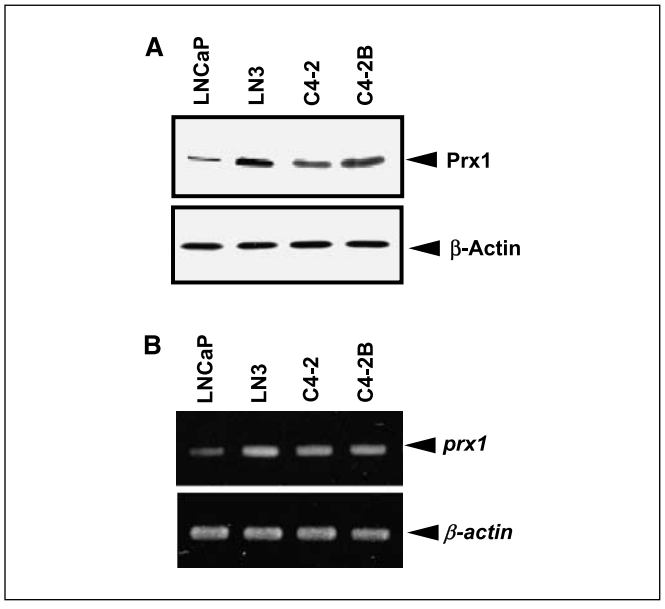

Figure 1. Elevated levels of Prx1 expression in LNCaP lineage progression cell models. *A,* equal amounts of protein extract from LNCaP, LN3, C4-2, and C4-2B cells were separated on 12% SDS-PAGE. Western blot analysis was done using an anti-Prx1 antibody as a probe. β-Actin (Sigma) was used as a loading control. Blots representative of three independent experiments. *B,* RT-PCR analysis of *prx1* mRNA with PCR primer pairs specific for the human *prx1* gene. The β-actin gene was amplified as a control. Gels representative of three independent experiments.

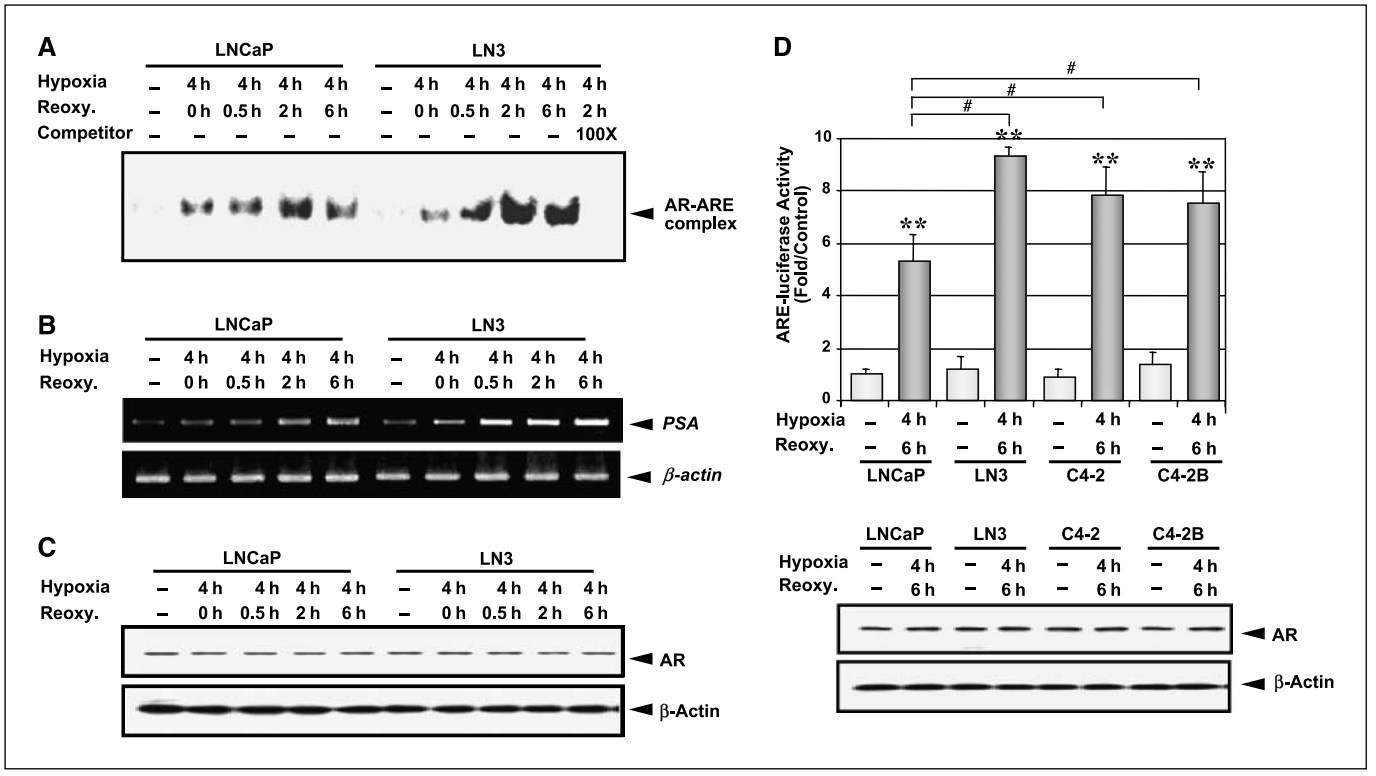

Figure 2. Effect of hypoxia/reoxygenation on AR-ARE binding activity and AR transactivation. *A,* LNCaP or LN3 cells were exposed to 4 h of hypoxia, and EMSA was done at the indicated times during reoxygenation. The ARE-containing oligonucleotides (Santa Cruz Biotechnology) radiolabeled with γ-^{32}P ATP (MP Biomedicals) were used as a probe. Location of the AR-ARE complex (*arrow*). To confirm the specificity of the AR-ARE binding, a molar excess of the unlabeled ARE was used as a competitor. *B,* LNCaP or LN3 were exposed to 4 h of hypoxia, and RT-PCR analysis was carried out using a PCR primer pair specific for the human *PSA* gene. The β-actin gene was amplified as a control. *C,* LNCaP or LN3 were exposed to 4 h of hypoxia, and Western blot analysis was carried out using an anti-AR antibody (Santa Cruz Biotechnology) as a probe. β-Actin antibody was used as a loading control. *D,* LNCaP, LN3, C4-2, or C4-2B cells were transfected with an ARE-luciferase construct (*top*). The pRL-TK vector containing the *Renilla* luciferase gene was cotransfected to normalize the transfection efficiency. At 24 h after transfection, cells were treated with 4 h hypoxia/6 h reoxygenation, and luciferase activity was determined. Normalized mean luciferase activity obtained from cells transfected with ARE-luciferase without hypoxia exposure was set at 1.0. *Columns,* mean ratio of the normalized luciferase activities; *bars,* SD. **, $P < 0.01$, compared with the respective non–hypoxia-treated control. #, $P < 0.05$, compared with hypoxia-treated LNCaP. Western blot analysis was done using an anti-AR antibody as a probe (*bottom*). β-Actin antibody was used as a loading control.

promoter region. LNCaP, LN3, C4-2, and C4-2B cells were transfected with an ARE-luciferase construct, and luciferase reporter activities were determined as a measure of AR transactivation by hypoxia/reoxygenation. Our results showed that increases of luciferase activity by hypoxia/reoxygenation were significantly higher in LN3, C4-2, and C4-2B when compared with that seen in LNCaP cells (Fig. 2*D*), although increases of luciferase activities were observed in all cell lines. The level of AR expression seemed to be comparable among the four cell lines; hypoxia/reoxygenation did not change the AR protein level.

Prx1 increases AR transactivation by hypoxia/reoxygenation. To test the role of Prx1 directly, Prx1 was introduced exogenously into LNCaP cells using an adenoviral vector carrying the *Prx1* gene (Ad.Prx1). As shown in Fig. 3*A*, the ARE-binding activity of AR was increased in cells transfected with Prx1 compared with that in the Ad.Con-infected control. Consistent with the enhanced ARE-binding activity, increased accumulation of PSA mRNA was observed in LNCaP cells infected with Ad.Prx1. The effect of Prx1 on AR transactivation was also examined by transfecting an ARE-luciferase construct. As shown in Fig. 3*B*, a significant increase of the reporter activity was observed in the Prx1-overexpressing cells, thus confirming that the enhanced AR activity by Prx1 was not limited to the *PSA* gene. We next examined the effect of reducing endogenous Prx1 expression on AR activity. To do this, LN3 cells were infected with a retroviral vector containing scramble-shRNA (scramble) or Prx1-shRNA (shPrx1). As shown in Fig. 3*C*, the level of Prx1 was markedly reduced in shPrx1-infected cells, but not in scramble shRNA-infected cells. The Prx1 expression level of mock-infected LN3 cells is shown for comparison. When scramble- or shPrx1-infected cells were exposed to hypoxia/reoxygenation, the accumulation of PSA mRNA was significantly reduced in shPrx1-infected cells. This result is consistent with the findings from Prx1-overexpressing cells. To further validate the functional significance of Prx1 in increasing AR activity, Prx1 was introduced into PC3-AR cells which stably express the wild-type AR. As shown in Fig. 3*D*, Prx1 overexpression increased the ARE-luciferase activity in response to hypoxia/reoxygenation in PC3-AR cells. Essentially identical results were obtained when Prx1 was overexpressed in the DU145 cells. Because DU145 cells are AR-null, the ARE-luciferase construct was cotransfected with the pSG5hAR vector containing the wild-type AR.

Prx1 increases ligand-stimulated AR transactivation. To examine whether Prx1 regulates ligand-stimulated AR activity independent of hypoxia/reoxygenation, LNCaP cells were switched to a CS-FBS medium to deplete residual androgens present in the regular FBS medium. Cells were exposed to a CS-FBS medium supplemented with 10 nmol/L of a synthetic androgen, R1881. It

was shown that prostate tissue contains ~10 nmol/L of dihydrotestosterone (16). A dominant tissue androgen in the prostate tissue is dihydrotestosterone. Our results show that Prx1 increased the ARE-binding activity of a ligand-stimulated AR (Fig. 4*A*). To test whether Prx1 sensitizes AR to low levels of androgen, we exposed the cells to a lower concentration of R1881. We chose to use 2 nmol/L of R1881 because prostate cancer tissues that recurred during ADT have been shown to contain approximately this level of dihydrotestosterone (16). Our results revealed that Prx1 overexpression significantly increased the ARE reporter activity at a subphysiologic level of R1881 (Fig. 4*B*). The activity of the ARE-luciferase reporter at 10 nmol/L of R1881 is shown for comparison.

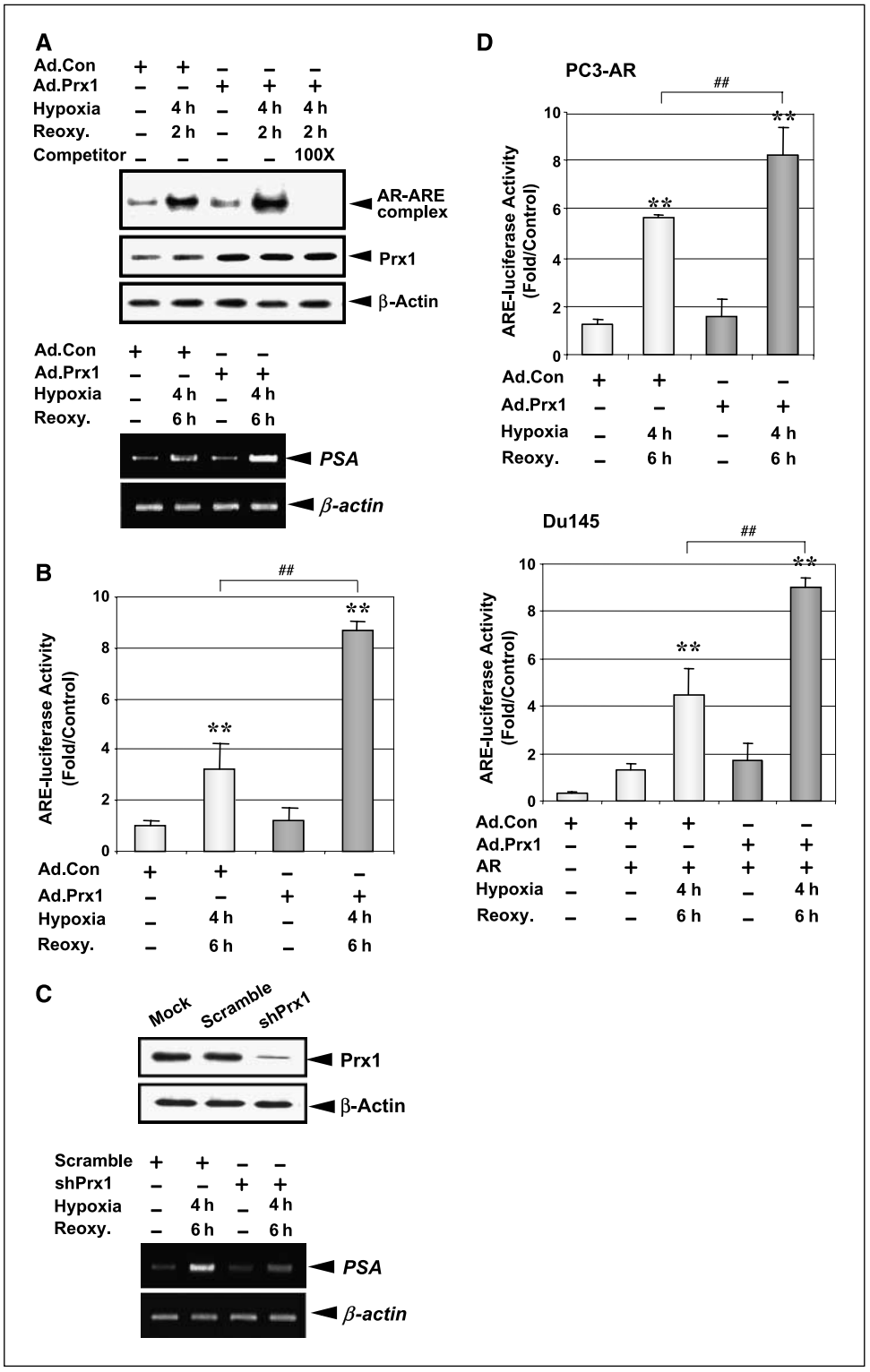

Figure 3. Prx1 increases the AR stimulatory effect of hypoxia/reoxygenation. *A,* LNCaP cells were infected with Ad.Con or Ad.Prx1 (*top*). At 24 h after infection, cells were exposed to 4 h of hypoxia. Cells were reoxygenated for 2 h, and EMSA was done as described above. Molar excess of the unlabeled ARE was used as a competitor. Prx1 Western blot was done to monitor the expression levels of Prx1 after adenovirus infection. β-Actin was used as a loading control. Ad.Con- or Ad.Prx1-infected LNCaP cells were treated with 4 h hypoxia/6 h reoxygenation (*bottom*). Total RNA was isolated, and RT-PCR analysis was carried out to amplify the *PSA* gene. β-Actin gene was amplified as a control. *B,* Ad.Con- or Ad.Prx1-infected LNCaP cells were transfected with the ARE-luciferase construct. At 24 h after transfection, cells were treated with 4 h hypoxia/6 h reoxygenation, and luciferase activities were measured. Normalized mean luciferase activity obtained from Ad.Con-infected cells without hypoxia exposure was set at 1.0. *Columns,* mean ratio of the normalized luciferase activities; *bars,* SD. **, $P < 0.01$, compared with non–hypoxia-treated control. ##, $P < 0.01$, between hypoxia-treated Ad.Con and Ad.Prx1 samples. *C,* LN3 cells were infected with retroviral vectors containing scramble shRNA (*Scramble*) and Prx1 shRNA (*shPrx1*), respectively (*top*). Western blot analysis was done to monitor the levels of Prx1 expression using an anti-Prx1 antibody as a probe. Mock-infected LN3 cells (*Mock*). β-Actin was used as a loading control. Scramble- or shPrx1-infected LN3 cells were treated with 4 h hypoxia/6 h reoxygenation (*bottom*). Total RNA was isolated, and RT-PCR analysis was carried out to evaluate the accumulation of PSA mRNA. β-Actin was amplified as a control. *D,* Ad.Con- or Ad.Prx1-infected PC3-AR cells were transfected with the ARE-luciferase construct (*left*). Cells were treated with 4 h hypoxia/6 h reoxygenation, and luciferase activity was determined. *Columns,* mean ratio of the normalized luciferase activities; *bars,* SD. **, $P < 0.01$ compared with non–hypoxia-treated control. ##, $P < 0.01$, between hypoxia-treated Ad.Con and Ad.Prx1 samples. Ad.Con- or Ad.Prx1-infected DU145 cells were cotransfected with wild-type AR containing pSG5hAR and the ARE-luciferase construct (*right*). Cells were treated with 4 h hypoxia/6 h reoxygenation, and luciferase activity was determined. *Columns,* mean ratio of the normalized luciferase activities; *bars,* SD. **, $P < 0.01$, compared with non–hypoxia-treated control. ##, $P < 0.01$, between hypoxia-treated Ad.Con and Ad.Prx1 samples.

To evaluate the effect of endogenous Prx1 knock-down on ligand-stimulated AR activity, scramble- or shPrx1-infected LN3 cells were exposed to 10 nmol/L of R1881. Our results clearly showed that the accumulation of PSA mRNA was much lower in shPrx1-infected cells compared with scramble-shRNA infected cells (Fig. 4*C*). Next, we examined the consequence of Prx1 knock-down on the growth-inhibitory effect of androgen deprivation. As shown in Fig. 4*D*, when cells were grown in an androgen-depleted medium containing CS-FBS, the growth rate of shPrx1-infected cells was significantly reduced compared with that of scramble shRNA–infected cells, showing that the growth-inhibitory effect of androgen deprivation is increased by Prx1 knock-down.

The AR stimulatory function of Prx1 is independent of its antioxidant activity. The ability of Prx1 to sensitize a ligand-stimulated AR indicated that the antioxidant activity of Prx1 may not be necessary for its AR stimulatory function in response to hypoxia/reoxygenation. When we examined the oxidation status of Prx1 in LNCaP and LN3 cells, we found that the active site Cys^{52} residue in Prx1 was oxidized and inactivated by hypoxia/reoxygenation. Figure 5*A* shows the two-dimensional Western blots of LN3 cells analyzed after 2 h of reoxygenation when the ARE-binding activity of AR was maximal based on EMSA results. Oxidation of Prx1 resulted in an acidic shift of the two-dimensional Western blot when probed with a Prx1 antibody (*top*). Oxidation of the active site Cys^{52}-SH to Cys^{52}-$SO_{2/3}H$ was further confirmed by using a Prx $SO_{2/3}H$ antibody, which specifically recognizes the oxidized Cys^{52} (*bottom*). The oxidation status of Prx1 was maintained at least 6 to 8 h after reoxygenation (data not shown). To test the effectiveness of an antioxidant activity-null Prx1 in modifying AR function, LNCaP cells were transfected with a plasmid containing a mutant Prx1 generated by replacing the catalytic site Cys^{52} with Ser^{52} (pCR C52S). As shown in Fig. 5*B*, regardless of whether the wild-type Prx1 (pCR Prx1WT) or the mutant Prx1 was overexpressed, the ARE-luciferase activity was consistently increased. The effect of hypoxia/reoxygenation on AR activity in mock-transfected cells with an empty plasmid (pCR3.1) is shown for comparison. The enhancement of AR activity in mutant Prx1-overexpressing cells was comparable to that seen in wild-type Prx1-overexpressing cells. This result clearly showed that the antioxidant activity of Prx1 was not essential for the AR-stimulatory function of Prx1.

F5 **Prx1 interacts with AR, and is recruited to the PSA promoter.** Because accumulating evidence suggests that Prx1 interacts with various proteins to modulate their activities (32, 34–36), we tested whether Prx1 interacts with AR. Immunoprecipitation and reciprocal immunoprecipitation experiments were carried out

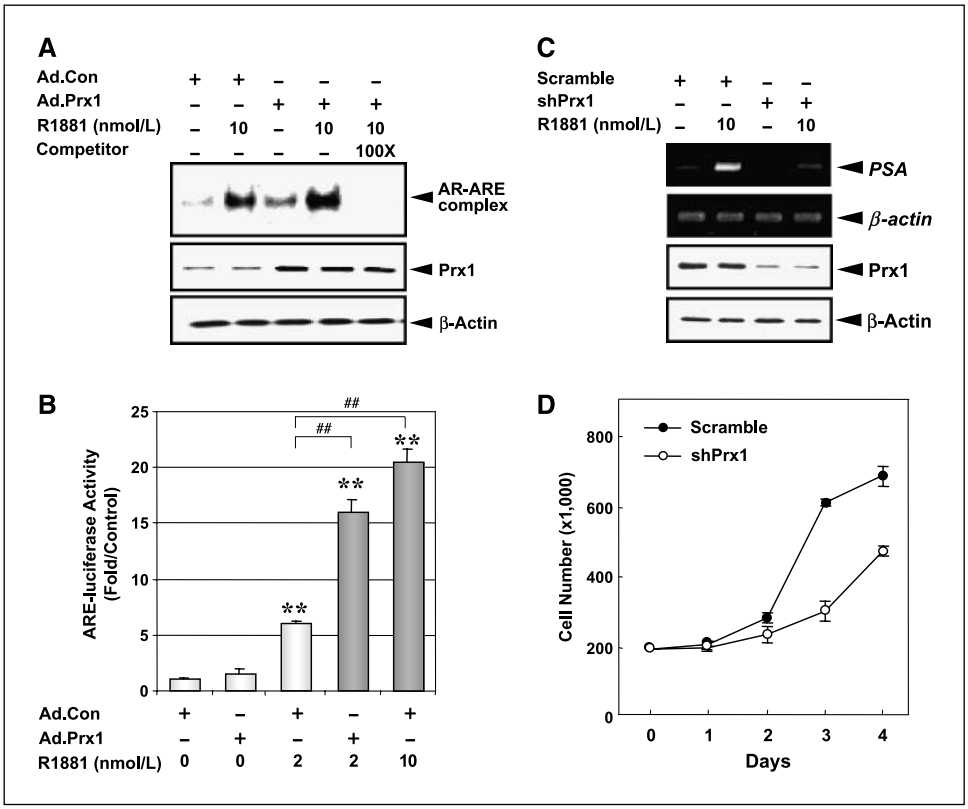

Figure 4. Prx1 enhances AR activation after exposure to synthetic androgen, R1881. *A,* Ad.Con- or Ad.Prx1-infected LNCaP cells grown in a CS-FBS containing medium were treated with 10 nmol/L of R1881 for 6 h. Nuclear extract was obtained, and EMSA was done using ARE-containing oligonucleotides as a probe. Western blot was carried out to monitor the expression levels of Prx1 at the time of experiment. β-Actin was used as a loading control. *B,* Ad.Con- or Ad.Prx1-infected cells grown in a CS-FBS–containing medium were transfected with the ARE-luciferase construct. Cells were treated with 2 or 10 nmol/L of R1881 for 6 h, and luciferase activities were determined. Normalized mean luciferase activity obtained from Ad.Con-infected cells without R1881 stimulation was set at 1.0. *Columns,* mean ratio of the normalized luciferase activities; *bars,* SD. **, $P < 0.01$, compared with unstimulated Ad.Con sample. ##, $P < 0.01$, compared with 2 nmol/L of R1881-stimulated Ad.Con sample. *C,* scramble- or shPrx1-infected LN3 cells grown in a CS-FBS medium were treated with 10 nmol/L of R1881 for 6 h. Total RNA was isolated and RT-PCR analysis was done to analyze the levels of PSA mRNA accumulation. Western blot analysis was carried out to monitor the expression levels of Prx1 in scramble- or shPrx1-infected cells at the time of experiment. *D,* scramble- and shPrx1-infected LN3 cells were grown in a CS-FBS medium. Cell growth was analyzed on days 1, 2, 3, and 4. *Points,* means of results from three separate experiments; *bars,* SD.

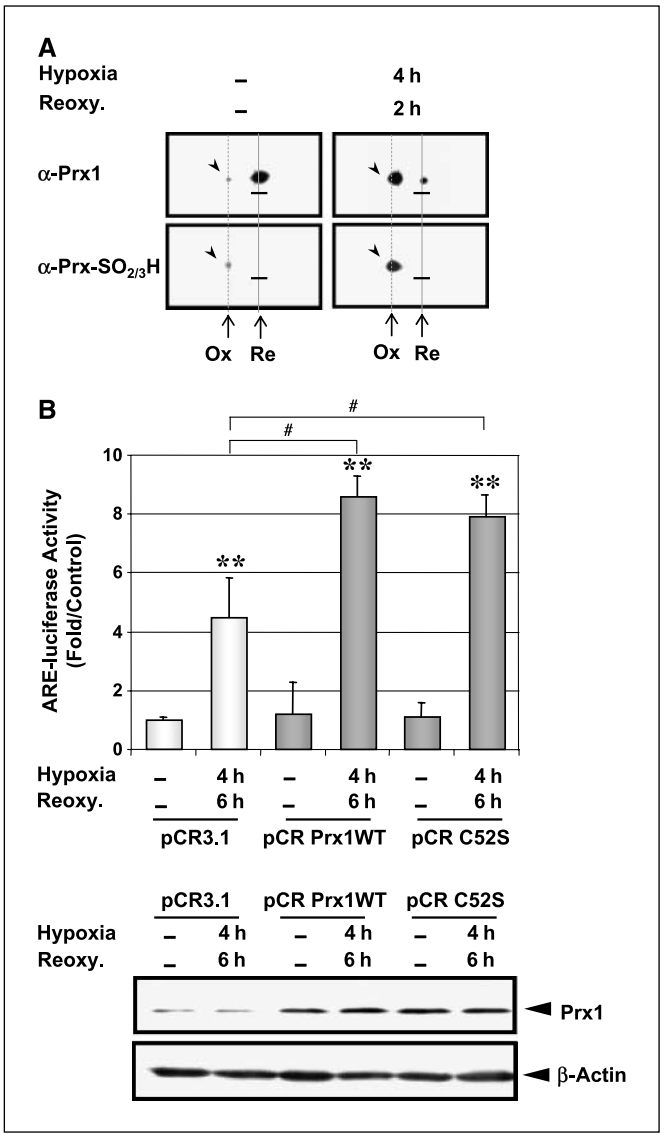

Figure 5. The antioxidant activity of Prx1 is not essential for AR transactivation by hypoxia/reoxygenation. *A,* LN3 cells were treated with 4 h hypoxia/2 h reoxygenation. The oxidation status of Prx1 was analyzed by two-dimensional gel electrophoresis followed by Western blot using a Prx1 antibody (*top*). The Prx1 antibody recognizes both oxidized (*Ox*) and reduced (*Re*) forms of Prx1. Note the acidic shift of oxidized Prx1 after hypoxia/reoxygenation. Oxidation status of the active site Cys^{52} was evaluated using Prx-$SO_{2/3}$H antibody (*bottom*). *B,* LNCaP cells were transfected with pCR vectors containing wild-type Prx1 (*pCR Prx1WT*) or mutant Prx1 lacking antioxidant activity (*pCR C52S; top*). Empty vector (*pCR3.1*) was transfected as a negative control. After 24 h of transfection, cells were treated with 4 h hypoxia/6 h reoxygenation. Normalized mean luciferase activity obtained from cells without hypoxia exposure was set at 1.0. *Columns,* mean ratio of the normalized luciferase activities; *bars,* SD. **, $P < 0.01$ compared with the respective non–hypoxia-treated control. #, $P < 0.05$, compared with hypoxia-treated pCR3.1 samples. Western blot analysis of Prx1 was carried out to monitor the levels of Prx1 expression after transfection (*bottom*). β-Actin was used as a loading control.

using a Prx1 antibody or an AR antibody in LN3 cells, these cells possess a relatively high level of endogenous Prx1. As shown in Fig. 6*A*, AR was coprecipitated with Prx1 after hypoxia/reoxygenation when a Prx1 antibody was used for immunoprecipitation. Similarly, Prx1 was coprecipitated with AR after hypoxia/reoxygenation when an AR antibody was used for immunoprecipitation, indicating a possible interaction of Prx1 and AR after hypoxia/reoxygenation. In order to examine whether Prx1 is recruited to the ARE of the PSA promoter in the natural chromatin milieu, ChIP assays were carried out using a Prx1 antibody. To control for possible nonspecific interactions and DNA contamination, samples precipitated with rabbit IgG were analyzed in parallel. As shown in Fig. 6*B*, our results reveal a recruitment of Prx1 to the ARE region in response to hypoxia/reoxygenation. The results obtained from DNA that was PCR-amplified from chromatin extracts before immunoprecipitation (*input*) are shown for comparison. The specific recruitment of AR to the same ARE region was also confirmed in cells treated with hypoxia/reoxygenation. Neither Prx1 nor AR were recruited to the nonspecific region (intervening) which does not contain an ARE site. No signal was detected in DNA samples obtained from the corresponding IgG samples.

We also examined whether Prx1 interacts directly with AR. To this end, we carried out pull-down experiments using purified Prx1 and *in vitro*–translated AR. The cell-free experiments showed a direct interaction between Prx1 and AR (Fig. 6*C*). When pull-down assays were carried out using a mutant Prx1 protein (*C52S*) or *in vitro* oxidized Prx1 (*Ox*), similar interactions between AR and these Prx1 proteins lacking antioxidant activity were observed. This result further corroborates the idea that the antioxidant function of Prx1 is not essential for its binding to the ARE.

Discussion

Recent advances in early detection and treatment led to a steady decline in prostate cancer mortality. Despite this improvement in survival outcome, prostate cancer is still the leading cause of cancer death in men in the U.S. An estimated 218,890 new cases and 27,050 deaths will occur from prostate cancer this year alone (12). The androgen signaling through AR plays a central role in the development and progression of prostate cancer. In this study, we showed that Prx1 is intimately involved in increasing AR activity in the context of an unstable oxygenation milieu of a tumor. We show that Prx1 interacts physically with AR, and enhances AR transactivation in response to hypoxia/reoxygenation in prostate cancer cells. We also show that Prx1 is capable of sensitizing ligand-stimulated AR activity. These findings suggest that Prx1 may play an important role in mediating the abnormal activation of AR in a subset of prostate cancer cells which are capable of maintaining survival in an unstable oxygenation condition and a reduced level of androgen. In fact, the inherently abnormal and unstable oxygenation of a tumor might be further perturbed by androgen deprivation. An unstable oxygenation can be exacerbated by vasculature destruction after castration, or during neoadjuvant ADT in conjunction with radiation therapy, or in recurrent tumors during ADT. Prostate cancer that recurs during ADT represents a lethal phenotype and poses serious clinical problems. There is mounting evidence to suggest that AR signaling plays an important role in prostate cancer recurrence (16–18, 37). The importance of the current study is underlined by the possibility that disrupting the interaction between Prx1 and AR may serve as a new therapeutic target in a wide range of clinical conditions.

The cell survival–enhancing function of Prx1 has traditionally been attributed to its antioxidant activity. However, despite the initial biochemical characterization of Prx1 as an antioxidant enzyme, the physiologic significance of its peroxidase function is unclear because Prx1 is highly susceptible to over-oxidation/inactivation during reactive oxygen species detoxification (38, 39). When the catalytic Cys is over-oxidized, the peroxidase activity is

lost. Recent studies suggest that the catalytic site over-oxidation of Prx1 may be physiologically significant because it may facilitate the structural and functional switching of Prx1 from an antioxidant enzyme to a molecular chaperone (32, 40, 41). This hypothesis is consistent with the behavior of Prx1 in interacting with various growth-regulating proteins to modulate their activities. The association of Prx1 with c-Abl, c-Myc, macrophage-inhibiting factor, and glutathione *S*-transferase π has been previously shown (32, 34–36). The current study shows that the interaction of Prx1 with AR is independent of the antioxidant function of Prx1. As studies of Prx1 progress, the spectrum of molecules interacting with Prx1 is likely to expand. The functional consequence of these interactions would need to be tested and interpreted in a cell type–and tissue context–dependent manner.

Although Prx1 is thought to be expressed primarily in the cytosol, several lines of evidence have suggested a localization of Prx1 to the nucleus. Using immunoelectron microscopy, Prx1 has been shown to be expressed in the nucleus as well as in the cytoplasm in the rat kidney (42). The presence of Prx1 in the nucleolus of hepatic parenchymal cells has also been shown in the rat liver using an immunogold technique (43). Immunohistochemical analysis of oral cancer tissue revealed a Prx1 staining in the nucleus (25). In addition, nuclear translocation of Prx1 has been reported in cultured cells (34). Collectively, these findings strongly suggest a potential role of Prx1 in the nucleus. Our study, showing the role of Prx1 in regulating AR activity, provides evidence supporting a physiologic function of Prx1 in the nucleus.

It is of note that Prx1 is elevated at the message level in the phenotypically aggressive LNCaP derivatives, LN3, C4-2, and C4-2B cells, which were established by different procedures. Although future studies will be necessary to elucidate the molecular basis of

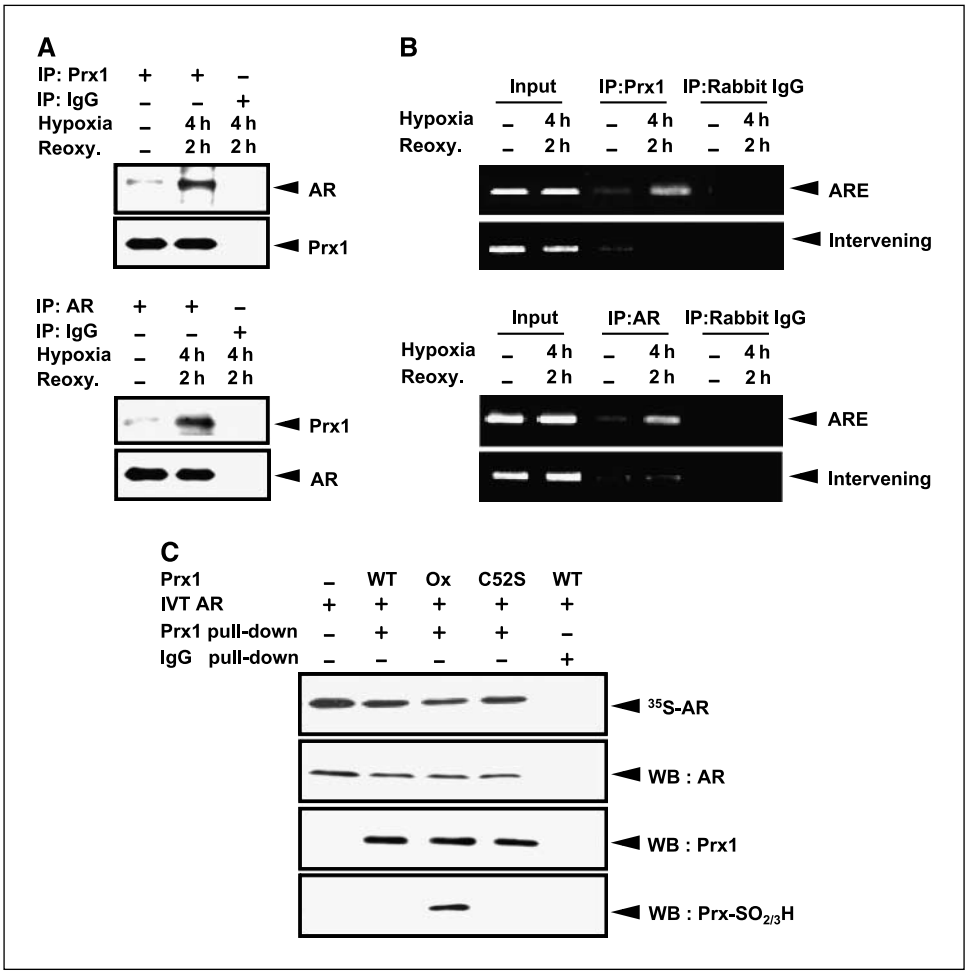

Figure 6. Prx1 interacts with AR, and is recruited to the PSA promoter with AR. *A,* LN3 cells were treated with 4 h hypoxia/2 h reoxygenation. Equal amounts of protein were used for immunoprecipitation (*IP*) with a Prx1 antibody (*top*). The immunoprecipitates were probed for the presence of AR by Western blot. Prx1 Western blot was done as a loading control. Rabbit IgG immunoprecipitation was done as a negative control. Aliquots of protein were subjected to reciprocal immunoprecipitation using an AR or rabbit IgG antibody (*bottom*). The immunoprecipitates were probed for the presence of Prx1 by Western blot. AR Western blot was done as a loading control. *B,* LN3 cells treated with 4 h hypoxia/2 h reoxygenation were processed for ChIP assays using an anti-Prx1 antibody (*top*). Primer pairs used to amplify the ARE-containing region (*ARE*) and the non–ARE-containing region (*Intervening*) are described in Materials and Methods. Results obtained from DNA that was PCR-amplified from chromatin extracts before immunoprecipitation (*Input*). PCR results obtained after immunoprecipitation with rabbit IgG (*Rabbit IgG*). The gels shown are representative of three independent experiments. Aliquots of samples were processed for ChIP assays using an anti-AR antibody (*bottom*). The ARE region and intervening regions were amplified with the respective primer pairs. *C,* equal amounts of purified wild-type Prx1 (*WT*), *in vitro* oxidized Prx1 (*Ox*), or mutant Prx1C52S (*C52S*) were incubated with *in vitro*–translated, [^{35}S]methionine-labeled AR. Physical interaction of Prx1 and AR was tested using a Prx1 antibody pull-down assay. The proteins were separated by SDS-PAGE, and the presence of AR was visualized by autoradiogram with X-ray film (^{35}S-AR) and Western blot. The presence of Prx1 was detected by Western blot using an anti-Prx1 antibody.

Prx1 up-regulation in these LNCaP progeny cell lines, it is tempting to speculate a possible existence of altered molecular mechanisms that are shared among the three cell lines compared with the parental LNCaP cells. Recently, we have cloned and characterized the human *prx1* promoter, and identified NF-E2–related factor 2, or Nrf2, as one of the key transcription factors responsible for *prx1* up-regulation (44). The activation of Nrf2 seems to be dependent on a number of regulatory mechanisms to increase Nrf2 protein level and/or promote its stabilization and accumulation in the nucleus. Phosphorylation of Nrf2 by various kinases, including mitogen-activated protein kinase, has been implicated as an important mechanism in regulating Nrf2 transactivation (45–47). Considering that mitogen-activated protein kinase signaling by epidermal growth factor receptor, HER-2/neu tyrosine kinase, and other growth factor signaling pathways are known to increase the activation of AR (48, 49), cross-talk mechanisms may exist between the Nrf2 and AR signaling pathways acting in concert to promote the malignant progression of prostate cancer.

The hypoxic and unstable oxygenation milieu of a tumor has been proposed to function as a microenvironmental pressure that selects for a subset of cancer cells with an increased ability to survive and proliferate. The current study revealed that elevated expression of Prx1 enhances AR transactivation by hypoxia/reoxygenation and sensitizes a ligand-stimulated AR, thereby providing a survival advantage to cancer cells subjected to an adverse microenvironment. Future research will be aimed at determining whether aberrant Prx1 up-regulation could be suppressed by genetic and/or pharmacologic approaches, and whether reducing Prx1 expression levels could suppress prostate cancer progression or reverse resistance to ADT in preclinical models. It may be worthwhile to investigate whether the Nrf2-Prx1 axis is dysregulated in human prostate cancer tissues, and whether it correlates with disease progression and poor clinical outcome.

Acknowledgments

Received 2/16/2007; revised 6/22/2007; accepted 7/16/2007.

Grant support: NIH grants CA111846, CA109480, and CA77739, Department of Defense grant PC050127, and Cancer Center Support grant CA16056.

The costs of publication of this article were defrayed in part by the payment of page charges. This article must therefore be hereby marked *advertisement* in accordance with 18 U.S.C. Section 1734 solely to indicate this fact.

References

1. Brizel DM, Dodge RK, Clough RW, et al. Oxygenation of head and neck cancer: changes during radiotherapy and impact on treatment outcome. Radiother Oncol 1999;53:113–7.

2. Brizel DM, Scully SP, Harrelson JM, et al. Tumor oxygenation predicts for the likelihood of distant metastases in human soft tissue sarcoma. Cancer Res 1996;56:941–3.

3. Movsas B, Chapman JD, Greenberg RE, et al. Increasing levels of hypoxia in prostate carcinoma correlate significantly with increasing clinical stage and patient age: an Eppendorf pO(2) study. Cancer 2000;89:2018–24.

4. Movsas B, Chapman JD, Hanlon AL, et al. Hypoxic prostate/muscle pO2 ratio predicts for biochemical failure in patients with prostate cancer: preliminary findings. Urology 2002;60:634–9.

5. Nordsmark M, Overgaard J. A confirmatory prognostic study on oxygenation status and loco-regional control in advanced head and neck squamous cell carcinoma treated by radiation therapy. Radiother Oncol 2000;57:39–43.

6. Hockel M, Schlenger K, Aral B, et al. Association between tumor hypoxia and malignant progression in advanced cancer of the uterine cervix. Cancer Res 1996;56:4509–15.

7. Zander R, Vaupel P. Proposal for using a standardized terminology on oxygen transport to tissue. Adv Exp Med Biol 1985;191:965–70.

8. Jain RK. Molecular regulation of vessel maturation. Nat Med 2003;9:685–93.

9. Jain RK. Normalization of tumor vasculature: an emerging concept in antiangiogenic therapy. Science 2005;307:58–62.

10. Vaupel P, Okunieff P, Neuringer LJ. Blood flow, tissue oxygenation, pH distribution, and energy metabolism of murine mammary adenocarcinomas during growth. Adv Exp Med Biol 1989;248:835–45.

11. Kimura H, Braun RD, Ong ET, et al. Fluctuations in red cell flux in tumor microvessels can lead to transient hypoxia and reoxygenation in tumor parenchyma. Cancer Res 1996;56:5522–8.

12. Jemal A, Siegel R, Ward E, et al. Cancer statistics, 2007. CA Cancer J Clin 2007;57:43–66.

13. Isaacs JT. Role of androgens in prostatic cancer. Vitam Horm 1994;49:433–502.

14. Isaacs JT. The biology of hormone refractory prostate cancer. Why does it develop? Urol Clin North Am 1999;26:263–73.

15. Trapman J, Cleutjens KB. Androgen-regulated gene expression in prostate cancer. Semin Cancer Biol 1997;8:29–36.

16. Mohler JL, Gregory CW, Ford OH III, et al. The androgen axis in recurrent prostate cancer. Clin Cancer Res 2004;10:440–8.

17. van der Kwast TH, Schalken J, Ruizeveld de Winter JA, et al. Androgen receptors in endocrine-therapy-resistant human prostate cancer. Int J Cancer 1991;48:189–93.

18. de Vere White R, Meyers F, Chi SG, et al. Human androgen receptor expression in prostate cancer following androgen ablation. Eur Urol 1997;31:1–6.

19. Shabsigh A, Chang DT, Heitjan DF, et al. Rapid reduction in blood flow to the rat ventral prostate gland after castration: preliminary evidence that androgens influence prostate size by regulating blood flow to the prostate gland and prostatic endothelial cell survival. Prostate 1998;36:201–6.

20. Jain RK, Safabakhsh N, Sckell A, et al. Endothelial cell death, angiogenesis, and microvascular function after castration in an androgen-dependent tumor: role of vascular endothelial growth factor. Proc Natl Acad Sci U S A 1998;95:10820–5.

21. Hayek OR, Shabsigh A, Kaplan SA, et al. Castration induces acute vasoconstriction of blood vessels in the rat prostate concomitant with a reduction of prostatic nitric oxide synthase activity. J Urol 1999;162:1527–31.

22. Park SY, Kim YJ, Gao AC, et al. Hypoxia increases androgen receptor activity in prostate cancer cells. Cancer Res 2006;66:5121–9.

23. Chang JW, Jeon HB, Lee JH, et al. Augmented expression of peroxiredoxin I in lung cancer. Biochem Biophys Res Commun 2001;289:507–12.

24. Yanagawa T, Ishikawa T, Ishii T, et al. Peroxiredoxin I expression in human thyroid tumors. Cancer Lett 1999;145:127–32.

25. Yanagawa T, Iwasa S, Ishii T, et al. Peroxiredoxin I expression in oral cancer: a potential new tumor marker. Cancer Lett 2000;156:27–35.

26. Chen MF, Keng PC, Shau H, et al. Inhibition of lung tumor growth and augmentation of radiosensitivity by decreasing peroxiredoxin I expression. Int J Radiat Oncol Biol Phys 2006;64:581–91.

27. Wu HC, Hsieh JT, Gleave ME, et al. Derivation of androgen-independent human LNCaP prostatic cancer cell sublines: role of bone stromal cells. Int J Cancer 1994;57:406–12.

28. Thalmann GN, Anezinis PE, Chang SM, et al. Androgen-independent cancer progression and bone metastasis in the LNCaP model of human prostate cancer. Cancer Res 1994;54:2577–81.

29. Pettaway CA, Pathak S, Greene G, et al. Selection of highly metastatic variants of different human prostatic carcinomas using orthotopic implantation in nude mice. Clin Cancer Res 1996;2:1627–36.

30. McConkey DJ, Greene G, Pettaway CA. Apoptosis resistance increases with metastatic potential in cells of the human LNCaP prostate carcinoma line. Cancer Res 1996;56:5594–9.

31. Thalmann GN, Sikes RA, Wu TT, et al. LNCaP progression model of human prostate cancer: androgen-independence and osseous metastasis. Prostate 2000;44:91–103.

32. Kim YJ, Lee WS, Ip C, et al. Prx1 suppresses radiation-induced c-Jun NH2-terminal kinase signaling in lung cancer cells through interaction with the glutathione S-transferase π/c-Jun NH2-terminal kinase complex. Cancer Res 2006;66:7136–42.

33. Lowry OH, Rosebrough NJ, Farr AL, et al. Protein measurement with the Folin phenol reagent. J Biol Chem 1951;193:265–75.

34. Wen ST, Van Etten RA. The PAG gene product, a stress-induced protein with antioxidant properties, is an Abl SH3-binding protein and a physiological inhibitor of c-Abl tyrosine kinase activity. Genes Dev 1997;11:2456–67.

35. Mu ZM, Yin XY, Prochownik EV. Pag, a putative tumor suppressor, interacts with the Myc box II domain of c-Myc and selectively alters its biological function and target gene expression. J Biol Chem 2002;277:43175–84.

36. Jung H, Kim T, Chae HZ, et al. Regulation of macrophage migration inhibitory factor and thiol-specific antioxidant protein PAG by direct interaction. J Biol Chem 2001;276:15504–10.

37. Chen CD, Welsbie DS, Tran C, et al. Molecular determinants of resistance to antiandrogen therapy. Nat Med 2004;10:33–9.

38. Rabilloud T, Heller M, Gasnier F, et al. Proteomics analysis of cellular response to oxidative stress. Evidence for *in vivo* overoxidation of peroxiredoxins at their active site. J Biol Chem 2002;277:19396–401.

39. Yang KS, Kang SW, Woo HA, et al. Inactivation of human peroxiredoxin I during catalysis as the result of the oxidation of the catalytic site cysteine to cysteine-sulfinic acid. J Biol Chem 2002;277:38029–36.

40. Jang HH, Lee KO, Chi YH, et al. Two enzymes in one; two yeast peroxiredoxins display oxidative stress-dependent switching from a peroxidase to a molecular chaperone function. Cell 2004;117:625–35.

41. Jang HH, Kim SY, Park SK, et al. Phosphorylation and concomitant structural changes in human 2-Cys peroxiredoxin isotype I differentially regulate its peroxidase and molecular chaperone functions. FEBS Lett 2006;580:351–5.
42. Oberley TD, Verwiebe E, Zhong W, et al. Localization of the thioredoxin system in normal rat kidney. Free Radic Biol Med 2001;30:412–24.
43. Immenschuh S, Baumgart-Vogt E, Tan M, et al. Differential cellular and subcellular localization of heme-binding protein 23/peroxiredoxin I and heme oxygenase-1 in rat liver. J Histochem Cytochem 2003;51:1621–31.
44. Kim YJ, Ahn JY, Liang P, et al. Human prx1 gene is a target of Nrf2 and is up-regulated by hypoxia/reoxygenation: implication to tumor biology. Cancer Res 2007;67:546–54.
45. Kong AN, Owuor E, Yu R, et al. Induction of xenobiotic enzymes by the MAP kinase pathway and the antioxidant or electrophile response element (ARE/EpRE). Drug Metab Rev 2001;33:255–71.
46. Huang HC, Nguyen T, Pickett CB. Phosphorylation of Nrf2 at Ser-40 by protein kinase C regulates antioxidant response element-mediated transcription. J Biol Chem 2002;277:42769–74.
47. Numazawa S, Ishikawa M, Yoshida A, et al. Atypical protein kinase C mediates activation of NF-E2-related factor 2 in response to oxidative stress. Am J Physiol Cell Physiol 2003;285:C334–42.
48. Craft N, Shostak Y, Carey M, et al. A mechanism for hormone-independent prostate cancer through modulation of androgen receptor signaling by the HER-2/neu tyrosine kinase. Nat Med 1999;5:280–5.
49. Gioeli D, Ficarro SB, Kwiek JJ, et al. Androgen receptor phosphorylation. Regulation and identification of the phosphorylation sites. J Biol Chem 2002;277:29304–14.

THE JOURNAL OF BIOLOGICAL CHEMISTRY VOL. 282, NO. 30, pp. 22011–22022, July 27, 2007

Human Peroxiredoxin 1 and 2 Are Not Duplicate Proteins

*THE UNIQUE PRESENCE OF CYS^{83} IN Prx1 UNDERSCORES THE STRUCTURAL AND FUNCTIONAL DIFFERENCES BETWEEN Prx1 AND Prx2**

Received for publication, November 6, 2006, and in revised form, April 18, 2007 Published, JBC Papers in Press, May 22, 2007, DOI 10.1074/jbc.M610330200

WeonSup Lee[‡], Kyoung-Soo Choi[‡], Jonah Riddell[‡], Clement Ip[§], Debashis Ghosh[¶‖], Jong-Hoon Park[**], and Young-Mee Park[‡1]

*From the Departments of [‡]Cell Stress Biology, [§]Cancer Prevention, and [¶]Pharmaology and Therapeutics, Roswell Park Cancer Institute, Buffalo, New York 14263, the [‖]Department of Structural Biology, Hauptman-Woodward Medical Research Institute, Buffalo, New York 14203, and the **Department of Biological Sciences, Sookmyung Women's University, Seoul 140-742, Korea*

Human peroxiredoxins 1 and 2, also known as Prx1 and Prx2, are more than 90% homologous in their amino acid sequences. Prx1 and Prx2 are elevated in various cancers and are shown to influence diverse cellular processes. Although their growth regulatory role has traditionally been attributed to the peroxidase activity, the physiological significance of this function is unclear because the proteins are highly susceptible to inactivation by H_2O_2. A chaperone activity appears to emerge when their peroxidase activity is lost. Structural studies suggest that they may form a homodimer or doughnut-shaped homodecamer. However, little information is available whether human Prx1 and Prx2 are duplicative in structure and function. We noted that Prx1 contains a cysteine (Cys^{83}) at the putative dimer-dimer interface, which is absent in Prx2. We studied the role of Cys^{83} in regulating the peroxidase and chaperone activities of Prx1, because the redox status of Cys^{83} might influence the oligomeric structure and consequently the functions of Prx1. We show that Prx1 is more efficient as a molecular chaperone, whereas Prx2 is better suited as a peroxidase enzyme. Substituting Cys^{83} with Ser^{83} (Prx1C83S) results in dramatic changes in the structural and functional characteristics of Prx1 in a direction similar to those of Prx2. Here we also report the first crystal structure of human Prx1 and the presence of the Cys^{83}–Cys^{83} bond at the dimer-dimer interface of decameric Prx1. These findings are consistent with the hypothesis that human Prx1 and Prx2 possess unique functions and regulatory mechanisms and that Cys^{83} bestows a distinctive identity to Prx1.

Human Prx1[2] and Prx2 are highly homologous members of the peroxiredoxin protein family (1). Prx1 and Prx2 are shown to be elevated in several human cancers. Prx1 is elevated in oral, esophageal, pancreatic, follicular thyroid, and lung cancers (2–10). Both Prx1 and Prx2 are elevated in mesothelioma, breast, and head-and-neck cancers (11–14). Elevation of Prx1 correlates with resistance to chemotherapy in breast cancer (15). In contrast, down-regulation of Prx1 has been shown to sensitize lung cancer cells to radiation and reduce metastasis of lung cancer xenografts (16). Similarly, overexpression of Prx2 renders leukemia and stomach cancer cells resistant to chemotherapeutic agents (17, 18), and down-regulation of Prx2 sensitizes head-and-neck cancer cells to radiation (14) and gastric carcinoma cells to cisplatin (19). These studies suggest that both Prx1 and Prx2 confer resistance to therapy and promote an aggressive survival phenotype of the cancer cells.

The cell survival enhancing functions of Prx1 and Prx2 are generally attributed to their H_2O_2 scavenging activities. The H_2O_2 catalytic mechanism of Prxs is unique among the peroxide-detoxifying enzymes. For example, glutathione peroxidase reduces peroxides while oxidizing glutathione as a co-substrate. The H_2O_2 eliminating action of Prx1, on the other hand, is mediated by a transient inter-molecular disulfide bond formation between the catalytic Cys^{52} of one Prx1 molecule and the Cys^{173} residue of another Prx1 molecule (1). Likewise, the H_2O_2 catalytic action of Prx2 is mediated through a disulfide bond formation between Cys^{51} and Cys^{172}. The formation of an inter-molecular disulfide bond between Prx1 and Prx2 does not appear to occur. Transiently formed disulfide bond is reduced back to Cys-SH by the action of disulfide oxidoreductase, thioredoxin. The Cys^{173} residue of Prx1 (Cys^{172} in Prx2) has traditionally been referred to as a "resolving" Cys. This is based on the fact that the transient inter-molecular disulfide bond formation between the Cys$^{173/172}$-SH of one Prx molecule and the Cys$^{52/51}$-SOH of another Prx molecule engaged in peroxide catalysis is a necessary step for reduction of the Cys$^{52/51}$-SOH back to Cys$^{52/51}$-SH. Despite the initial biochemical characterization of Prxs as peroxide-removing enzymes, the physiological significance of their peroxidase activity is unclear, because the catalytic Cys of a Prx is highly susceptible to loss of activity as a result of its overoxidation to sulfenic ($-SO_2H$) or sulfonic

* This work was supported by National Institutes of Health Grants CA109480 (to Y. M. P.), CA111846 (to Y. M. P.), CA105500 (to D. G.), GM62794 (to D. G.), and EY09412 (to D. G.), Department of Defense Grant PC050127 (to Y. M. P.), Cancer Center Support Grant CA16056, and KOSEF NRL Program 05J0000-10110 (to J. H. P.) through the Ministry of Science and Technology of Korea. The costs of publication of this article were defrayed in part by the payment of page charges. This article must therefore be hereby marked "*advertisement*" in accordance with 18 U.S.C. Section 1734 solely to indicate this fact.

[1] To correspondence should be addressed: Dept. of Cell Stress Biology, Roswell Park Cancer Institute, Buffalo, NY 14263. Tel.: 716-845-3190; Fax: 716-845-8899; E-mail: young-mee.park@roswellpark.org.

[2] The abbreviations used are: Prx1, peroxiredoxin 1; Prx2, peroxiredoxin 2; MALDI-TOF, matrix-assisted laser adsorption ionization-time of flight; Q-TOF, quadruple-time of flight; DTT, dithiothreitol; MDH, malate dehydrogenase; IAA, iodoacetamide; yTR, yeast thioredoxin reductase; yTrx, yeast thioredoxin; MS, mass spectrometry, MS/MS, tandem mass spectrometry; PDGF, platelet-derived growth factor; Gpx, glutathione peroxidase; PHGpx, phospholipid hydroperoxide Gpx; KO, knock-out; JNK, c-Jun N-terminal kinase.

acid ($-SO_3H$) during peroxide detoxification (20–22). When the catalytic Cys is overoxidized, the peroxidase activity is lost.

Structural studies from various species suggest that Prx proteins may exist as an α_2 homodimer or a doughnut-shaped $(\alpha_2)_5$ homodecamer (23–25). Two molecules of reduced Prxs form an α_2 homodimer, which in turn serves as a building block for decamer formation. According to x-ray crystallographic studies, the inter-molecular disulfide bond that occurs transiently during the catalytic cycle requires local unfolding because the distance between the catalytic Cys and the resolving Cys is too far apart at ~13 Å (24, 25). The latter effect destabilizes the dimer-dimer (DD) interface and, by extension, the decameric structure. The stability of the DD interface is quickly restored when the disulfide bond is reduced back to Cys-SH by thioredoxin. This completes a cycle of H_2O_2 catalysis by the Prx protein. If the mechanics of unfolding or the conditions for disulfide formation are unfavorable for various reasons, the catalytic Cys becomes overoxidized to sulfenic ($-SO_2H$) or sulfonic acid ($-SO_3H$) and loses its H_2O_2 catalytic activity. The DD interface of an overoxidized Prx dimer, however, appears to be more stable than that of a fully reduced Prx dimer, and it may in fact lead to a more compact decamer (23–25). Recent studies suggest that high molecular weight Prx may function as a molecular chaperone (26–28). The information above suggests that the redox status of the catalytic Cys and the molecular chaperone activities of Prx may be closely linked.

Human Prx1 and Prx2 are 91% homologous and 78% identical in their amino acid sequences. Are Prx1 and Prx2 duplicate proteins or do they have unique functions and regulatory mechanisms? Although Prx1 and Prx2 have been studied independently in a number of cell and animal systems, little information is available regarding this fundamental question. Studies of Prx1 knock-out (KO) and Prx2KO mice illustrate the complexity of addressing this deceivingly simple question. One of the major phenotypes of Prx1KO was uncontrolled cell proliferation and the development of tumors in certain cell types (29). This striking observation led to the suggestion that Prx1 may act as a tumor suppressor. This is contradictory to the proposed role of Prx1 in promoting cell survival, treatment resistance, and malignant progression of various cancer cells (1–16). Absence of Prx2, on the other hand, resulted in splenomegaly caused by the congestion of red pulp with hemosiderin accumulation in Prx2KO mice (30). No tumor development was observed in any cell types or tissues of Prx2KO mice. Based on this finding, it was suggested that Prx2 is essential for sustaining the life span of erythrocytes in mice. Although there are no data available comparing the levels of H_2O_2 in different tissues of the Prx1KO or Prx2KO mice, or between the same tissue or cells obtained from Prx1KO and Prx2KO mice, elevated levels of H_2O_2 were observed in certain tissues of both Prx1KO and Prx2KO mice. Obviously, reduced peroxide removal resulting from the absence of either Prx1 or Prx2 cannot offer an answer to the drastically different phenotypes observed in these studies. The above information and findings from various human cancer cells and tissues, however, clearly indicate the following: 1) Prx1 and Prx2 may not be identical in function and are distinguishable by their regulatory mechanisms; 2) maintaining an adequate level of these proteins may be important in keeping normal cell proliferation/apoptosis in check; 3) the functions of Prx1 and Prx2 may be regulated in a cell type- and tissue context-dependent manner; and 4) their functions would need to be tested (and interpreted) in light of the various genetic and environmental factors that could affect the molecular behavior of Prx1 and Prx2.

```
Prx1  MSSGNAKIGHPAPNFKATAVMPDGQFKDISLSDYKGKYVVFFFYPLDFTF

Prx2  MASGNARIGKPAPDFKATAVVDG-AFKEVKLSDYKGKYVVLFFYPLDFTF
      *:****:**:***:******: .  **::.**********:*********
                52              71          83
Prx1  VCPTEIIAFSDRAEEFKKLNCQVIGASVDSHFCHLAWVNTPKKQGGLGPM
                51              70
Prx2  VCPTEIIAFSNRAEDFRKLGCEVLGVSVDSQFTHLAWINTPRKEGGLGPL
      **********:***:*:**.*:*:*.****:* ****:***:*:*****:

Prx1  NIPLVSDPKRTIAQDYGVLKADEGISFRGLFIIDDKGILRQITVNDLPVG

Prx2  NIPLLADVTRRLSEDYGVLKTDEGIAYRGLFIIDGKGVLRQITVNDLPVG
      ****::*_.* :::******:****::*******.**:***********
                              173                     199
Prx1  RSVDETLRLVQAFQFTDKHGEVCPAGWKPGSDTIKPDVQKSKEYFSKQK
                              172                     198
Prx2  RSVDEALRLVQAFQYTDEHGEVCPAGWKPGSDTIKPNVDDSKEYFSKHN
      *****:********:**:******************:*:.*******::
```

FIGURE 1. **Alignment of the amino acid sequences of human Prx1 and Prx2.** The amino acid sequences of human Prx1 and Prx2 are aligned using ClustalW program (version 1.83) (53). Note that the amino acid corresponding to position 24 of Prx1 is missing in Prx2. The locations of the Cys residues are marked. In addition to the catalytic Cys and the resolving Cys, one extra Cys is shared by Prx1 and Prx2 at positions 71 and 70, respectively. The presence of Cys^{83} is unique to Prx1. Identical residues (*) and strong (:) or weak (.) homologous residues are indicated *below* the sequences. The amino acid residues located at the putative DD interface are *underlined*.

When we examined the amino acid sequences of human Prx1 and Prx2, we noted that in addition to the well characterized catalytic Cys (Cys^{52} in Prx1 and Cys^{51} in Prx2) and resolving Cys (Cys^{173} in Prx1 and Cys^{172} in Prx2) residues, there is a Cys^{83} that is unique to Prx1 and not found in Prx2 (Fig. 1). According to available structural information from various Prx species (24, 25), the Cys^{83} of human Prx1 appears to be located at the putative DD interface. The goal of this study was to investigate whether there is a functional and/or structural difference between human Prx1 and Prx2 at the protein level, and if so, whether Cys^{83} in Prx1 contributes to the difference. Our approach was to employ defined experimental systems and to compare the molecular behaviors of these two proteins side by side. We purified recombinant human Prx1 and Prx2 proteins and evaluated their peroxidase and molecular chaperone activities. We also examined the biochemical and structural characteristics of the $Cys^{83} \rightarrow$ Ser substituted Prx1 (Prx1C83S) with those of wild type Prx1 and Prx2. Based on the results from a combination of mutagenesis, biochemical, computer modeling, mass spectrometry, and x-ray crystallographic studies, we conclude that Prx1 and Prx2 are not redundant proteins and that the Cys^{83} of Prx1 plays a critical role in bestowing a distinctive identity on Prx1, which is not shared by Prx2.

EXPERIMENTAL PROCEDURES

Materials—Dithiothreitol (DTT), iodoacetamide (IAA), NADPH, hydrogen peroxide, citrate synthase, and insulin were obtained from Sigma. Tris-(2-carboxyethyl)phosphine hydrochloride was from Invitrogen. Malate dehydrogenase (MDH) was from Roche Applied Science.

Expression and Purification of Recombinant Proteins—The Prx1/pET-17b and Prx2/pET-17b vectors containing the entire coding regions of human Prx1 and Prx2 were constructed. Site-directed mutagenesis of Cys^{83} to Ser^{83} was performed to generate the Prx1C83S with the QuikChange mutagenesis kit (Stratagene) using the Prx1/pET-17b as a template. Recombinant human Prx1, Prx2, and Prx1C83S proteins were purified by sequential ion exchange chromatography and size exclusion chromatography as described previously (31). Briefly, the cell extract was loaded onto DEAE-Sepharose (GE Healthcare) and equilibrated with 20 mM Tris-Cl (pH 7.5). The proteins were dialyzed with 50 mM sodium phosphate buffer (pH 6.5). The dialyzed proteins were loaded onto SP-Sepharose (GE Healthcare) and equilibrated with 50 mM sodium phosphate buffer (pH 6.5). The bound proteins were eluted with a linear gradient of sodium chloride. The fractions containing Prx1, Prx2, or Prx1C83S were pooled, loaded onto Superdex 200 (16:60, GE Healthcare), and equilibrated with 50 mM sodium phosphate buffer (pH 7.0) containing 0.1 M NaCl. The fractions containing Prx1, Prx2, or Prx1C83S were pooled and stored at −80 °C. Unless otherwise specified, all proteins were treated with 0.5 mM DTT for 30 min prior to their use. DTT was removed with Hitrap desalting column (5 ml; GE Healthcare). Full-length clones of yeast thioredoxin (yTrx) and yeast thioredoxin reductase (yTR) were obtained from yeast genomic DNA (Clontech). The yTrx and yTR proteins were purified as described previously (32).

Peroxidase Activity Assay—The thioredoxin-dependent peroxidase activity of the purified Prxs was measured as described previously with minor modifications (32). A total of 1.1 μg each of Prx1, Prx2, or Prx1C83S was incubated in 50 mM Hepes (pH 7.0) containing 200 μM NADPH, 3 μM yTrx, and 1.5 μM yTR. The reaction mixture was incubated at 30 °C for 5 min, followed by the addition of a 10-μl aliquot of H_2O_2 at various concentrations. NADPH oxidation was monitored for the next 10 min by a decrease in absorbance at 340 nm measured with the Ultrospec 2100 pro (GE Healthcare) spectrophotometer.

Molecular Chaperone Activity Assay—Molecular chaperone activity was determined as described previously (33) by assessing the ability of the recombinant Prxs to inhibit the thermal aggregation of substrate proteins (26–28). Briefly, 1 μM of MDH, citrate synthase, or insulin was mixed with various concentrations of Prx1, Prx2, or Prx1C83S, in a degassed 50 mM Hepes (pH 7.0) solution containing 0.1 M NaCl. The reaction mixture was incubated at 45 °C for 30 min, and the increase of light scattering as a result of thermal aggregation of substrate proteins was monitored at 360 nm.

Statistical Analysis—Statistical significance was examined using Student's *t* tests. The two-sample *t* test was used for two group comparisons. Values were reported as means ± S.D. *p* values <0.05 were considered significant.

Western Blot Analysis—A total of 1.1 μg each of Prx1, Prx2, or Prx1C83S was incubated in 50 mM Hepes (pH 7.0) containing 200 μM NADPH, 3 μM yTrx, and 1.5 μM yTR. The reaction mixture was incubated at 30 °C for 5 min, and various concentrations of 10 μl H_2O_2 were added to the mixture. After 5 min of incubation, 0.6 μmol of IAA was added to block the residual free thiol (−SH) group. The reaction was allowed to go in the dark for 5 min and then quenched by adding 100 nmol of Tris-(2-carboxyethyl)phosphine hydrochloride. An aliquot of 100 ng of Prxs from each reaction mixture was taken and subjected to Western blot analysis with Prx1, Prx2, or Prx-$SO_{2/3}$H antibodies (Lab Frontier Life Science Institute, Seoul, Korea).

Gel Filtration Chromatography—A total of 0.45 mg each of Prx1, Prx1C83S, or Prx2 protein was loaded onto a Superdex 200 column (1.6 × 60 cm) equilibrated with buffer containing 50 mM sodium phosphate, pH 7.0, and 0.1 M NaCl. Thyroglobulin (699 kDa), aldolase (150 kDa), bovine serum albumin (67 kDa), and bovine trypsinogen (24 kDa) were used as molecular weight standards.

Intrinsic Tryptophan Fluorescence Spectroscopy—Intrinsic Trp fluorescence spectra were recorded using an LB-45 spectrofluorometer (PerkinElmer Life Sciences) with an excitation wavelength of 295 nm. Samples of Prx1, Prx1C83S, or Prx2 protein were used at a concentration of 10 μg/ml in 50 mM sodium phosphate buffer (pH 7.0) containing 0.1 mM NaCl. The excitation and emission band passes were set at 3 nm. Spectra were monitored from 300 to 500 nm at room temperature.

Homology Modeling—A model of decameric human Prx1 was built based on the atomic structure of well characterized bacterial Prx protein, AhpC (Protein Data Bank code 1YEP). A molecular operating environment (version 2005.06, Chemical Computing Group, Montreal, Canada) running on a G5 dual 2.7-GHz PowerPC workstation was used for homology modeling. The best intermediate model was energy-minimized to remove unfavorable van der Waals contacts. PyMOL (34) was used for analysis and illustration purposes.

Intact Protein Analysis by MALDI-TOF Mass Spectrometry—Samples of Prx1, Prx1C83S, or Prx2 in water, 0.1% trifluoroacetic acid were mixed with a solution of 3,5-dimethoxy-4-hydroxycinnamic acid, sinapinic acid matrix. Five pmol each of the proteins was applied to a sample plate. The MALDI micro-MX™ mass spectrometer (Waters, Milford, MA) was operated in positive linear mode (post acceleration dynode, 5 kV; sample period, 1 ns). Data acquisition was performed over the *m/z* ranges of 25,000–250,000. Mass spectra were calibrated by the default method and verified by using bovine serum albumin for external calibration.

In-solution Digestion of Recombinant Proteins with Trypsin—Samples of Prx1, Prx1C83S, or Prx2 proteins were diluted to 1 μM concentration with 10% acetonitrile, 40 mM ammonium bicarbonate buffer. After brief sonication to dissolve the samples, 200 μl each of protein solution was transferred to Eppendorf tubes. For some experiments, the protein solution was reduced with 20 μl of DTT (50 mM in 10% acetonitrile, 40 mM ammonium bicarbonate buffer) at 60 °C for 30 min. After it was cooled to room temperature, iodoacetamide solution was added (20 μl, 200 mM in 10% acetonitrile, 40 mM ammonium bicarbonate buffer), and the reaction mixture was incubated at room temperature for 30 min in the dark. A solution of sequencing grade trypsin (10 μg of trypsin dissolved in 500 μl of 10% acetonitrile, 40 mM ammonium bicarbonate buffer) was added to the mixture to achieve an enzyme/protein ratio of 1:10 (w/w). The solution was digested at 37 °C for 16 h.

MALDI-TOF Analysis of Trypsin-digested Peptides—After trypsin digestion, the peptide mixtures were dried in a Speedvac

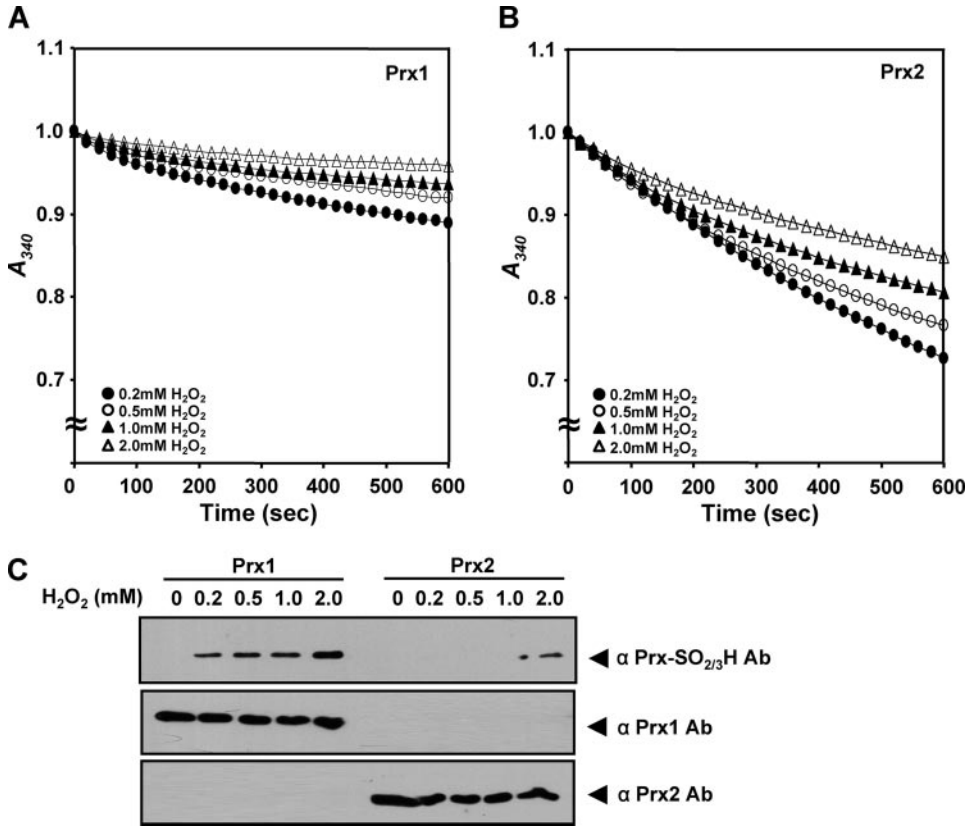

FIGURE 2. **Inactivation of human Prx1 and Prx2 peroxidase activity during H_2O_2 catalytic cycle.** *A,* reaction mixtures containing equal amounts of Prx1 were assayed for peroxidase activity with the increasing concentrations of H_2O_2 from 0.2 to 2.0 mM. The oxidation of NADPH was monitored at 30 °C by the decrease in absorbance at 340 nm (A_{340}). The results shown are the means of three independent experiments. *B,* inactivation of Prx2 peroxidase activity was monitored as described above. The results are the means of three independent experiments. *C,* effect of H_2O_2 on the overoxidation of the catalytic Cys in Prx1 and Prx2. The Prx1 and Prx2 proteins were reacted with the increasing concentrations of H_2O_2 and were subjected to Western blot analysis using a Prx-$SO_{2/3}$H antibody (*Ab*) (Lab Frontier Life Science Institute), which specifically recognizes the overoxidized catalytic Cys residue. Aliquots of samples were also probed with a Prx1 or a Prx2 antibody (Lab Frontier Life Science Institute). The experiments were repeated at least three times, and the representative blots are shown.

concentrator and dissolved in water containing 0.1% trifluoroacetic acid. Samples were mixed 1:1 (v/v) with 10 mg/ml α-cyano-4-hydroxycinnamic acid in 400:400:200 (v/v) acetonitrile/ethanol/water. A total of 1.3 μl of sample/matrix mixture was spotted onto a MALDI target plate, allowed to dry in air at room temperature, and analyzed on a MALDI micro MX™ mass spectrometer. The machine was operated in a positive reflectron mode with an accelerating voltage of 25 kV, and a time lag focusing delay of 500 ns. Data acquisition was performed over the *m/z* ranges of 900–4000. Calibration mixture containing polyethylene glycol in a range of molecular weights and sodium iodide was used to generate a multipoint external calibration. The MS data were externally corrected by using the adrenocorticotropic hormone as a lock mass.

Q-TOF Analysis of Trypsin-digested Peptides—A hybrid quadruple/orthogonal time-of-flight mass spectrometer Q-TOF API US (Waters, Milford, MA) was used to carry out a tandem mass spectrometry (MS/MS) analysis. Two μl of digested peptide solution were injected into the LC system (nanoACQUITY UPLC, Waters) that was interfaced with a Q-TOF mass spectrometer at a flow rate of 4 μl/min. The solution was pre-concentrated on a symmetry C18 column (180 μm × 20 mm; Waters). The peptides were eluted onto a nanoACQUITY C18 column (100 μm × 100 mm; Waters) and were separated over a 75-min period at a flow rate of 400 nl/min with a gradient of acetonitrile solution containing 0.1% formic acid. The samples were directed to the electrospray source. The Q-TOF mass spectrometer was operated in a positive ion mode with a source temperature of 120 °C and a cone voltage of 45 eV in V-mode. The collision energies were set at 10 and 30 V for MS and MS/MS scans, respectively. The MS/MS spectra were obtained in a data-dependent acquisition mode.

Crystallization, Data Collection, and Structure Solution—Human Prx1 was crystallized as described previously with minor modifications (35). The crystals were obtained by hanging drop vapor diffusion experiments using a reservoir solution of 100 mM citrate (pH 4.6) and 10% polyethylene glycol at a protein concentration of 15 mg/ml. X-ray diffraction data collection was carried out at the Cornell High Energy Synchrotron Source A-1 beam line. One hundred eighty 1° oscillation frames of data from one crystal were recorded on a CCD detector and processed with HKL2000 and SCALEPACK software packages (36). The space group is $P2_1$ and the unit cell dimensions are $a = 89.3$Å, $b = 111.1$Å, $c = 120.4$Å, $\beta = 111.8°$, with one complete decamer in the asymmetric unit. A total of 94,269 diffraction intensities was measured yielding 33,727 unique data to a maximum of 3.20 Å resolution. The overall *R*-merge for the data set was 0.152 and was 95.1% complete. The $I/\sigma I$ value for the data set was 8.16 overall and 1.75 in the highest resolution shell (3.31-3.20 Å). The structure was determined by the molecular replacement method using the AhpC structure as the search model and refined with Refmac5 in the CCP4 crystallographic package (37). After one cycle of refinement with tight noncrystallographic restraints (1980 amino acids and 15,520 atoms; no solvent molecules were included), the crystallographic *R*-factor and *R*-free values were 0.299 and 0.328, respectively. The root mean squared deviations from ideality of bond distances and angles are 0.023 Å and 2.14°, respectively, without any major violation in the Ramachandran plot.

RESULTS

Comparison of Peroxidase and Molecular Chaperone Activities of Prx1 and Prx2—To compare the H_2O_2 catalytic activities of human Prx1 and Prx2, the standard peroxidase reaction was carried out by using the yeast Trx system (yTrx, yTR, and

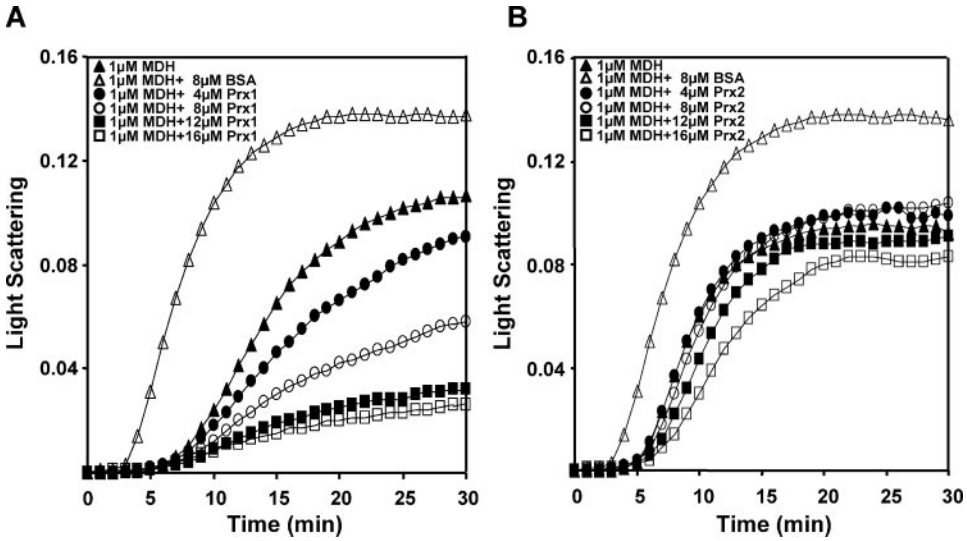

FIGURE 3. **Molecular chaperone activity of human Prx1 and Prx2.** The molecular chaperone activities of Prx1 (*A*) and Prx2 (*B*) were monitored by using MDH as a substrate. The effect of the increasing concentrations of Prx1 or Prx2 on the thermal aggregation of MDH (1 μM) was monitored at 45 °C for 30 min. The effect of bovine serum albumin (8 μM) on the MDH aggregation was evaluated as a negative control.

NADPH) as an electron donor. The activities were evaluated by monitoring the decrease in absorbance at 340 nm (A_{340}) because of the oxidation of NADPH. As shown in Fig. 2, *A* and *B*, the peroxidase activities of both Prx1 and Prx2 diminished progressively in a time-dependent manner as the concentration of H_2O_2 was increased from 0.2 to 2.0 mM, as evidenced by the increases of A_{340} values. However, the inactivation of Prx1 was much more severe than that of Prx2 at all H_2O_2 concentrations. The peroxidase activity of Prx2 was fairly well maintained with a concentration of H_2O_2 as high as 2.0 mM. Even at 600 s after starting the reaction, Prx2 was still capable of reducing H_2O_2 as evidenced by the appreciable decrease of an A_{340} value. Although the activities of Prx1 at 0.2 mM and 2.0 mM H_2O_2 were reduced to 36.5 ± 0.4 and 24.8 ± 0.2%, respectively, Prx2 activities remained at levels of 55.8 ± 1.1 and 35.7 ± 0.6% at those same respective concentrations of H_2O_2. In fact, the activity of Prx2 at 2.0 mM H_2O_2 was comparable with that of Prx1 at 0.2 mM H_2O_2. The degree of inactivation of Prx1 was greater than that of Prx2 at all concentrations with a p value of less than 0.001. The greater sensitivity of Prx1 to H_2O_2-induced inactivation was confirmed by probing with a Prx-$SO_{2/3}$H antibody that specifically recognizes the overoxidized (*i.e.* inactivated) catalytic Cys. Although the sulfenic/sulfonic (–$SO_{2/3}$H) form of Prx1 was detectable at all concentrations of H_2O_2, the overoxidation of Prx2 was visible only at a level of H_2O_2 greater than 1 mM (Fig. 2*C*).

Next, we compared the molecular chaperone activities of Prx1 and Prx2 by using MDH as a substrate. As shown in Fig. 3*A*, Prx1 displayed a robust capacity to suppress the thermal aggregation of MDH. The molecular chaperone activity of Prx1 increased in a concentration-dependent manner, peaking at 12 μM. In contrast, the chaperone activity of Prx2 was considerably less than that of Prx1 on an equimolar basis (Fig. 3*B*). Similar results were obtained when citrate synthase or insulin was used as a substrate (data not shown).

Effect of Cys^{83} to Ser^{83} Substitution of Prx1 on Peroxidase and Molecular Chaperone Activities—To investigate a possible role of Cys^{83} in influencing the function of Prx1, the Cys^{83} residue of Prx1 was replaced by Ser^{83}. Fig. 4*A* shows the peroxidase activity of Prx1C83S in the presence of increasing concentrations of H_2O_2. It is clear that the peroxidase function of Prx1C83S was robust and not as easily inactivated as the wild type Prx1 during H_2O_2 catalysis. In contrast to the wild type Prx1, a significant peroxidase activity was observed in Prx1C83S at all H_2O_2 concentrations. The activity of Prx1C83S at 2.0 mM H_2O_2 remained as high as 47 ± 1.0% at 600 s after starting the reaction. The peroxidase activities of Prx1 at 1.0 and 2.0 mM H_2O_2 are shown for comparison; the peroxidase activities of Prx1C83S were significantly greater than those of wild type Prx1 at both concentrations ($p < 0.001$). The resistance of Prx1C83S to overoxidation by H_2O_2 was confirmed by the negative Western blot data with a Prx-$SO_{2/3}$H antibody (Fig. 4*B*). Prx1C83S also appeared to have completely lost its ability to suppress the thermal aggregation of MDH (Fig. 4*C*). The chaperone activities of wild type Prx1 at 8 and 12 μM are shown for comparison.

The Oligomeric Status of Prx1 Differs Significantly from That of Prx2 and Prx1C83S—The results above suggest that the molecular properties of Prx1C83S are significantly changed from those of the wild type Prx1, and in a direction that resembles the characteristics of Prx2. Because the structure of Prxs may be closely linked to the peroxidase and molecular chaperone activities, we next carried out gel filtration chromatography to examine the oligomeric status of Prx1, Prx1C83S, and Prx2. The elution profile of Prx1C83S and Prx2 was significantly different from that of Prx1 (Fig. 5*A*). The position of Prx1 at its peak corresponded approximately to a molecular mass of 340 kDa, which is somewhat greater than the expected molecular mass (220 kDa) of a decameric structure. The position of Prx1C83S was similar to that of Prx2. The apparent molecular masses of Prx1C83S and Prx2 at their peaks were 57 and 67 kDa, respectively. These values were also slightly higher than the expected molecular mass of a dimer (44 kDa). Considering that hydrodynamic radius influences the elution pattern of a protein on gel filtration chromatography, it is likely that the differences between the expected and observed molecular masses resulted from the differential compactness of these proteins in solution. Nonetheless, the results strongly suggested the presence of differences in the oligomerization characteristics of Prx1 compared with that of Prx1C83S or Prx2.

We also examined the intrinsic tryptophan fluorescence profiles of Prx1, Prx1C83S, and Prx2 (Fig. 5*B*). The intensities of the Trp fluorescence spectra of Prx1 were much lower than those of

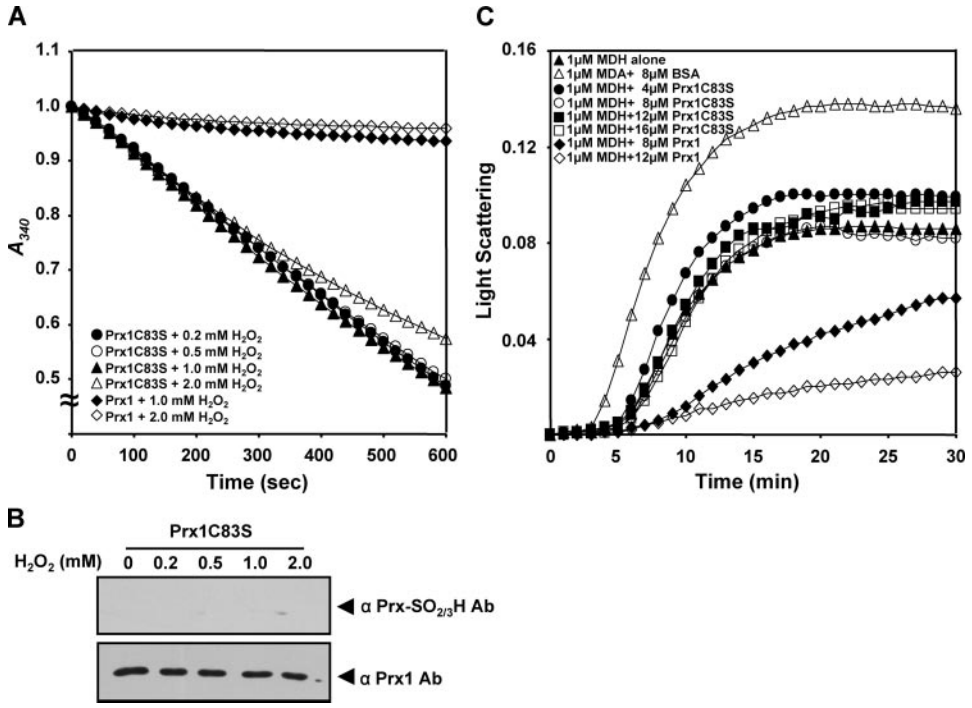

FIGURE 4. **Effect of Cys^{83} to Ser^{83} substitution on the peroxidase and molecular chaperone activities of human Prx1.** *A,* equal amount of Prx1C83S was reacted with the increasing concentration of H_2O_2. The absorbance at 340 nm (A_{340}) was monitored to evaluate the inactivation of Prx1C83S during the catalytic cycle. Values are the means of three independent experiments. *B,* equal amount of Prx1C83S was reacted with the increasing concentrations of H_2O_2 and was subjected to Western blot by using a Prx-$SO_{2/3}$H antibody (*Ab*) (Lab Frontier Life Science Institute). Aliquots of the same reaction mixture were probed with a Prx1 antibody. Representative blots from the three independent experiments are shown. *C,* molecular chaperone activity of Prx1C83S was determined by measuring its ability to inhibit the thermal aggregation of MDH. *BSA,* bovine serum albumin.

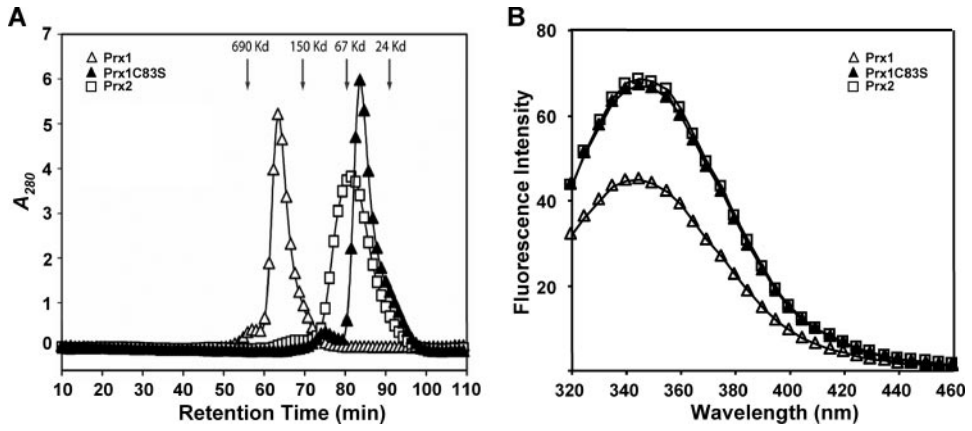

FIGURE 5. **Gel filtration chromatography and intrinsic Trp spectra analysis.** *A,* Prx1, Prx1C83S, or Prx2 protein was loaded onto Superdex-200 column pre-equilibrated with 50 mM sodium phosphate buffer (pH 7.0) containing 0.1 M NaCl. The samples were eluted at a flow rate of 1 ml/min. *Arrows* indicate the elution positions of the molecular weight standards. *B,* intrinsic Trp fluorescence spectra of Prx1, Prx1C83S, or Prx2 were recorded with an excitation wavelength of 295 nM. The excitation and emission band passes were set at 3 nm. Spectra were monitored from 300 to 500 nm at room temperature.

Prx1C83S and Prx2. Lower intensities in the Prx1 Trp spectra are indicative of a greater propensity to form an oligomeric structure (38). Consistent with the result obtained from the gel filtration study, the Trp fluorescence spectra indicated that the tertiary packing property of Prx1 is significantly different from that of Prx1C83S or Prx2.

Molecular Mass Determination by Mass Spectrometry Reveals That Prx1 Is Present as a Decamer, whereas Prx2 and Prx1C83S Are Primarily in a Dimeric Form—MALDI-TOF mass spectrometry was employed to determine the molecular masses of the intact Prx1, Prx2C83S, and Prx2 proteins in high resolution. The molecular mass/charge (*m/z*) values of 219,746.17, 110,201.47, 73,554.93, and 55,373.06 represent the singly, doubly, triply, and quadruply charged Prx1 decamer, respectively, further corroborating that Prx1 is present predominantly as a decamer (Fig. 6*A*). The minor peaks at *m/z* of 44,202.26 and 882,902.29 represent the singly charged Prx1 dimer and tetramer ion, respectively. We found that the decamer signature of Prx1 is completely lost in Cys^{83}- to Ser^{83}-substituted Prx1. As shown in Fig. 6*B*, Prx1C83S is present predominantly in a dimeric form. The intense signal shown at *m/z* value of 44,000.22 represents a Prx1C83S dimer with a charge state of +1. The weak signal of the Prx1C83S tetramer ion is detected at *m/z* value of 88,286.76. Consistent with the functional similarity between Prx1C83S and Prx2, Prx2 is also present primarily as a dimer (Fig. 6*C*). The intense peak at *m/z* of 43,627.27 is a Prx2 dimer with a charge state of +1. Similar to Prx1C83S, a weak signal of the Prx2 tetramer ion (*m/z* 87,373.28) was also detected. The molecular mass determination of intact protein by MALDI-TOF mass spectrometry is highly accurate. The % errors of all the experimental *m/z* values were less than 0.5% of the theoretical values (Table 1), except for the singly charged Prx1 decamer ion in which the % error of experimental mass is 0.55%.

The Cys^{83} of Prx1 Is Located at the Dimer-Dimer Interface—To gain insight as to how Cys^{83} may impact on the structural and functional characteristics of Prx1, we carried out a homology modeling study. Because the crystal structure of human Prx1 has not been determined, the atomic structure of the well characterized bacterial Prx, AhpC (Protein Data Bank code 1YEP), was used as a basis for homology modeling. Our modeling results indicated that the

DD interface of human Prx1 decamer contains a local 2-fold symmetry axis close to Cys^{83} of each peptide chain. The Cys^{83} residue in either $\chi_1 = -180°$ or $\chi_1 = -60°$ conformation packs at the DD interface in a manner similar to the packing of AhpC. The distance between the two Cys residues is at (Cys^{83} at $\chi_1 = -180°$) or slightly above (Cys^{83} at $\chi_1 = -60°$) the sum of van der Waals radii, thus ensuring a tight fit and perhaps entropic gain because of the burial of hydrophobic surfaces. Fig. 7 illustrates the DD interface of the Prx1 decamer model with the Cys^{83} side chain in $\chi_1 = -180°$ conformation. The presence of the Asp^{79} and Asp^{47} pairs at the DD interface does not appear to be destabilizing, because the side chains are likely be shielded by water molecules at the interface as is the case with the AhpC crystal structure. Consequently, repulsive negative charges at the DD interface or energy costs for burial of charged side chains are probably of little concern.

The Cys^{83} Residue of Prx1 Is Oxidized under an Ambient Atmosphere—Because of the specific location of Cys^{83} at the DD interface, we questioned whether the disulfide bond between the dimer units contributes to the preferential decamer structure of Prx1. Although the distance between the two dimer Cys^{83} sulfur atoms (2.42 Å) is slightly longer than the ideal disulfide bond distance of 2.03 Å (39), a Cys^{83}–Cys^{83} disulfide bond appears to be plausible with some adjustment to the backbone conformation in this region. We looked for a Cys^{83}–Cys^{83}-containing peptide ion or the MS/MS fragments of such ion by using MALDI-TOF and Q-TOF mass spectrometry, respectively. We did not find corresponding molecular masses under the experimental conditions that we tested. Nonetheless, when we analyzed the tryptic digests of Prx1 by MALDI-TOF, the 68–92 peptide that contains the reduced Cys^{83} was not detected, indicating that Cys^{83} may be oxidized under an ambient atmosphere. As shown in Fig. 8*A*, except for the 68–92 residue, the Cys^{52} containing the 38–62 peptide ion (*m/z* 3036.7607) and the Cys^{173} containing the 169–190 peptide ion (*m/z* 2349.2420) were clearly detected. The fact that the 68–92 ion (*m/z* 2751.6653) was clearly detected in Prx1C83S (Fig. 8*B*) further corroborated the idea that the loss of the 68–92 peptide signal in the wild type Prx1 may be because of the oxidation of Cys^{83}. The theoretical and experimental masses as well as the sequences of

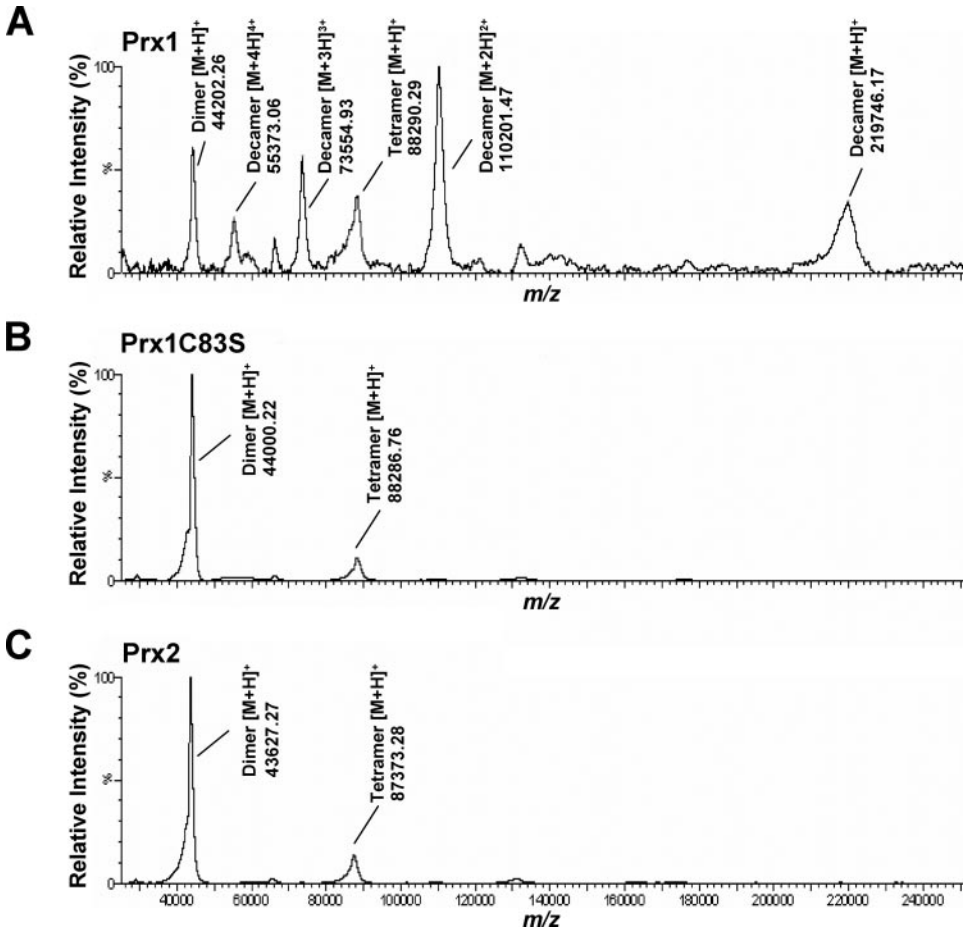

FIGURE 6. **MALDI-TOF mass spectrum of intact human Prx1, Prx1C83S, and Prx2 proteins.** The oligomeric status of Prx1 (*A*), Prx1C83S (*B*), and Prx2 (*C*) was determined by measuring the accurate molecular masses of the intact proteins by MALDI-TOF mass spectrometry.

TABLE 1
Theoretical and experimental molecular masses of Prx1, Prx1C83S, and Prx2 protein ions

		Dimer $[M + H]^+$	Tetramer $[M + H]^+$	Decamer			
				$[M + H]^+$	$[M + 2H]^{2+}$	$[M + 3H]^{3+}$	$[M + 4H]^{4+}$
Prx1	Theoretical	44,192.55	88,385.11	220,962.79	110,482.39	73,655.26	55,241.70
	Experimental	44,202.26	88,290.29	219,746.17	110,201.47	73,554.93	55,373.06
	% error	0.02	0.11	0.55	0.25	0.14	0.24
Prx1C83S	Theoretical	44,160.42	88,320.85	220,802.12	110,402.06	73,601.71	55,201.53
	Experimental	44,000.22	88,286.76	ND[a]	ND	ND	ND
	% error	0.36	0.04				
Prx2	Theoretical	43,756.48	87,512.95	218,782.38	109,392.19	72,928.46	54,696.60
	Experimental	43,627.27	87,373.28	ND	ND	ND	ND
	% error	0.30	0.16				

[a] ND indicates not detected.

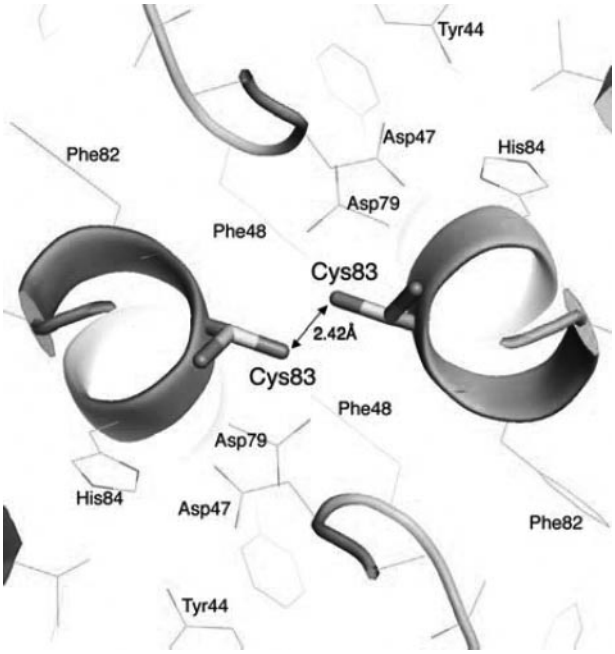

FIGURE 7. **Structure of human Prx1 at the DD interface.** A decamer structure of Prx1 was built based on the crystal structure of AhpC (Protein Data Bank code 1YEP). A close up of the Cys^{83} residue-containing region shows that Cys^{83} is proximal to the local 2-fold related Cys^{83} at the dimer-dimer interface. When the two Cys^{83} side chains are modeled in $\chi_1 \sim -180°$ conformation, the S-γ atoms have a closest approach distance of 2.42 Å.

the 38–62, 68–92, and 169–190 residues of Prx1 and Prx1C83S are shown in Table 2.

To test whether the disappearance of the Cys^{83}-containing peptide in Prx1 is because of the oxidation of Cys^{83}, an aliquot of Prx1 was incubated with DTT, and the thiol (–SH) moieties were alkylated with IAA. The MALDI-TOF analysis revealed that the 68–92 residue with the *m/z* of 2881.6497 was fully restored in the DTT-treated and -alkylated wild type Prx1 digests. Fig. 8*C* shows an overlay of the isotopic clusters of the alkylated 68–92 peptide ion of Prx1 with or without DTT treatment. In contrast, when the 68–92 peptide ion of Prx1C83S was alkylated with or without DTT treatment, no difference was observed. Fig. 8*D* displays an overlay of the isotopic clusters of the alkylated 68–92 of Prx1C83S at *m/z* values of 2808.6533 (with DTT) and 2808.5066 (without DTT). These results further confirmed that the oxidation of Cys^{83} contributes to the loss of the 68–92 ion signal of wild type Prx1.

The Cys^{83}-Cys^{83} Disulfide Bond Is Present at the Dimer-Dimer Interface of Prx1 Decamer—X-ray crystallographic studies were conducted to determine the three-dimensional structure of human Prx1 protein. The crystal structure determined at 3.2 Å (*R*-factor value of 0.299 and *R*-free value of 0.328) clearly demonstrated that human Prx1 is present as a decamer, in which five homodimers associate around a local 5-fold rotational axis forming a doughnut-shaped oligomer (Fig. 9*A*). The crystallographic data also provided direct evidence that the Cys^{83} residues at the DD interfaces are all involved in the formation of disulfide bridges across dimers. The electron density maps of the five interfaces show the presence of disulfide bonds at DD interfaces (Fig. 9*B*), demonstrating that Prx1 is locked into a decameric form through interfacial disulfide bond formation. One homodimeric Prx1 molecule is shown in Fig. 9*C*, pointing out the locations of interfacial Cys^{83}–Cys^{83} disulfide bonds. The locations of the Cys^{52} and Cys^{172} residues are shown for reference. Given that the Cys^{52} residue is approximately 13 Å apart from the Cys^{173} in each homodimer unit, it is unlikely that the Cys^{52} and Cys^{172} are linked by a disulfide bond. The overoxidation status of Cys^{52} could not be ascertained from the crystallographic information.

DISCUSSION

Human Prx1 and Prx2 have been studied independently in a number of cell and animal systems and have been shown to influence the survival, proliferation, and treatment response of cancer cells. In this study, we demonstrated that human Prx1 and Prx2 possess unique functions and regulatory mechanisms. Prx1 displays a greater molecular chaperone activity than Prx2 as assessed by its ability to inhibit the thermal aggregation of substrate proteins such as MDH. The peroxidase activity of Prx1, on the other hand, is more susceptible to inactivation by H_2O_2 than that of Prx2. Consistent with this finding, the catalytic Cys residue of Prx1 is more prone to overoxidation than that of Prx2. Amino acid sequence analysis indicates that there is a cysteine residue at position 83 that is unique to Prx1. Our mutagenesis, biochemical, mass spectrometry, computer modeling, and x-ray crystallographic results are congruent with the hypothesis that the redox-sensitive Cys^{83} of human Prx1 plays an important role in modifying the molecular characteristics of Prx1. The substitution of Cys^{83} to Ser^{83} (Prx1C83S) results in dramatic changes in the structural and functional properties of human Prx1 in a direction that aligns more closely to human Prx2.

Our results show that compared with Prx1, the peroxidase activity of Prx2 is not as easily inactivated as Prx1 during a catalytic cycle. Although our studies are done using purified proteins in cell-free systems, we propose that Prx2 may be physiologically better suited as a peroxidase enzyme. This hypothesis is consistent with the recent study demonstrating the H_2O_2 catalytic activity of Prx2 in regulating PDGF signaling. Prx2, but not Prx1, translocates to the membrane and eliminates H_2O_2 that was generated upon PDGF receptor activation in response to PDGF binding to the receptor (40). The catalytic Cys residue of Prx2 is not overoxidized in this condition. According to the available x-ray crystallographic information and the results presented in this study, the regional structure surrounding the active site Cys appears to differ between Prx1 and Prx2; the catalytic Cys in Prx1 appears to be surrounded by several hydrophobic residues (41), whereas access to the active site Cys in Prx2 appears to be restricted by Phe^{81} of the adjacent Prx2 dimer (23). This may account in part for the resistance of Prx2 to overoxidation during the catalytic cycle. Because the *de novo* synthesis of H_2O_2 during PDGF signaling is likely occur in a very restricted region localized around the PDGF receptor, a preferential translocation of Prx2 from the cytosol to the membrane may also contribute to the peroxidase function of Prx2 during PDGF signaling.

The Cys^{83} residue of Prx1 is located at the DD interface. Sequence alignment indicates that Cys^{83} is conserved only in mammalian Prx1, including human, bovine, rat, and mouse, but

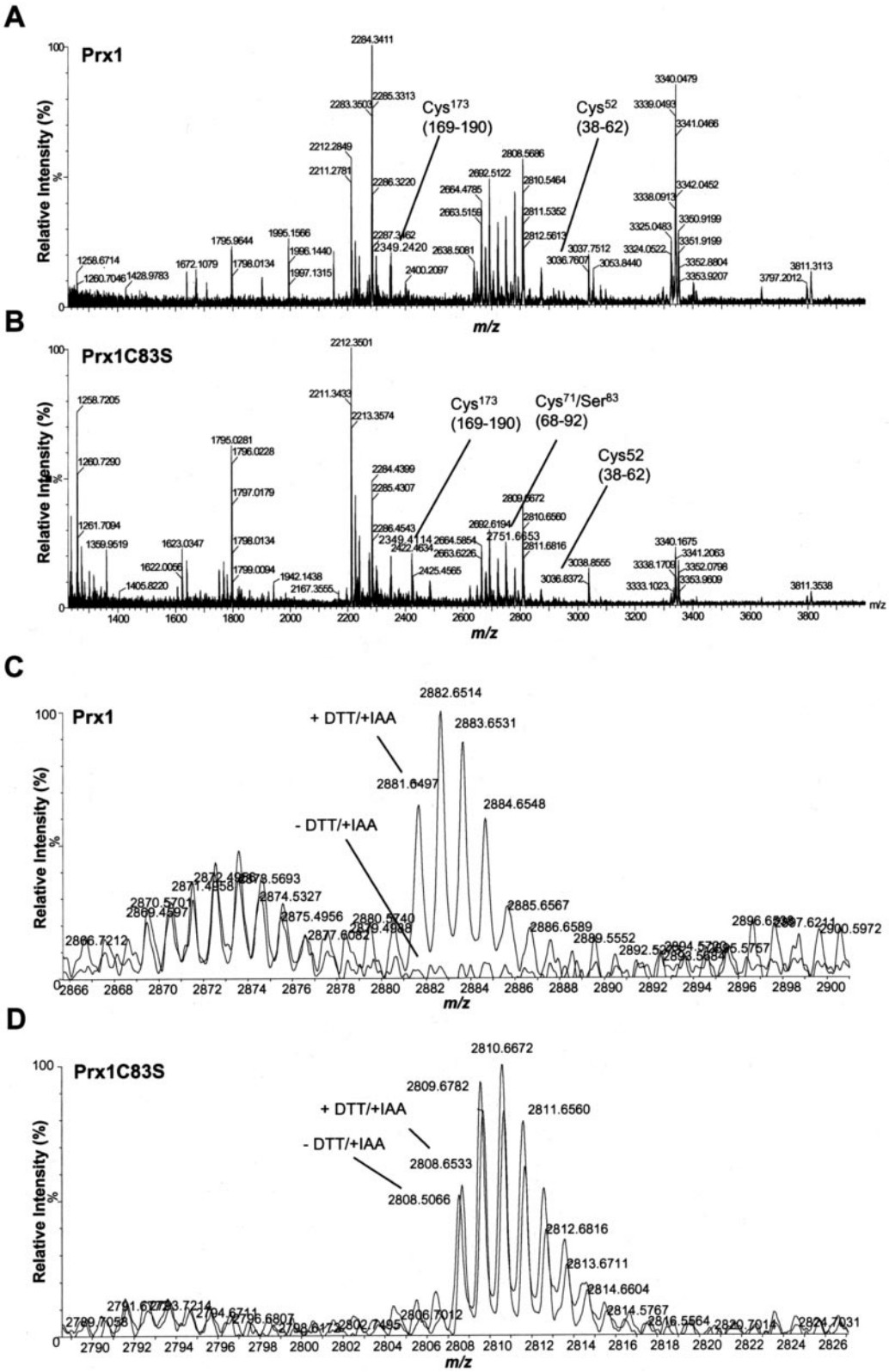

FIGURE 8. **Analysis of digested human Prx1 and Prx1C83S by MALDI-TOF mass spectrometry.** *A,* Prx1 protein was digested with trypsin, and MALDI-TOF mass spectrometry was performed in a positive reflectron mode. The locations of the peptide ions containing the Cys^{52} and Cys^{173} residue are marked. *B,* MALDI-TOF mass spectra of the trypsin-digested Prx1C83S. The locations of the peptide ions containing the Cys^{52}, Cys^{71}/Ser^{83}, and Cys^{173} are marked. *C,* Cys residues in Prx1 were alkylated with IAA followed by the presence (+DTT/+IAA) or absence (−DTT/+IAA) of DTT treatment. The protein was digested with trypsin and subjected to MALDI-TOF mass spectrometry, and the natural isotopic patterns of the Cys^{83} containing peptide ion were obtained. Note the restoration of the Cys^{83}-containing peptide ion with the *m/z* value of 2881.6497 in the DTT-treated sample (+DTT/+IAA). The theoretical *m/z* value of Cys^{72}- and Cys^{83}-alkylated 68–92 peptide ion is 2881.4221. *D,* natural isotopic patterns of the alkylated Cys^{83}-containing peptide ion at 2808.6533 (+DTT/+IAA) were overlaid with those of the 2808.5066 ion (−DTT/−IAA). The theoretical *m/z* value of Cys^{72} alkylated 68–92 Prx1C83S peptide ion is 2808.4208.

TABLE 2

Theoretical and experimental molecular masses of the Cys^{52}-, Cys^{71}/Cys^{83}-, Cys^{71}/Ser^{83}-, and Cys^{173}-containing peptide ions of Prx1 and PrxC83S tryptic digests

The underline indicates the position of the Cys residue. The location of the Ser^{83} is also underlined.

	Residues	Peptide sequence	Theoretical $[M + H]^+$	Experimental $[M + H]^+$
Prx1	38–62	(K)YVVFFFYPLDFTFVCPTEIIAFSDR(A)	3036.4900	3036.7607
	68–92	(K)KLNCQVIGASVDSHFCHLAWVNTPK(K)	2767.3800	ND[a]
	169–190	(K)HGEVCPAGWKPGSDTIKPDVQK(S)	2349.1700	2349.2420
Prx1C83S	38–62	(K)YVVFFFYPLDFTFVCPTEIIAFSDR(A)	3036.4900	3036.8372
	68–92	(K)KLNCQVIGASVDSHFSHLAWVNTPK(K)	2751.3134	2751.6653
	169–190	(K)HGEVCPAGWKPGSDTIKPDVQK(S)	2349.1700	2349.4114

[a] ND indicates not detected.

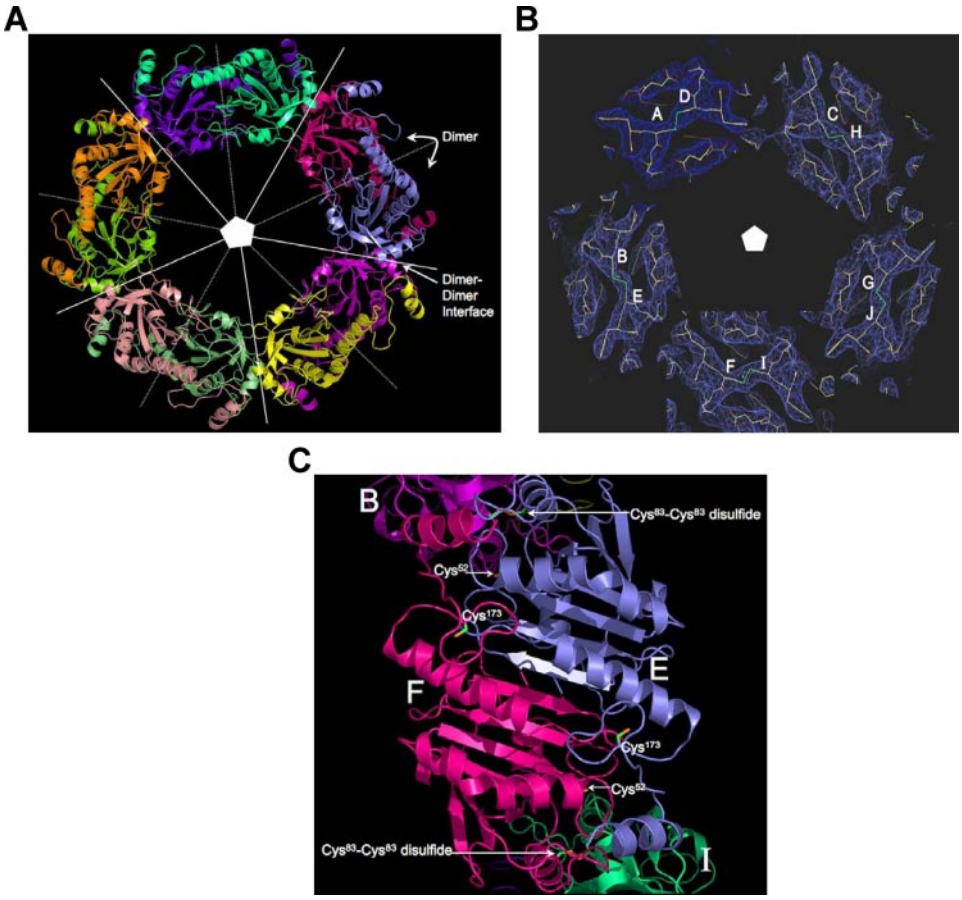

FIGURE 9. **The presence of Cys^{83}-Cys^{83} disulfide bond at the DD interface of the decameric structure of human Prx1.** *A,* ribbon diagram of the decameric structure of human Prx1 as determined at 3.2 Å resolution. Each polypeptide chain is shown in a different color. The DD interface and the homodimer serving as a building block for a decamer are indicated. The 5-fold rotational symmetry axis is at the center of the doughnut-shaped structure and nearly perpendicular on its plane. *B,* five sections of electron density maps (drawn in *blue*) from five DD interfaces showing the experimental electron densities of the Cys^{83}–Cys^{83} disulfide bonds (in *green*) at the DD interfaces of a decameric Prx1. The sections are arranged about the 5-fold rotation axis to illustrate the orientations of the dimers. Homodimer pairs are labeled as *A-B, C-D, E-F, G-H,* and *I-J. C,* close-up view of a Prx1 dimer along the local 2-fold rotational symmetry axis. The locations of the Cys^{52} and domain-swapped Cys^{173} in monomers E and F are shown. Two Cys^{83}–Cys^{83} disulfide bonds linking the EF dimer to AB and IJ dimers at the DD interfaces are also visible.

not in bacteria, yeast, or parasite orthologs of Prxs (Fig. 10). We propose that Cys^{83} may have been gained later in evolution, perhaps for the functional specialization of Prx1 in mammalian species. Our results indicate that Cys^{83} may increase the affinity between the dimers at the DD interface, thereby enabling the formation of a decamer as a preferred structure. How might the substitution of Cys^{83} to Ser^{83} decrease the stability of the DD interface? A disulfide bridge across the DD interface may be a possibility. Our crystallographic analysis of the molecular structure of human Prx1 demonstrated the presence of Cys^{83}–Cys^{83}-linked disulfide bond at each of the five DD interfaces of the decameric Prx1. Although our mass spectrometry studies provided an accurate molecular mass corresponding to the Prx1 decamer, we were not able to detect the Cys^{83}–Cys^{83}-linked peptide ion under the mass spectrometry conditions that were tested. It is possible that our inability to obtain a Cys^{83}–Cys^{83} peptide ion or its fragments could result from deformation of the peptide during the gas phase ionization by some unknown mechanisms. Because the nonbonded contact distance is very close (the nonbonded S–S distance is ≈2.42Å at $\chi_1 = -180°$ or ≈4.0Å at $\chi_1 = -60°$) with a possible entropic gain of a hydrophobic surface, we cannot exclude the possibility that Prx1 could pack tightly at the DD interface without having to form a Cys^{83}–Cys^{83} covalent linkage across the dimers. A Ser^{83} substitution is likely to alter the DD interface in at least two ways. First, it makes the surface less hydrophobic and more polar. Second, the van der Waals radius of oxygen (in Ser^{83}) is 1.40 Å, as opposed to 1.85 Å for sulfur (in Cys^{83}). Thus, Ser will render the DD packing less tight. These consequences would have a destabilizing effect in Ser^{83}-substituted Prx1 and make decamer formation energetically less favorable.

How might the structural property of Prx1 explain its molecular chaperone activity and greater sensitivity to inactivation by H_2O_2? According to the previously proposed mechanism (24, 25), the H_2O_2 catalytic cycle of Prxs requires a decamer to dimer transition through local unfolding of the loops containing the catalytic Cys^{52} and the Cys^{173}. If Cys^{83} stabilizes the DD interface of Prx1 and discourages local unfolding, the active site Cys engaged in a catalytic cycle would not be able to form an inter-molecular disulfide bond and its subsequent reduction by

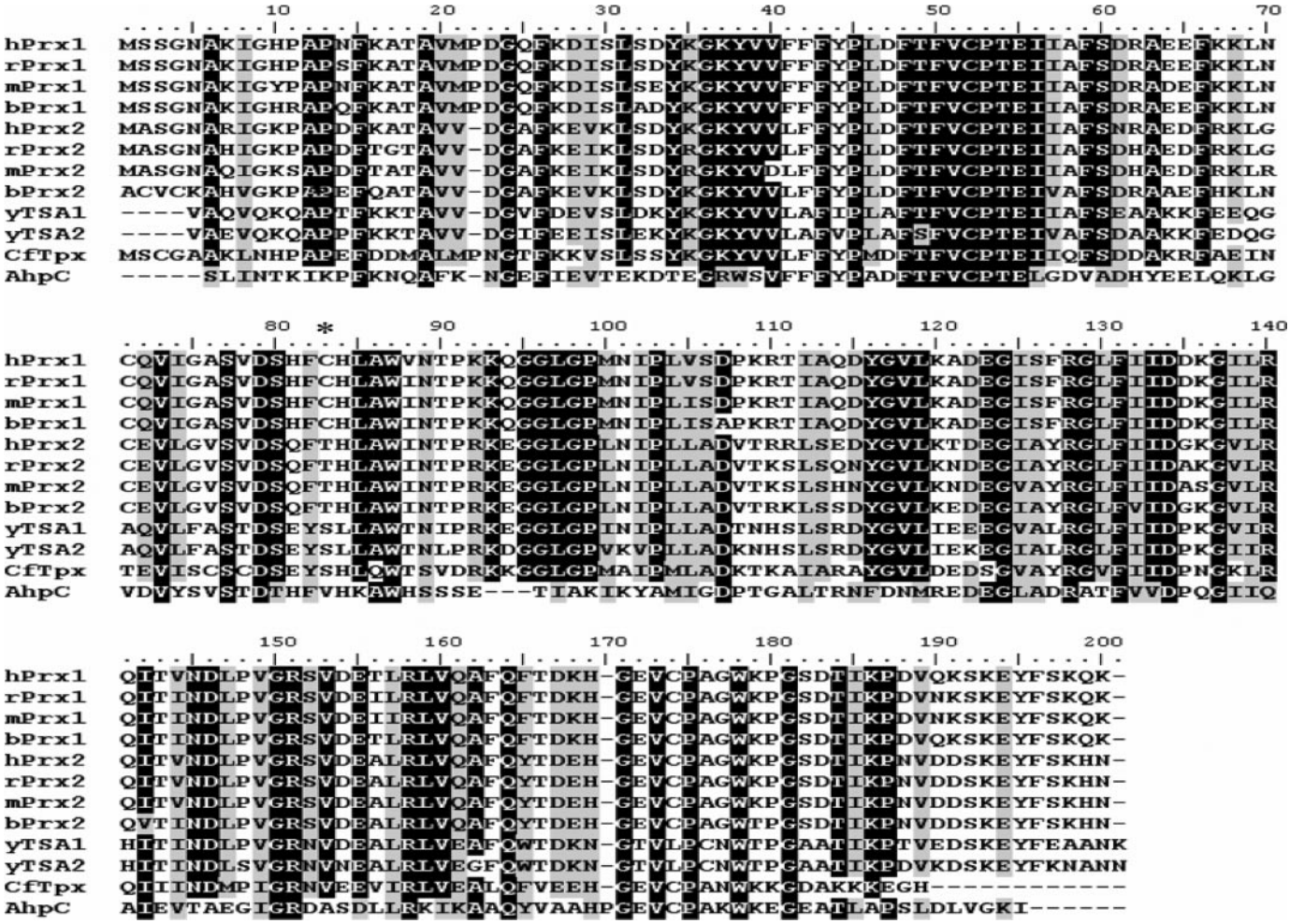

FIGURE 10. **Multiple sequence alignments of mammalian Prx1, Prx2, and Prx orthologs across species.** The respective Prx1 and Prx2 amino acid sequences of human (*hPrx1* and *hPrx2*), rat (*rPrx1* and *rPrx2*), mouse (*mPrx1* and *mPrx2*), and bovine (*bPrx1* and *bPrx2*) are aligned with those of *Saccharomyces cerevisiae* (yTSA1 and yTSA2), *Crithidia fasciculata* (*CfTpx*), and *Salmonella typhimurium* (*AhpC*) Prx orthologs using ClustalW. The conserved (identical or similar) amino acid residues are shown by *shading*; *darker shading* indicates identical residues, and *lighter shading* indicates similar residues. The location of the Cys residue corresponding to the Cys^{83} of human Prx1 is marked with an *asterisk*.

thioredoxin to complete the cycle. As a result, Prx1 is more prone to overoxidation, which in turn may lead to a more stable and compact oligomeric structure. This property may explain why Prx1 is a better molecular chaperone than Prx2. An interesting analogy appears to exist in the isoforms of glutathione peroxidase (Gpx). Although several Gpx isoforms act primarily as an antioxidant peroxidase, the phospholipid hydroperoxide Gpx (PHGpx) forms a capsule around sperm mitochondrion in the testis (42, 43). The PHGpx in the capsule is oxidatively cross-linked and enzymatically inactive. Because both Prx and Gpx systems utilize NADPH as an ultimate reducing source, the functions of the two peroxidase systems can be complementary or inter-dependent in certain cell types and tissues. Similar to the Prx system, functional specialization of the Gpx system might have been developed during evolution.

Lines of evidence suggests that overoxidation of the catalytic Cys may allow a mechanism of structural and functional switching of Prx from a peroxidase enzyme to a molecular chaperone. This hypothesis is consistent with the behavior of Prx1 in interacting physically with various cellular proteins. Using a yeast two-hybrid system, the interaction of Prx1 with the Src homology 3 domain of c-Abl, the Myc Box II domain of c-Myc, and the macrophage inhibiting factor has been demonstrated (44–46). We recently reported that Prx1 suppresses radiation-induced JNK signaling and apoptosis in lung cancer cells (31). Our results demonstrated that the JNK inhibitory effect is mediated through the interaction of Prx1 with the GSTpi-JNK complex, thereby preventing JNK release from the complex. The interaction of Prx1 with growth regulatory and signaling proteins may be responsible for the wide range of effects attributed to Prx1 (29, 47–50). Whether Prx2 behaves similarly to Prx1 in this respect is presently unknown.

In addition, the regulation of Prx1 and Prx2 expression appears to vary widely among different cell types. In the brain, Prx1 is expressed in astrocytes, whereas Prx2 is expressed in neurons (51). Prx1 is preferentially expressed in the Leydig cells, whereas Prx2 predominates in the Sertoli cells in the testis (52). These observations indicate that the cell type- and tissue-specific expression of Prx1 and Prx2 would also contribute to their respective activities in certain cells and tissues, but not in others. In this study, we provide

evidence to support the existence of inherent structural and functional differences between Prx1 and Prx2 at the protein level. We show that the differences between the two highly homologous proteins are attributable in part to the unique presence of Cys^{83} in Prx1. The significance of this study is underlined by the realization that the differential molecular characteristics of Prx1 and Prx2 would continue to influence their molecular behaviors in various biological systems and also under a diverse environmental and genetic context. The information obtained in this study would provide a conceptual framework for further studies to delineate the physiological (or pathophysiological) functions of Prx1 and Prx2.

Acknowledgments—MALDI- and Q-TOF mass spectrometry studies were supported by the Proteomics Resources at Roswell Park Cancer Institute.

REFERENCES

1. Rhee, S. G., Kang, S. W., Chang, T. S., Jeong, W., and Kim, K. (2001) *IUBMB Life* **52,** 35–41
2. Yanagawa, T., Iwasa, S., Ishii, T., Tabuchi, K., Yusa, H., Onizawa, K., Omura, K., Harada, H., Suzuki, H., and Yoshida, H. (2000) *Cancer Lett.* **156,** 27–35
3. Qi, Y., Chiu, J. F., Wang, L., Kwong, D. L., and He, Q. Y. (2005) *Proteomics* **5,** 2960–2971
4. Shen, J., Person, M. D., Zhu, J., Abbruzzese, J. L., and Li, D. (2004) *Cancer Res.* **64,** 9018–9026
5. Yanagawa, T., Ishikawa, T., Ishii, T., Tabuchi, K., Iwasa, S., Bannai, S., Omura, K., Suzuki, H., and Yoshida, H. (1999) *Cancer Lett.* **145,** 127–132
6. Chang, J. W., Jeon, H. B., Lee, J. H., Yoo, J. S., Chun, J. S., Kim, J. H., and Yoo, Y. J. (2001) *Biochem. Biophys. Res. Commun.* **289,** 507–512
7. Lehtonen, S. T., Svensk, A. M., Soini, Y., Paakko, P., Hirvikoski, P., Kang, S. W., Saily, M., and Kinnula, V. L. (2004) *Int. J. Cancer* **111,** 514–521
8. Chang, J. W., Lee, S. H., Jeong, J. Y., Chae, H. Z., Kim, Y. C., Park, Z. Y., and Yoo, Y. J. (2005) *FEBS Lett.* **579,** 2873–2877
9. Kim, H. J., Chae, H. Z., Kim, Y. J., Kim, Y. H., Hwangs, T. S., Park, E. M., and Park, Y. M. (2003) *Cell Biol. Toxicol.* **19,** 285–298
10. Kinnula, V. L., Paakko, P., and Soini, Y. (2004) *FEBS Lett.* **569,** 1–6
11. Kinnula, V. L., Lehtonen, S., Sormunen, R., Kaarteenaho-Wiik, R., Kang, S. W., Rhee, S. G., and Soini, Y. (2002) *J. Pathol.* **196,** 316–323
12. Noh, D. Y., Ahn, S. J., Lee, R. A., Kim, S. W., Park, I. A., and Chae, H. Z. (2001) *Anticancer Res.* **21,** 2085–2090
13. Karihtala, P., Mantyniemi, A., Kang, S. W., Kinnula, V. L., and Soini, Y. (2003) *Clin. Cancer Res.* **9,** 3418–3424
14. Park, S. H., Chung, Y. M., Lee, Y. S., Kim, H. J., Kim, J. S., Chae, H. Z., and Yoo, Y. D. (2000) *Clin. Cancer Res.* **6,** 4915–4920
15. Iwao-Koizumi, K., Matoba, R., Ueno, N., Kim, S. J., Ando, A., Miyoshi, Y., Maeda, E., Noguchi, S., and Kato, K. (2005) *J. Clin. Oncol.* **23,** 422–431
16. Chen, M. F., Keng, P. C., Shau, H., Wu, C. T., Hu, Y. C., Liao, S. K., and Chen, W. C. (2006) *Int. J. Radiat. Oncol. Biol. Phys.* **64,** 581–591
17. Chung, Y. M., Yoo, Y. D., Park, J. K., Kim, Y. T., and Kim, H. J. (2001) *Anticancer Res.* **21,** 1129–1133
18. Zhang, P., Liu, B., Kang, S. W., Seo, M. S., Rhee, S. G., and Obeid, L. M. (1997) *J. Biol. Chem.* **272,** 30615–30618
19. Yo, Y. D., Chung, Y. M., Park, J. K., Ahn, C. M., Kim, S. K., and Kim, H. J. (2002) *Exp. Mol. Med.* **34,** 273–277
20. Rabilloud, T., Heller, M., Gasnier, F., Luche, S., Rey, C., Aebersold, R., Benahmed, M., Louisot, P., and Lunardi, J. (2002) *J. Biol. Chem.* **277,** 19396–19401
21. Wagner, E., Luche, S., Penna, L., Chevallet, M., Van Dorsselaer, A., Leize-Wagner, E., and Rabilloud, T. (2002) *Biochem. J.* **366,** 777–785
22. Yang, K. S., Kang, S. W., Woo, H. A., Hwang, S. C., Chae, H. Z., Kim, K., and Rhee, S. G. (2002) *J. Biol. Chem.* **277,** 38029–38036
23. Schroder, E., Littlechild, J. A., Lebedev, A. A., Errington, N., Vagin, A. A., and Isupov, M. N. (2000) *Structure* (*Lond.*) **8,** 605–615
24. Wood, Z. A., Schroder, E., Robin Harris, J., and Poole, L. B. (2003) *Trends Biochem. Sci.* **28,** 32–40
25. Parsonage, D., Youngblood, D. S., Sarma, G. N., Wood, Z. A., Karplus, P. A., and Poole, L. B. (2005) *Biochemistry* **44,** 10583–10592
26. Jang, H. H., Lee, K. O., Chi, Y. H., Jung, B. G., Park, S. K., Park, J. H., Lee, J. R., Lee, S. S., Moon, J. C., Yun, J. W., Choi, Y. O., Kim, W. Y., Kang, J. S., Cheong, G. W., Yun, D. J., Rhee, S. G., Cho, M. J., and Lee, S. Y. (2004) *Cell* **117,** 625–635
27. Moon, J. C., Hah, Y. S., Kim, W. Y., Jung, B. G., Jang, H. H., Lee, J. R., Kim, S. Y., Lee, Y. M., Jeon, M. G., Kim, C. W., Cho, M. J., and Lee, S. Y. (2005) *J. Biol. Chem.* **280,** 28775–28784
28. Jang, H. H., Kim, S. Y., Park, S. K., Jeon, H. S., Lee, Y. M., Jung, J. H., Lee, S. Y., Chae, H. B., Jung, Y. J., Lee, K. O., Lim, C. O., Chung, W. S., Bahk, J. D., Yun, D. J., Cho, M. J., and Lee, S. Y. (2006) *FEBS Lett.* **580,** 351–355
29. Neumann, C. A., Krause, D. S., Carman, C. V., Das, S., Dubey, D. P., Abraham, J. L., Bronson, R. T., Fujiwara, Y., Orkin, S. H., and Van Etten, R. A. (2003) *Nature* **424,** 561–565
30. Lee, T. H., Kim, S. U., Yu, S. L., Kim, S. H., Park, D. S., Moon, H. B., Dho, S. H., Kwon, K. S., Kwon, H. J., Han, Y. H., Jeong, S., Kang, S. W., Shin, H. S., Lee, K. K., Rhee, S. G., and Yu, D. Y. (2003) *Blood* **101,** 5033–5038
31. Kim, Y. J., Lee, W. S., Ip, C., Chae, H. Z., Park, E. M., and Park, Y. M. (2006) *Cancer Res.* **66,** 7136–7142
32. Kim, J. A., Park, S., Kim, K., Rhee, S. G., and Kang, S. W. (2005) *Anal. Biochem.* **338,** 216–223
33. Hendrick, J. P., and Hartl, F. U. (1993) *Annu. Rev. Biochem.* **62,** 349–384
34. DeLano, W. L. (2003) *The PyMOL Molecular Graphics System.* DeLano Scientific LLC, San Carlos, CA
35. Ghosh, D., Sawicki, M., Lala, P., Erman, M., Pangborn, W., Eyzaguirre, J., Gutierrez, R., Jornvall, H., and Thiel, D. J. (2001) *J. Biol. Chem.* **276,** 11159–11166
36. Otwinowski, Z., and Minor, W. (1997) *Methods Enzymol.* **276,** 307–326
37. Collaborative Computational Project Number Four (1994) *Acta Crystallogr. Sect. D Biol. Crystallogr.* **50,** 760–763
38. Pasta, S. Y., Raman, B., Ramakrishna, T., and Rao Ch, M. (2004) *Mol. Vis.* **10,** 655–662
39. Engh, R. A., and Huber, R. (1991) *Acta Crystallogr. Sect.* A **47,** 392–400
40. Choi, M. H., Lee, I. K., Kim, G. W., Kim, B. U., Han, Y. H., Yu, D. Y., Park, H. S., Kim, K. Y., Lee, J. S., Choi, C., Bae, Y. S., Lee, B. I., Rhee, S. G., and Kang, S. W. (2005) *Nature* **435,** 347–353
41. Hirotsu, S., Abe, Y., Okada, K., Nagahara, N., Hori, H., Nishino, T., and Hakoshima, T. (1999) *Proc. Natl. Acad. Sci. U. S. A.* **96,** 12333–12338
42. Trujillo, M., Mauri, P., Benazzi, L., Comini, M., De Palma, A., Flohe, L., Radi, R., Stehr, M., Singh, M., Ursini, F., and Jaeger, T. (2006) *J. Biol. Chem.* **281,** 20555–20566
43. Ursini, F., Heim, S., Kiess, M., Maiorino, M., Roveri, A., Wissing, J., and Flohe, L. (1999) *Science* **285,** 1393–1396
44. Wen, S. T., and Van Etten, R. A. (1997) *Genes Dev.* **11,** 2456–2467
45. Mu, Z. M., Yin, X. Y., and Prochownik, E. V. (2002) *J. Biol. Chem.* **277,** 43175–43184
46. Jung, H., Kim, T., Chae, H. Z., Kim, K. T., and Ha, H. (2001) *J. Biol. Chem.* **276,** 15504–15510
47. Ishii, T., Yamada, M., Sato, H., Matsue, M., Taketani, S., Nakayama, K., Sugita, Y., and Bannai, S. (1993) *J. Biol. Chem.* **268,** 18633–18636
48. Prosperi, M. T., Ferbus, D., Karczinski, I., and Goubin, G. (1993) *J. Biol. Chem.* **268,** 11050–11056
49. Kawai, S., Takeshita, S., Okazaki, M., Kikuno, R., Kudo, A., and Amann, E. (1994) *J. Biochem.* (*Tokyo*) **115,** 641–643
50. Shau, H., and Kim, A. (1994) *Biochem. Biophys. Res. Commun.* **199,** 83–88
51. Sarafian, T. A., Verity, M. A., Vinters, H. V., Shih, C. C., Shi, L., Ji, X. D., Dong, L., and Shau, H. (1999) *J. Neurosci. Res.* **56,** 206–212
52. Lee, K., Park, J. S., Kim, Y. J., Soo Lee, Y. S., Sook Hwang, T. S., Kim, D. J., Park, E. M., and Park, Y. M. (2002) *Biochem. Biophys. Res. Commun.* **296,** 337–342
53. Thompson, J. D., Higgins, D. G., and Gibson, T. J. (1994) *Comput. Appl. Biosci.* **10,** 19–29